

AD-A045 466

AIR FORCE GEOPHYSICS LAB HANSCOM AFB MASS  
LWIR (7-24-MICROMETER) MEASUREMENTS FROM THE LAUNCH OF A ROCKET--ETC(U)  
MAY 77 J W ROGERS, A T STAIR, N B WHEELER  
AFOL-TR-77-0113 DNA-HAES-64

F/O 1/13

UNCLASSIFIED

NL

1 OF 2

AD  
A045466



AD A 045466

AFOL-TR-77-0113

ENVIRONMENTAL RESEARCH PAPERS, NO. 597

HAES REPORT-NO. 64

DNW

12



# LWIR (7-24 $\mu$ m) Measurements From the Launch of a Rocketborne Spectrometer Into a Quiet Atmosphere (1974)

JAMES W. ROGERS

A.T. STAIR, Jr.

NED B. WHEELER

CLAIR L. WYATT

DORAN J. BAKER

24 May 1977

Approved for public release; distribution unlimited.

This research was sponsored by the Defense Nuclear Agency under contract N110AX72534, Task Unit 10, entitled "Infrared Sensor Measurements".

DDC  
RECEIVED  
OCT 25 1977  
B

AU NO. \_\_\_\_\_  
DDC FILE COPY

OPTICAL PHYSICS DIVISION PROJECT 220  
AIR FORCE GEOPHYSICS LABORATORY  
WRIGHT PAFB, WRIGHT-PATTERSON AFB, OHIO 45433

AIR FORCE SYSTEMS COMMAND, USAF

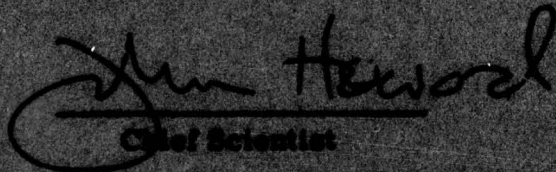




This report has been reviewed by the ESD Information Office (OI) and is releasable to the National Technical Information Service (NTIS).

This technical report has been reviewed and is approved for publication.

FOR THE COMMANDER

  
Chief Scientist

Qualified requestors may obtain additional copies from the Defense Documentation Center. All others should apply to the National Technical Information Service.

micrometers

Unclassified

SECURITY CLASSIFICATION OF THIS PAGE (When Data Entered)

REPORT DOCUMENTATION PAGE		READ INSTRUCTIONS BEFORE COMPLETING FORM
1. REPORT NUMBER	2. REPORT ACCESSION NO.	3. RECIPIENT'S CATALOG NUMBER
14 AFGL-TR-77-0113, AFGL-ERP-597		
4. TITLE (and Subtitle)	5. TYPE OF REPORT & PERIOD COVERED	
6 LWIR (7-24 $\mu$ m) MEASUREMENTS FROM THE LAUNCH OF A ROCKETBORNE SPECTROMETER INTO A QUIET ATMOSPHERE (1974)	Scientific Interim (HAES Report No. 64)	
7. AUTHOR(s)	8. CONTRACT OR GRANT NUMBER(s)	
10 James W. Rogers, Clair L. Wyatt A. T. Stair, Jr., Doran J. Baker Ned B. Wheeler		
9. PERFORMING ORGANIZATION NAME AND ADDRESS	10. PROGRAM ELEMENT, PROJECT, TASK AREA & WORK UNIT NUMBERS	
Air Force Geophysics Laboratory (OPR) Hanscom AFB, Massachusetts 01731	61102F 2310G404 17G4	
11. CONTROLLING OFFICE NAME AND ADDRESS	12. REPORT DATE	
Air Force Geophysics Laboratory (OPR) Hanscom AFB, Massachusetts 01731	24 May 1977	
14. MONITORING AGENCY NAME & ADDRESS (if different from Controlling Office)	15. SECURITY CLASS. (of this report)	
18 DNA 19 HAES-64	Unclassified 17p	
DECLASSIFICATION/DOWNGRADING SCHEDULE		
16. DISTRIBUTION STATEMENT (of this Report)		
Approved for public release; distribution unlimited.		
9 Environmental research papers		
17. DISTRIBUTION STATEMENT (of the abstract entered in Block 20, if different from Report)		
B		
18. SUPPLEMENTARY NOTES		
This research was sponsored by the Defense Nuclear Agency under Subtask K11BAXHX 534, Work Unit 18, entitled "Infrared Auroral Measurements." *Utah State University, Electro Dynamics Laboratories, Logan, Utah 84321		
19. KEY WORDS (Continue on reverse side if necessary and identify by block number)		
Long-wavelength infrared Rocketborne spectrometer CO <sub>2</sub> emission O <sub>3</sub> emission		
20. ABSTRACT (Continue on reverse side if necessary and identify by block number)		
A liquid-helium-cooled, long-wavelength infrared (LWIR) spectrometer was successfully launched by the Air Force Geophysics Laboratory onboard a Black Brant VC rocket (A18.006-4) on 14 Feb 1974 from the University of Alaska's Poker Flat Research Range at Chatanika, Alaska. This flight was part of the Defense Nuclear Agency ICECAP 74 Program. The spectrometer, which employs a circular-variable filter (CVF), was developed by AFGL and Utah State University and was almost identical to the one flown a year earlier on 22 Mar 1973 that provided the first measurements of the altitude profile of the		

DD FORM 1 JAN 73 1473A EDITION OF 1 NOV 65 IS OBSOLETE

Unclassified

SECURITY CLASSIFICATION OF THIS PAGE (When Data Entered)

409548

11/5



Unclassified

SECURITY CLASSIFICATION OF THIS PAGE(When Data Entered)

micrometers.

20. (Cont) *8 A P 1473 A*

→ infrared spectrum of the upper-atmospheric emissions between 7 and 24  $\mu$ m.

The 1973 measurements were from an energetically pumped atmosphere during the occurrence of an IBC II aurora. Altitude profiles of the 15  $\mu$ m carbon dioxide, 9.6  $\mu$ m ozone, and a portion of the 6.3  $\mu$ m water band were obtained. In addition, unidentified emissions were observed above 100 km.

→ The objective of the 1974 flight was to obtain emission data from an aurorally quiet atmosphere to determine the contribution of the auroral energy input to the data obtained in 1973. Specifically, the effect on the 15  $\mu$ m carbon dioxide and 9.6  $\mu$ m ozone emissions was to be investigated along with possible auroral sources for the unidentified emitters.

→ The payload was successfully launched during nonauroral conditions, and data were obtained on the 15  $\mu$ m carbon dioxide (*nu 2*) emission from 74 to 160 km and on the 9.6  $\mu$ m ozone (*nu 3*) emission between 74 and 110 km. Above 110 km, significant unidentified emission was again observed at 9.3  $\mu$ m.

This report documents in detail the data obtained under quiet atmospheric conditions along with rocket and payload performance, launch conditions, and a comparison with data obtained during aurorally disturbed atmospheric conditions.

ACCESSION for	
NTIS	White Section <input checked="" type="checkbox"/>
DDC	Buff Section <input type="checkbox"/>
UNANNOUNCED	<input type="checkbox"/>
JUDICIAL	<input type="checkbox"/>
BY	
DISTRIBUTION/AVAILABILITY CODES	
Dist.	SPECIAL
A	

1473B

Unclassified

SECURITY CLASSIFICATION OF THIS PAGE(When Data Entered)



## Preface

The High Altitude Effects Simulation (HAES) Program, sponsored by the Defense Nuclear Agency since early 1970, comprises several groupings of separate but interrelated technical activities, for example, ICECAP (Infrared Chemistry Experiments - Coordinated Auroral Program). Each of the latter has the common objective of providing information essential to the development and validation of predictive computer codes designed for use with high priority DoD radar, communications, and optical defensive systems.

Since the inception of the HAES Program, significant achievements and results have been described in reports published by DNA, participating service laboratories, and supportive organizations. In order to provide greater visibility for such information and enhance its timely applications, significant reports published since early calendar 1974 have been identified with an assigned HAES serial number and the appropriate activity acronym (for example, ICECAP) as part of the report title. A complete and current bibliography of all HAES reports issued prior to and subsequent to HAES Report No. 1\* is maintained and available on request from DASIAC, DoD Nuclear Information and Analysis Center, 816 State Street, Santa Barbara, California 93102, Telephone (805) 965-0551.

This report, the sixty-fourth in the HAES series, presents the data obtained from the launch of a liquid-helium-cooled, long-wavelength, infrared spectrometer into a quiet atmosphere, discusses rocket and payload performance, describes the launch conditions, and compares the data with that reported in HAES Report No. 51 that was obtained during aurorally disturbed atmospheric conditions.

\*Rocket Launch of an SWIR Spectrometer into an Aurora (ICECAP 72) AFCRL-TR-74-0077, 5 Feb 1974.

The authors wish to thank the personnel from various organizations who made significant contributions to the success of this experiment, including: Dr. H.C. Fitz, Jr., and Mr. Herb Mitchell\* of DNA; Neil Brown of the University of Alaska; Tom Condron, Ed McKenna, Ray Wilton, and Phil Doyle of AFGL; Gary Frodsham of Utah State University; Ed Allen of Space Data Corporation; Ed Butterfield of White Sands Missile Range; and Larry O'Connor and Dick Morin of Northeastern University. The efficiency and assistance of Ms. Gloria Foss in the preparation of this report is gratefully acknowledged.

---

\* Presently with R&D Associates.



Contents	
1. INTRODUCTION	9
2. PAYLOAD CONFIGURATION	10
2.1 LWIR CVF Spectrometer Description	10
2.2 Photometer Description	12
2.3 Dust Detector Description	13
3. LAUNCH CONDITIONS	13
4. FLIGHT PERFORMANCE	14
4.1 LWIR CVF Spectrometer Performance	15
4.2 Photometer Performance	16
4.3 Dust Detector Performance	16
5. EXPERIMENTAL RESULTS	17
5.1 $N_2(1N)$ Altitude Profile	18
5.2 LWIR CVF Infrared Spectra	19
5.3 $O_3$ and $CO_2$ Zenith Radiance Profiles	21
5.4 Unidentified Emissions	23
6. COMPARISON OF AURORA AND QUIET LWIR EMISSION DATA	24
7. CONCLUSIONS	26
REFERENCES	27
APPENDIX A: Instrumentation Analysis for Spectrometer Model HS-1B-2B Flown on Rocket A18.006-4	29
APPENDIX B: Ascent Intensity Correction	35
APPENDIX C: Spectral Data Scans Obtained During the Flight	39



## Contents

APPENDIX D: List of HAES Reports	105
APPENDIX E: Distribution List	113

## Illustrations

1. Cutaway View of the Liquid-Helium-Cooled CVF Spectrometer Used for IR Atmospheric Emissions	11
2. Final Flight Calibration of the CVF Spectrometer	12
3. Spectrometer Detector and Baffle Temperatures During Flight	15
4. Dust Detector Output Between Cover Opening and Closing	17
5. Correlation of Dust Detector Signals With Anomalous Spectrometer Signals	17
6. The Altitude Profile of Overhead Radiance at $3914 \text{ \AA}$ as Measured Onboard the Rocket	18
7. Spectral Values for Scan 432 at 200 km	19
8. Spectral Radiance Values for Scan 736 at 95 km During Descent	19
9. Spectral Radiance Values at Apogee Obtained by Averaging Over 36 Scans	20
10. Altitude Dependence of the Spectral Radiance During Ascent From 105 to 200 km	20
11. Altitude Dependence of the Spectral Radiance During Descent From 200 to 105 km	21
12. Altitude Dependence of the Spectral Radiance During Descent From 110 to 75 km	21
13. Zenith Radiance Altitude Profile at $9.6 \text{ }\mu\text{m}$ Measured With the LWIR Spectrometer	22
14. Zenith Radiance Altitude Profile at $15 \text{ }\mu\text{m}$ Measured With the LWIR Spectrometer	22
15. Zenith Radiance Altitude Profile of the Strong Unidentified Emission at $9.3 \text{ }\mu\text{m}$	23
16. Zenith Radiance of the Unidentified Emission Feature at $9.3 \text{ }\mu\text{m}$ as a Function of Time After Launch	23
17. Comparison of the Zenith Radiance Altitude Profiles at $9.6 \text{ }\mu\text{m}$ During Quiet Conditions (1974) and an Aurora (1973)	24
18. Comparison of the Zenith Radiance Altitude Profiles at $15 \text{ }\mu\text{m}$ During Quiet Conditions (1974) and an Aurora (1973)	25
19. Comparison of the Zenith Radiance Altitude Profiles of the Unidentified Emission Feature at $9.3 \text{ }\mu\text{m}$ During Quiet Conditions (1974) and an Aurora (1973)	25

## Illustrations

20.	Comparison of the Spectral Bandshape at Apogee of the Unidentified Emission Feature at $9.3 \mu\text{m}$ During Quiet Conditions (1974) and at Aurora (1973)	26
A1.	dc Zero Reset Values of Each Data Channel During the Entire Flight	30
A2.	Averages of 58 Background Scans Before Cover Opening of the CVF Spectrometer	33
A3.	Standard Deviations of the 58 Averaged Background Scans for Each Data Channel	34
B1.	Ascent Intensity Corrections to the $\text{CO}_2$ Zenith Radiance Altitude Profile at $15 \mu\text{m}$	36
B2.	Ascent Intensity Corrections to the Zenith Radiance Altitude Profile of the Unidentified Emission at $9.3 \mu\text{m}$	36

## Tables

1.	Poker Flat Temperatures ( $^{\circ}\text{C}$ ) From Rocket Sounding Data at 0540 UT on 14 February 1974	14
A1.	List of Channels and Scans With Unreliable Zero Values for Scans 117 through 766	31
A2.	Summary of Discarded and "Good" Data Scans	31



## LWIR (7-24 $\mu\text{m}$ ) Measurements From the Launch of a Rocketborne Spectrometer Into a Quiet Atmosphere (1974)

### 1. INTRODUCTION

On 14 February 1974, a Black Brant VC rocket (A18.006-4) carrying a liquid-helium-cooled, long-wavelength-infrared (LWIR) spectrometer was successfully launched by the Air Force Geophysics Laboratory (AFGL) from the University of Alaska's Poker Flat Research Range at Chatanika, Alaska. This flight was part of the Defense Nuclear Agency (DNA) ICECAP 74 Program. The spectrometer was almost identical to the one flown a year earlier on 22 March 1973 that provided the first measurements of the altitude profile of the infrared spectrum of the upper-atmospheric emissions between 7 and 24  $\mu\text{m}$ .<sup>1</sup>

The 1973 measurements were from an energetically pumped atmosphere during the occurrence of an IBC II aurora. Altitude profiles of the 15  $\mu\text{m}$  carbon dioxide, 9.6  $\mu\text{m}$  ozone, and a portion of the 6.3  $\mu\text{m}$  water band were obtained. In addition, unidentified emissions were observed above 100 km.

The objective of the 1974 flight was to obtain emission data from an aurorally quiet atmosphere to determine the contribution of the auroral energy input to the data obtained in 1973. Specifically, the effect on the 15  $\mu\text{m}$  carbon dioxide and

(Received for publication 24 May 1977)

1. Rogers, J. W., Stair, A. T., Jr., Wheeler, N. B., Wyatt, C. L., and Baker, D. J. (1976) LWIR (7-24  $\mu\text{m}$ ) Measurements From the Launch of a Rocketborne Spectrometer Into an Aurora (1973), ERP No. 583, AFGL-TR-76-0274, HAES Report No. 51.



9.6  $\mu\text{m}$  ozone emissions was to be investigated along with possible auroral sources for the unidentified emitters.

The payload was successfully launched during non-auroral conditions, and data were obtained on the 15  $\mu\text{m}$  carbon dioxide ( $\nu_2$ ) emission from 74 to 160 km and on the 9.6  $\mu\text{m}$  ozone ( $\nu_3$ ) emission between 74 and 110 km. Above 110 km, significant unidentified emission was again observed at 9.3  $\mu\text{m}$ .

This report documents in detail the data obtained under quiet atmospheric conditions, describes rocket performance, payload performance and launch conditions, and compares data obtained with that obtained during aurorally disturbed atmospheric conditions, which was initially reported by Stair, et al.<sup>2</sup>

## 2. PAYLOAD CONFIGURATION

The payload configuration was identical to the payload flown in 1973. In addition to the liquid-helium-cooled LWIR CVF spectrometer, the payload was instrumented with diagnostic sensors to provide information on local atmospheric conditions plus rocket and payload performance. These included a 3914 Å photometer, a light-scattering dust detector, mechanical vibration spectrometers, an aspect gyro, and a spin magnetometer.

The rocket was assembled with a "clamshell" split-nosecone that could be opened during ascent at a predetermined altitude above which the LWIR sensor would not seriously cryo-pump. The clamshell could be closed during descent. The payload was outfitted with a recovery system employing a parachute and beacon. The dust detector was provided to indicate the presence of local particulate matter that might pass through the field of view of the spectrometer. To minimize possible dust contamination problems, all portions of the payload were sealed, and both the sensor and the payload were assembled in a clean room. The final payload was enclosed in a large plastic bag until launch.

### 2.1 LWIR CVF Spectrometer Description

The spectrometer flown was Model HS-1B-2B; it was developed by Utah State University (USU) and is described as follows: The spectral region from 23.4 to 7  $\mu\text{m}$  is scanned at a rate of two scans per second with a full-angle field of view of 2 deg ( $9.6 \times 10^{-4}$  sr). The entire optical subsection is cooled to liquid-helium temperature, including an arsenic-doped silicon detector that is thereby operated with an effective zero radiation background. A key element of the spectrometer is

2. Stair, A. T., Jr., Ulwick, J. C., Baker, D. J., Wyatt, C. L., and Baker, K. D. (1974) Altitude profiles of infrared radiance of O<sub>3</sub> (9.6  $\mu\text{m}$ ) and CO<sub>2</sub> (15  $\mu\text{m}$ ), Geophysical Research Letters, 1, No. 3:117-118.

the rotating variable interference filter that was developed by Optical Coating Laboratories, Inc. (OCLI). The spectral resolution of the filter was measured at AFGL by Condron<sup>3</sup> and the best estimate of the half-bandwidth for the flight-configured spectrometer is that it may be 25 percent greater than the spectrometer launched in 1973. This results in a 3.29 percent half-bandwidth for the short-wavelength filter half and 3.65 percent for the long-wavelength filter half. This circular variable filter element has led to this class of instruments being referred to as CVF spectrometers. A dynamic range of  $5 \times 10^4$  is achieved by providing four data channels with different gains. The output data from the spectrometer along with the diagnostic information were transmitted to a ground telemetry site during the flight.

Many technical breakthroughs had to be achieved in order to assure satisfactory measurements. Most of these problems dealt with the cryogenics and the stringent requirements placed on the electronics and optics to perform remotely in a severe environment. A cutaway view of the spectrometers is shown in Figure 1. Specific details on the spectrometer can be found in Reference 1 and the references it lists.

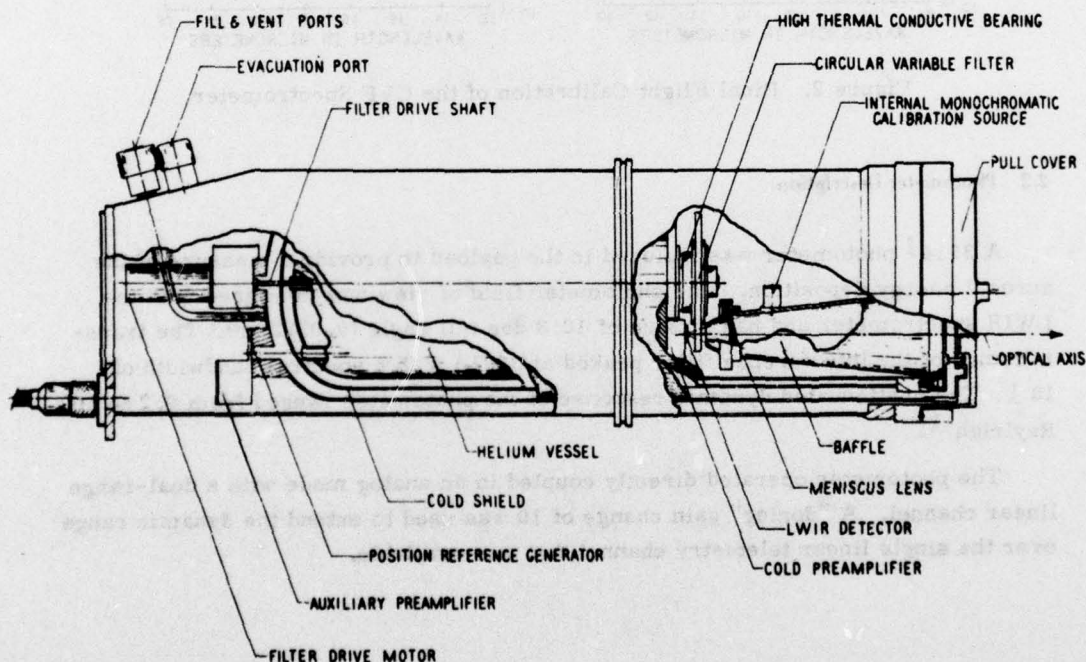


Figure 1. Cutaway View of the Liquid-Helium-Cooled CVF Spectrometer Used for IR Atmospheric Emissions

3. Condron, T. P. (1973) Calibration Data for the HS-1B-2B Radiometer, December 1973 (unpublished report).



The final flight calibration of the spectrometer's absolute spectral response was performed at AFGL and is contained in a report by Condron.<sup>3</sup> The spectral response in  $\text{W cm}^{-2} \text{sr}^{-1} \mu\text{m}^{-1} / \text{V}$  of the highest gain channel is shown in Figure 2 for both halves of the filter and is accurate to within a factor of two.

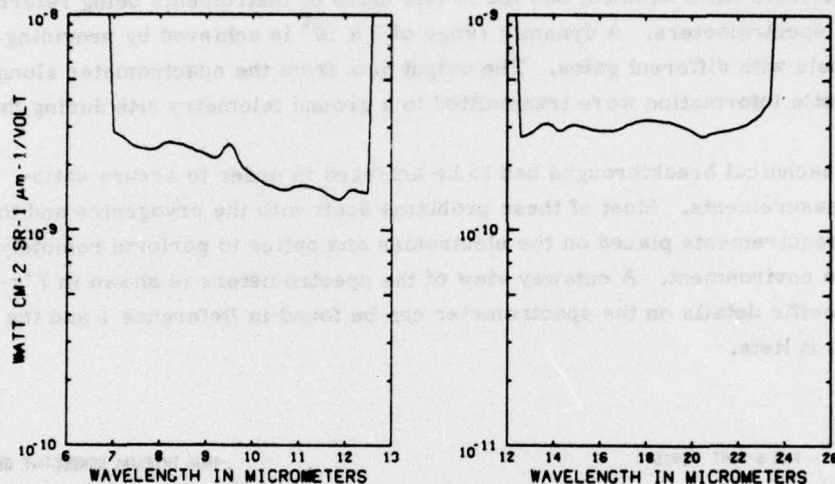


Figure 2. Final Flight Calibration of the CVF Spectrometer

## 2.2 Photometer Description

A  $3914 \text{ \AA}$  photometer was included in the payload to provide a measure of the auroral energy deposition. The photometer field of view was coaligned with the LWIR spectrometer and had a value of  $10.8 \text{ deg}$  full angle ( $0.0282 \text{ sr}$ ). The transmittance of the interference filter peaked at  $3907 \text{ \AA}$  with a spectral bandwidth of  $18 \text{ \AA}$ . The unattenuated dynamic response of the photometer ranged from  $0.2$  to  $500 \text{ Rayleigh/\AA}$ .

The photometer operated directly coupled in an analog mode with a dual-range linear channel. A "dogleg" gain change of 10 was used to extend the dynamic range over the single linear telemetry channel that was available.



### 2.3 Dust Detector Description

The dust detector, Model DD-1, consists of an emitter head, a detector head, and an electronics box. The emitter consists of a bank of eight light-emitting diodes, and the detector head contains a silicon detector and preamplifier. The coherent detector system is phase-locked to the emitters, which are pulsed with 50 percent duty cycle at 400 Hz.

The dust detector is tied into the HS-1B-2B Logic in such a way that the emitters are turned off when the HS-1B system internal calibrate is activated every tenth scan, and turned back on after 250 msec. The dust detector is oriented so that the maximum intersection of its field of view with the spectrometer's field-of-view occurs 13.5 cm forward of the spectrometer entrance aperture.

Calculations based upon the emitter and detector data indicate that a signal-to-noise ratio of 10 would be obtained for a single particle of  $60 \mu$  diameter ( $6 \times 10^{-3}$  cm) that re-radiates all incident energy as a Lambertian radiator at 300°K. No quantitative calibrations were made on the dust detector.

### 3. LAUNCH CONDITIONS

The mission criteria were such that the payload would be launched into non-auroral conditions. Electron densities should be low and magnetometer and riometer readings quiet. Although overcast skies and a light snowfall at the multiple supporting sites precluded the clear visual conditions that were desirable as a prerequisite to launch, it was predetermined that evidence of the lack of auroral activity (from the Chatanika incoherent backscatter radar and from optical observations at one site) would provide justification for launch of the vehicle.

The radar data obtained were presented in a report by Perrault and Baron<sup>4</sup> of The Stanford Research Institute. Radar azimuth scan observations were made prior to and during the launch, and typical peak electron densities of  $0.5 \times 10^5/\text{cm}^3$  were observed. Particle precipitation energy, calculated from the 6-min-averaged electron-density profiles, was, of course, also very low, with an energy deposition rate of less than  $0.05 \text{ ergs}/\text{cm}^2\text{-sec}$ . Since this is effectively at the radar threshold of detection, determinations of temperature and vector quantities were precluded. In addition, no auroral activity was recorded by the Chatanika all-sky camera during the evening of the launch.

The University of Alaska's Fort Yukon H-component magnetometer data indicated levels of less than 10 gammas above the quiet-time level throughout the

4. Perrault, P. D., and Baron, M. J. (1975) ICECAP '74 - Chatanika Radar Results, HAES Report No. 47, Topical Report, DNA3871T, Contract No. DNA 001-74-C-0167, Stanford Research Institute, Menlo Park, California.

evening of the launch. The Poker Flat Magnetometer also indicated quiet conditions at this time.

Visual observation of quiet auroral conditions were obtained at the Poker Flat site until about an hour before launch. The University of Alaska's Fort Yukon optics site became relatively clear about 30 min before launch. The 5577 Å meridian-scanning photometer data indicate near airglow intensity levels at the anticipated rocket penetration of the 100 km level. The intensity overhead at Fort Yukon was only slightly enhanced, with a maximum intensity of about 5 kR occurring approximately 450 km north of the site.

The data from the Chatanika backscatter radar indicated that the ionosphere was very quiet, and the confirming visual observation at Fort Yukon of the relative absence of auroral activity in the region of the rocket trajectory satisfied the basic conditions for launch.

Table 1 lists the atmospheric temperature profiles obtained from sounding rocket data approximately 28 min before launch.<sup>5</sup> These temperatures are necessary to describe the atmospheric environment and analyze the flight data.

Table 1. Poker Flat Temperatures (°C) From Rocket Sounding Data at 0540 UT on 14 February 1974

Altitude (km)	25	30	35	40	45	50	55	60
Temperature (°C)	-47	-46	-40	-39	-41	-20	-21	-35

#### 4. FLIGHT PERFORMANCE

The Black Brant VC rocket (A18.006-4) with the LWIR CVF spectrometer payload was launched at 0607:53 UT on 14 February 1974 into a quiet night sky. The payload was integrated at AFGL under the direction of E. McKenna, with R. Wilton of AFGL responsible for telemetry and tracking. Trajectory and aspect data are contained in a report prepared by the Analysis and Simulation Branch of the AFGL Computation Center.<sup>6</sup> The altitudes reported are accurate to within 0.5 km and indicate that an apogee of 200.6 km was attained in 227.5 sec. The report also showed that the rocket attitude control system (ACS) maintained the look angle of the spectrometer to within 4 deg of the vertical.

5. Atmospheric Sciences Laboratory, White Sands Missile Range, New Mexico, private communication.

6. Aspect Report, Rocket No. A18-006-4 (1974) Aspect Report Number 4600, Analysis and Simulation Branch, AFGL Computation Center.



The rocket flight was extremely successful with associated physical functions accomplished as planned, including payload separation, attitude control, and nose tip and instrument deployment. Data were obtained from all instruments with successful telemetry, radar trackings, and payload recovery.

#### 4.1 LWIR CVF Spectrometer Performance

Excellent data were obtained from the LWIR spectrometer that was the primary payload sensor. A detailed analysis of the instrument performance, as was presented in a report by Rogers<sup>7</sup> for the 1973 flight, is given in Appendix A.

The effects of atmospheric heating on the spectrometer detector and optical baffle can be seen in Figure 3. After the vacuum cover was opened at 67 sec (87.7 km), the detector temperature rose to a maximum of 24.5°K at 74.5 sec (87.5 km), but returned to the temperature of liquid helium by 113 sec (141 km).

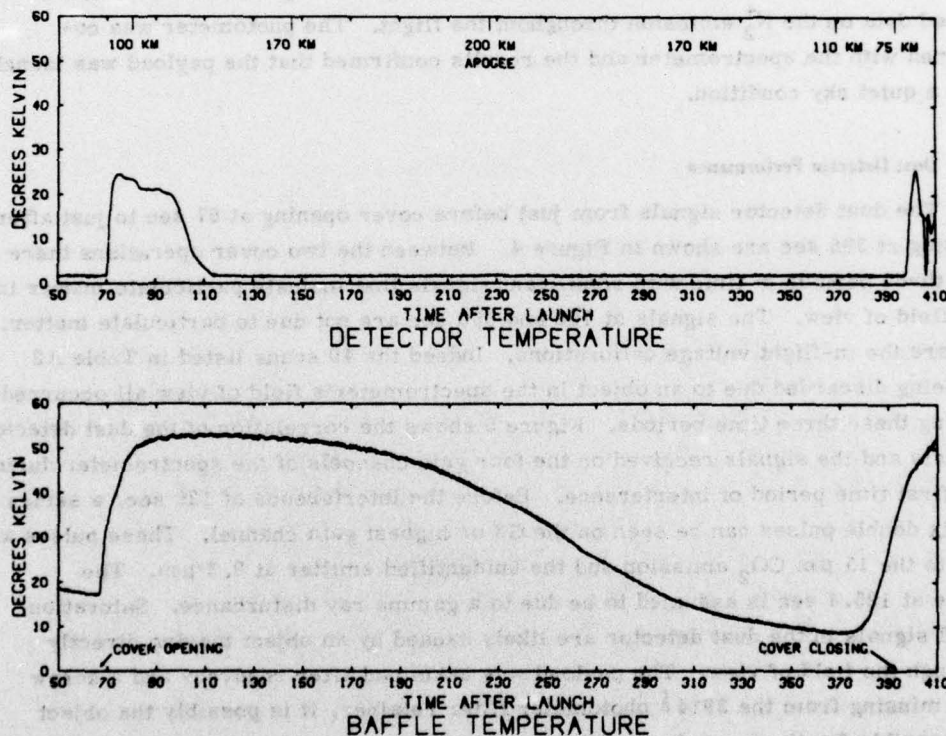


Figure 3. Spectrometer Detector and Baffle Temperatures During Flight

7. Rogers, J.W. (1975) Instrumentation Analysis and Data Processing for Rocket-borne LWIR Spectrometers (With Application to Rocket A18.006-2 of 22 March 1973), ERP No. 539, AFCRL-TR-75-0535, HAES Report No. 23.

During payload descent, the detector temperature did not start to rise again until 398 sec (70 km), which was after the last usable scan of data at 395 sec (74 km). The baffle temperature also rose after the vacuum cover was opened, and peaked at about 53°K around 95 sec (121 km). The baffle cooled off throughout the flight to a minimum temperature of around 9°K, and then started to rise again at 377 sec (89 km). During the last usable data scan, the baffle was at 38°K.

The baffle temperature never rose to a level high enough to affect the spectrometer performance in any way. However, the high detector temperature resulted in a sensitivity drop of about an order of magnitude during the initial portion of the flight. Emission intensities can be approximated during this time by using the internal calibration source as a reference. This procedure is explained in Appendix B.

#### 4.2 Photometer Performance

The 3914 Å photometer, with a field of view of 10.8 deg ( $2.82 \times 10^{-2}$  sr), obtained data on the  $N_2^+$  emission throughout the flight. The photometer was co-aligned with the spectrometer and the results confirmed that the payload was launched into a quiet sky condition.

#### 4.3 Dust Detector Performance

The dust detector signals from just before cover opening at 67 sec to just after closing at 395 sec are shown in Figure 4. Between the two cover operations there are three periods of time with significant signals that indicate particulate matter in the field of view. The signals at 180 and 360 sec are not due to particulate matter, but are the in-flight voltage calibrations. Indeed the 40 scans listed in Table A2 as being discarded due to an object in the spectrometer's field of view all occurred during these three time periods. Figure 5 shows the correlation of the dust detector signals and the signals received on the four gain channels of the spectrometer during the first time period of interference. Before the interference of 126 sec, a series of six double pulses can be seen on the G3 or highest gain channel. These pulses are due to the 15  $\mu$ m CO<sub>2</sub> emission and the unidentified emitter at 9.3  $\mu$ m. The pulse at 125.4 sec is assumed to be due to a gamma ray disturbance. Saturation level signals in the dust detector are likely caused by an object moving directly through the field of view. The payload was examined after recovery and a screw was missing from the 3914 Å photometer filter retainer, it is possibly the object responsible for the anomalous signals.

The anomalous signals during the time period shown in Figure 5 resulted in a loss of data during ascent between 153 and 168 km.



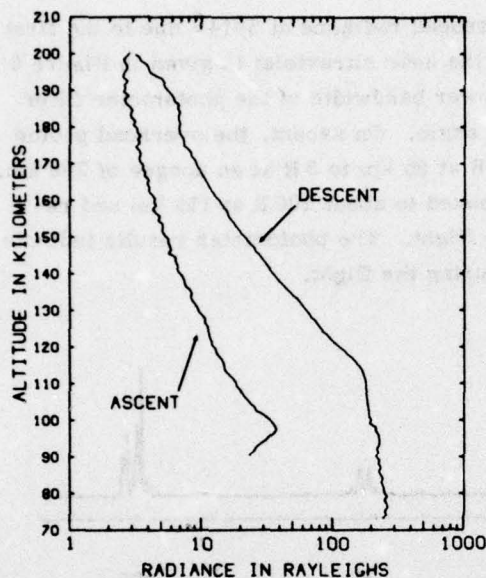


Figure 4. Dust Detector Output Between Cover Opening and Closing

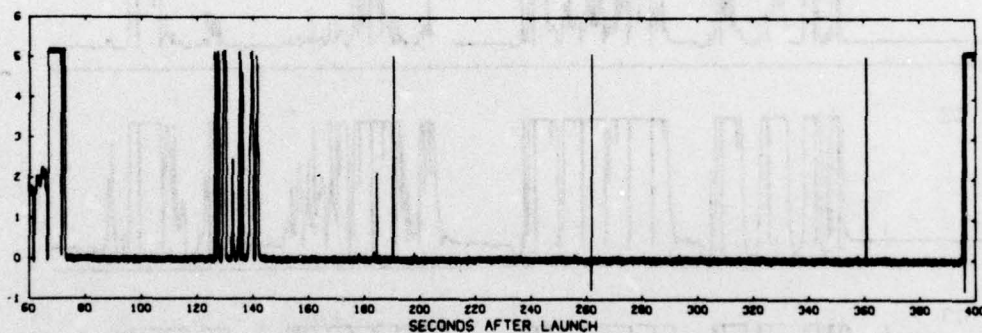


Figure 5. Correlation of Dust Detector Signals With Anomalous Spectrometer Signals. The lower plot is the dust detector output and the other four plots are the spectrometer output with G3 representing the highest gain channel

## 5. EXPERIMENTAL RESULTS

Excellent data were obtained from the LWIR spectrometer and the 3914 Å photometer. After the vacuum cover was opened at 87.7 km, 864 scans were obtained of which 542 were considered usable. Data were obtained on the 15 μm carbon dioxide ( $\nu_2$ ) emission from 74 to 160 km and on the 9.6 μm ozone ( $\nu_3$ ) emission between 74 and 110 km. Above 110 km, significant unidentified emission was again observed at 9.3 μm.

### 5.1 $N_2^+(1N)$ Altitude Profile

The measured altitude profile of the overhead radiance at  $3914 \text{ \AA}$  due to the first negative band ( $B^2 \Sigma_u^+ \rightarrow X^2 \Sigma_g^+$ ) of  $N_2^+(0,0)$  in the near ultraviolet is given in Figure 6 as a function of rocket altitude. The half-power bandwidth of the photometer filter was  $18 \text{ \AA}$  with a field of view of  $10.8 \text{ deg}$  full angle. On ascent, the overhead photon radiance decreased from a peak of about 40 R at 95 km to 3 R at an apogee of 200 km. During descent, the overhead intensity increased to about 200 R at 115 km and remained constant during the remainder of the flight. The photometer results indicate the lack of any significant auroral activity during the flight.

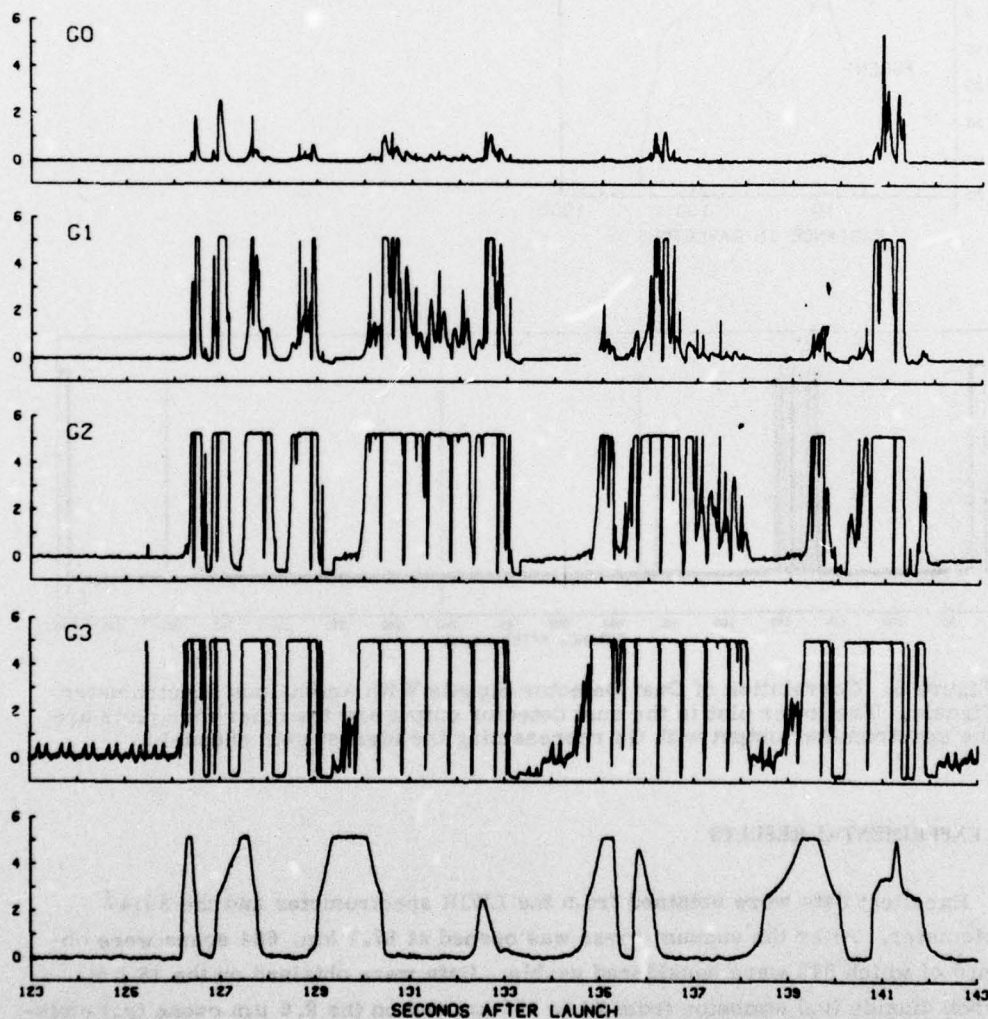


Figure 6. The Altitude Profile of Overhead Radiance at  $3914 \text{ \AA}$  as Measured Onboard the Rocket



## 5.2 LWIR CVF Infrared Spectra

Figures 7 and 8 show typical examples of individual scans obtained; the dashed lines represent  $\pm 3\sigma$  error limits. Scan 432 (Figure 7) was taken 300 sec after launch near apogee at 200 km, and scan 736 (Figure 8) was taken at 380 sec (95 km) during the downleg portion of the trajectory. At the higher altitudes, where the signals are weak and varying slowly, the data scans can be averaged to reduce the random noise at each wavelength. The resulting gain in signal-to-noise from this process is shown at apogee by Figure 9 where the spectral radiance values have been averaged over 36 scans. It is seen that the coherent background signals shown on the high gain channel (G3) in Figure A2 are evident in Figure 9. This indicates that the inherent spectrometer background has not been adequately removed from the emission spectra. However, the signal levels are very weak at the higher altitudes; the unidentified feature at  $9.3 \mu\text{m}$  is significantly above the background level and is caused by an external source or sources. Appendix C contains data scans obtained throughout the entire flight. Averaging has been performed as indicated in the figure captions.

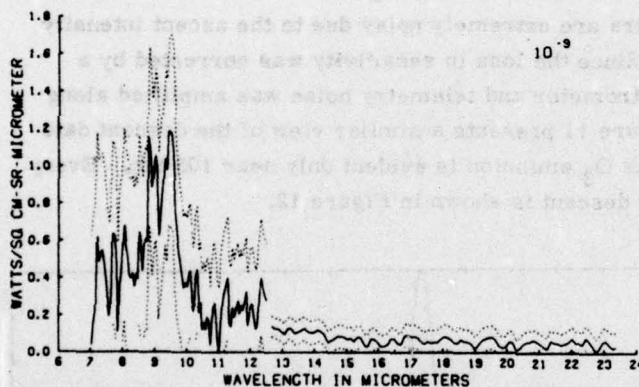


Figure 7. Spectral Radiance Values for Scan 432 at 200 km. The dashed curves are the  $\pm 3\sigma$  error bars

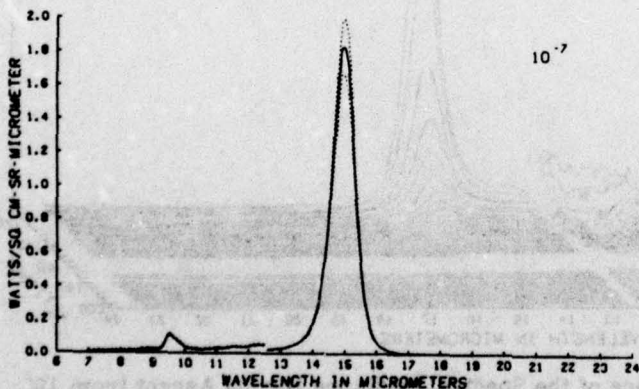


Figure 8. Spectral Radiance Values for Scan 736 at 95 km During Descent. The dashed curves are the  $\pm 3\sigma$  error bars

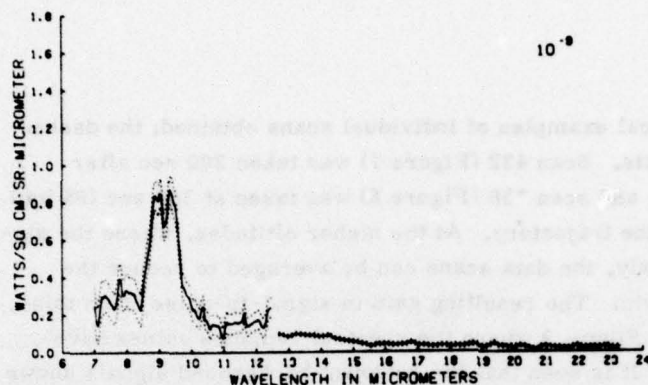


Figure 9. Spectral Radiance Values at Apogee Obtained by Averaging Over 36 Scans. The dashed curves are the  $\pm 3\sigma$  error bars

Graphic portrayals of the spectral intensities measured during this experiment are given by the three-dimensional presentations shown in Figures 10, 11, and 12. Due to the dynamic range of the spectrometer, some of the noise baseline features are lost in these plots. Figure 10 shows a portion of the ascent data between 105 and 200 km where the scans have been averaged over 2.5-km increments. The decay of the  $15\text{-}\mu\text{m}$   $\text{CO}_2$  emission is clearly seen. The loss of data between 153 and 168 km is due to the anomalous spectrometer signals described in Section 4.3. From 105 to 130 km, the spectra are extremely noisy due to the ascent intensity correction (see Appendix B). Since the loss in sensitivity was corrected by a multiplicative factor, the spectrometer and telemetry noise was amplified along with the infrared signals. Figure 11 presents a similar view of the descent data from 200 to 105 km; the  $9.6\text{ }\mu\text{m}$   $\text{O}_3$  emission is evident only near 105 km. Every scan from 110 to 75 km during descent is shown in Figure 12.

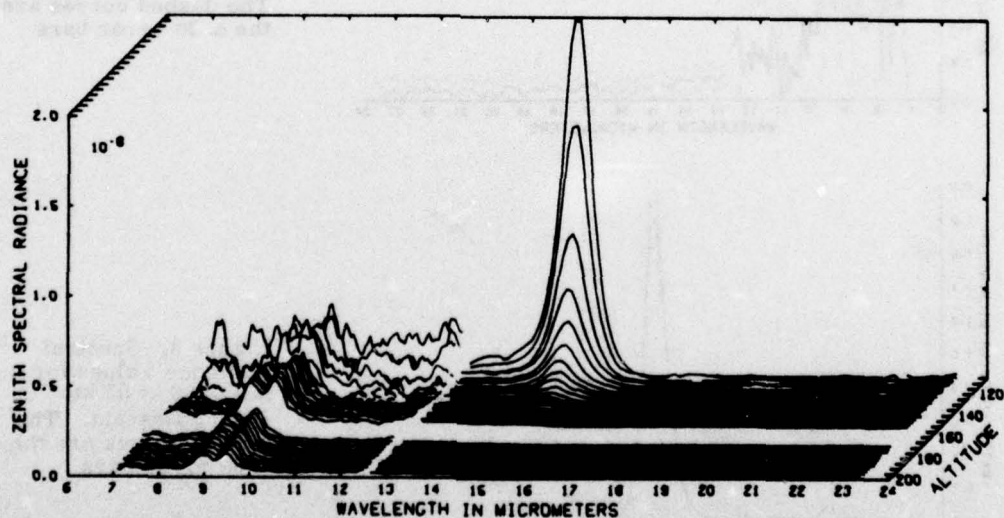


Figure 10. Altitude Dependence of the Spectral Radiance During Ascent from 105 to 200 km. Spectral scans are averages over 2.5-km increments



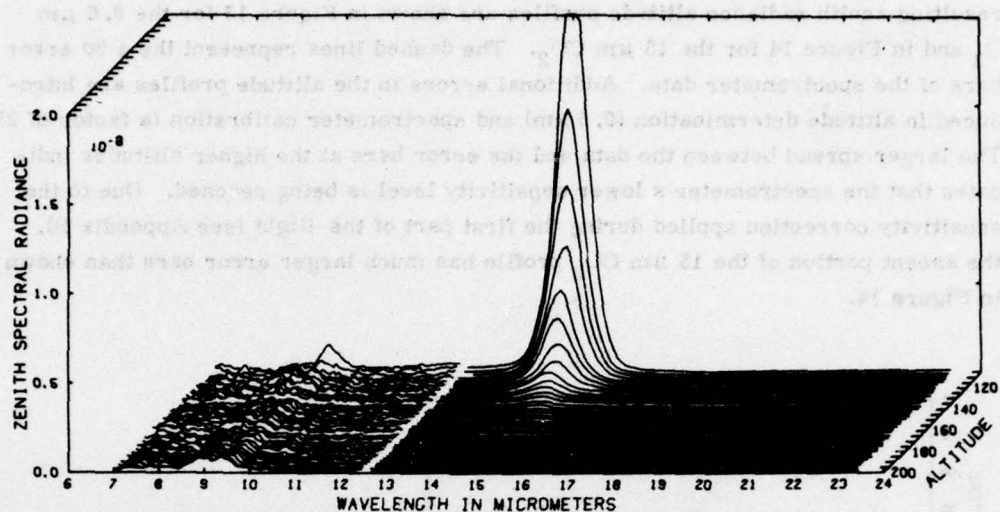


Figure 11. Altitude Dependence of the Spectral Radiance During Descent From 200 to 105 km. Spectral scans are averages over 2.5-km increments

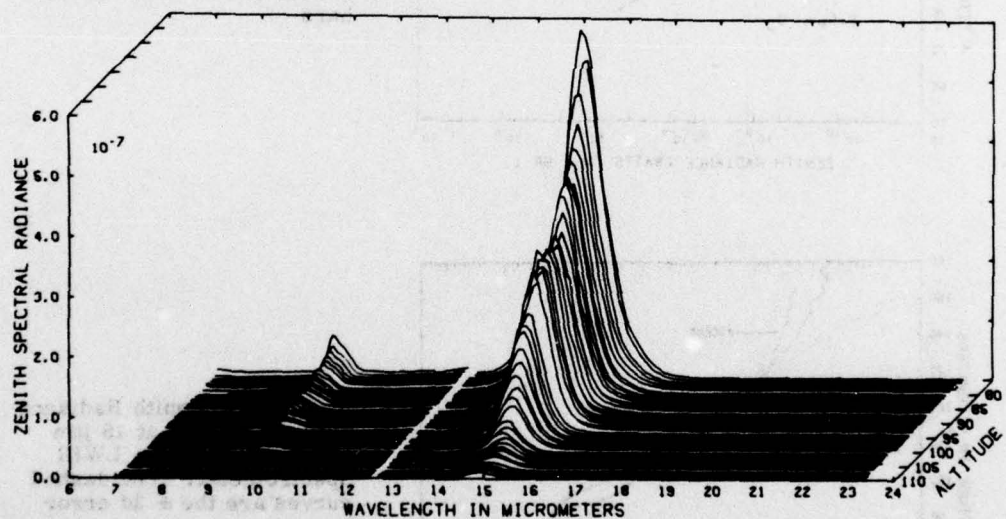


Figure 12. Altitude Dependence of the Spectral Radiance During Descent From 110 to 75 km

### 5.3 O<sub>3</sub> and CO<sub>2</sub> Zenith Radiance Profiles

Zenith radiance values are obtained by integrating every scan between 9.2 and 10  $\mu\text{m}$  for the 9.6  $\mu\text{m}$  O<sub>3</sub> band and between 14 and 16  $\mu\text{m}$  for the 15  $\mu\text{m}$  band. The

resulting zenith radiance altitude profiles are shown in Figure 13 for the  $9.6 \mu\text{m}$   $\text{O}_3$  and in Figure 14 for the  $15 \mu\text{m}$   $\text{CO}_2$ . The dashed lines represent the  $\pm 3\sigma$  error bars of the spectrometer data. Additional errors in the altitude profiles are introduced in altitude determination (0.5 km) and spectrometer calibration (a factor of 2). The larger spread between the data and the error bars at the higher altitudes indicates that the spectrometer's lower sensitivity level is being reached. Due to the sensitivity correction applied during the first part of the flight (see Appendix B), the ascent portion of the  $15 \mu\text{m}$   $\text{CO}_2$  profile has much larger error bars than shown in Figure 14.

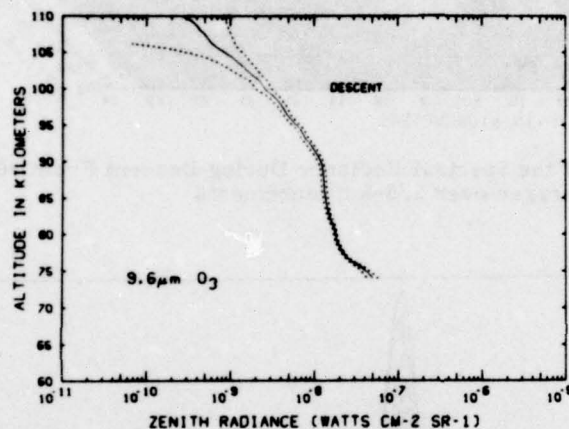


Figure 13. Zenith Radiance Altitude Profile at  $9.6 \mu\text{m}$  Measured With the LWIR Spectrometer. The dashed curves are the  $\pm 3\sigma$  error bars

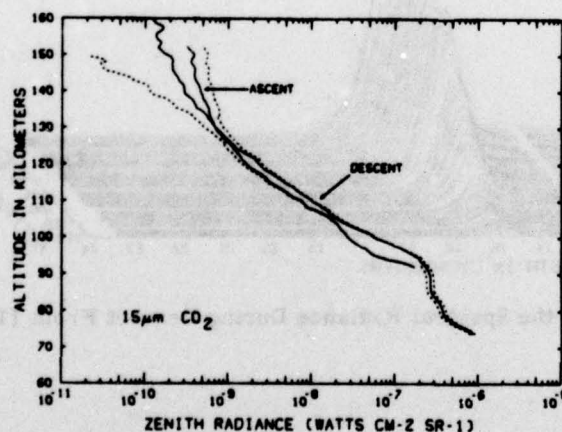


Figure 14. Zenith Radiance Altitude Profile at  $15 \mu\text{m}$  Measured With the LWIR Spectrometer. The dashed curves are the  $\pm 3\sigma$  error bars



#### 5.4 Unidentified Emissions

As in the 1973 flight, significant emission was observed at  $9.3 \mu\text{m}$  above 110 km; however, weaker features at other wavelengths were not as evident. The zenith altitude profile of the  $9.3 \mu\text{m}$  feature, obtained by integrating the spectral radiance data from  $8.5$  to  $10.9 \mu\text{m}$  (Figure 15), shows a marked asymmetry between ascent and descent. The observed radiance values plotted vs time in Figure 16 are less intense but similar to the 1973 flight values where, after an initial rise, the intensity decreases throughout the remainder of the flight. The gap in the data during ascent is due to the anomalous spectrometer signals discussed in Section 4.3. Further examination of Figure 9 and the scans above 110 km in Appendix C shows that there is little evidence of the intense background continuum that appeared during the 1973 flight.

The source of the 1973 emission has still not been identified. A number of possible explanations were presented in Reference 1, but it appears that additional experiments will have to be performed for positive identification.

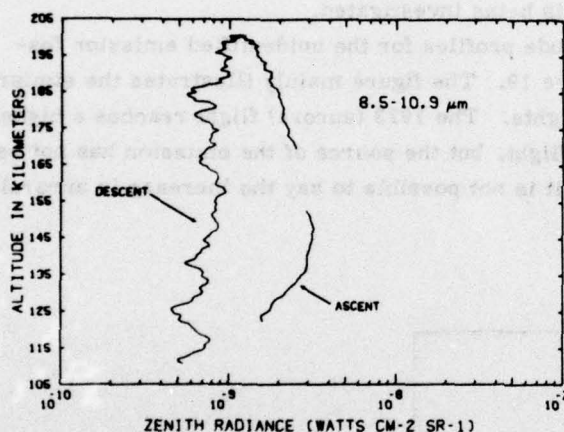


Figure 15. Zenith Radiance Altitude Profile of the Strong Unidentified Emission at  $9.3 \mu\text{m}$

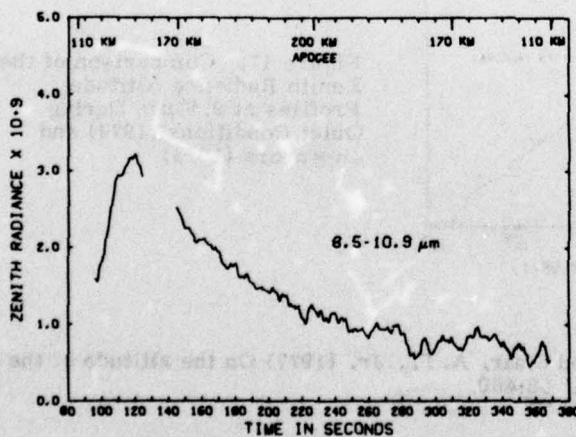


Figure 16. Zenith Radiance of the Unidentified Emission Feature at  $9.3 \mu\text{m}$  as a Function of Time After Launch

## 6. COMPARISON OF AURORA AND QUIET LWIR EMISSION DATA

The data obtained during the spectrometer launch into a quiet atmospheric background confirmed predictions that neither the  $9.3 \mu\text{m}$   $\text{O}_3$  nor the  $15 \mu\text{m}$   $\text{CO}_2$  band is enhanced to any significant degree for at least an IBC II aurora.

Comparison of the descent zenith altitude profile for the two flights is shown in Figure 17 for the  $9.6 \mu\text{m}$   $\text{O}_3$  emission and in Figure 18 for the  $15 \mu\text{m}$   $\text{CO}_2$  emission. Descent profiles are shown since the spectrometer performance was somewhat affected in both flights by the cover opening operation. Model calculations will be used to determine the ozone number density profiles and the  $\text{CO}_2$  mixing ratios that will be reported at a later date. It is evident from Figure 17 that the ozone layer is 5 to 10 km higher during the quiet launch than during the auroral launch. While the exact mechanism is not known, it has been reported that the peak of the OH layer can vary between 84 and 89 km.<sup>8</sup> The differences in the  $\text{CO}_2$  profiles shown in Figure 18, especially between 75 and 105 km, is not explainable at this time, but the possibility of high altitude temperature effects is being investigated.

A comparison of the zenith altitude profiles for the unidentified emission feature at  $9.3 \mu\text{m}$  is presented in Figure 19. The figure mainly illustrates the similarities in profile shapes for the two flights. The 1973 (aurora) flight reaches a higher radiance level than the 1974 (quiet) flight, but the source of the emission has not been identified at this time. Therefore, it is not possible to say the increase is aurorally induced.

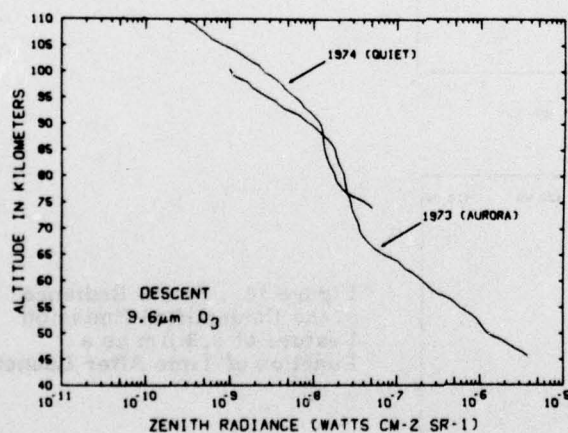


Figure 17. Comparison of the Zenith Radiance Altitude Profiles at  $9.6 \mu\text{m}$  During Quiet Conditions (1974) and an Aurora (1973)

8. Baker, D.J., Conley, T.D., and Stair, A.T., Jr. (1977) On the altitude of the OH airglow, EOS Trans. AGU 58:460.



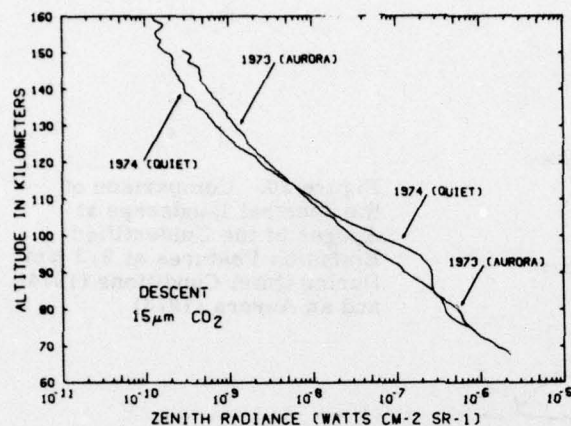


Figure 18. Comparison of the Zenith Radiance Altitude Profiles at  $15 \mu\text{m}$  During Quiet Conditions (1974) and an Aurora (1973)

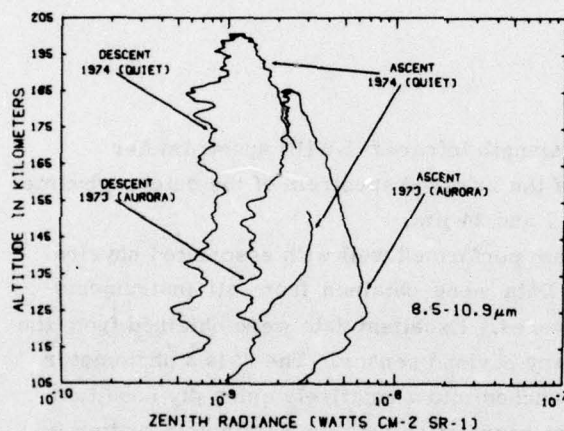


Figure 19. Comparison of the Zenith Radiance Altitude Profiles of the Unidentified Emission Feature at  $9.3 \mu\text{m}$  During Quiet Conditions (1974)

Figure 20 shows a comparison of the spectral bandshapes for the  $9.3 \mu\text{m}$  emission feature measured during both flights. From the figure, it would appear that the spectrometer launched in 1974 had a slightly higher resolution; however, this is contrary to the results obtained during preflight calibration.<sup>3</sup> The differences shown are actually very slight when the actual filter imperfections at these very weak signal levels are considered. It is clear that the observed unidentified emission at  $9.3 \mu\text{m}$  is due to the same species during both flights.

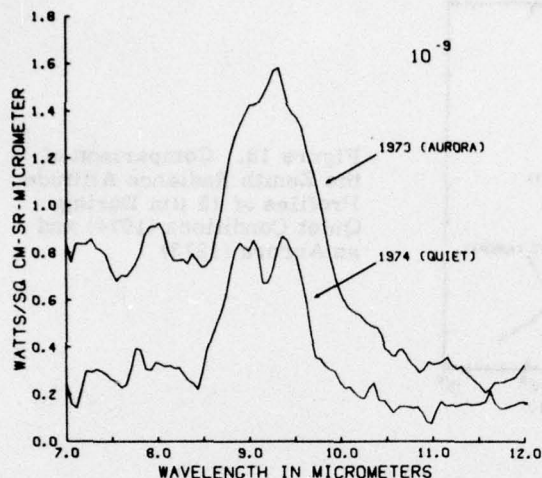


Figure 20. Comparison of the Spectral Bandshape at Apogee of the Unidentified Emission Features at  $9.3 \mu\text{m}$  During Quiet Conditions (1974) and an Aurora (1973)

## 7. CONCLUSIONS

A liquid-helium-cooled, long-wavelength infrared (LWIR) spectrometer successfully obtained measurements of the infrared spectrum of the quiet nighttime upper atmospheric emissions between 7 and  $24 \mu\text{m}$ .

All components of the rocket system performed well with associated physical functions accomplished as planned. Data were obtained from all instruments and the payload was successfully recovered. Excellent data were obtained from the LWIR spectrometer that was the primary payload sensor. The  $3914 \text{ \AA}$  photometer data confirmed that the payload was launched into a relatively quiet sky condition, and the dust detector provided excellent correlation between particulate matter in the field-of-view and anomalous spectrometer signals.

During the quiet background conditions, data were obtained on the  $15 \mu\text{m}$  carbon dioxide emission from 74 to 160 km and on the  $9.6 \mu\text{m}$  ozone emission between 74 and 110 km. Comparison with the 1973 auroral launch confirms the prediction that neither of these bands is enhanced to any degree by auroral activity at the IBC II level. The ozone layer does appear to be 5 to 10 km higher for the 1974 (quiet) launch than it was during the 1973 (auroral) launch, and there are differences in the  $15 \mu\text{m}$   $\text{CO}_2$  profile in the 75 to 105 km region.

Above 110 km, significant unidentified emission was again observed at  $9.3 \mu\text{m}$ . As with the 1973 flight, these emissions showed a marked asymmetry between ascent and descent. Identification of the species that produce this observed radiation has not been accomplished at this time; additional experiments will have to be performed for positive identification.



## References

1. Rogers, J.W., Stair, A.T., Jr., Wheeler, N.B., Wyatt, C.L., and Baker, D.J. (1976) LWIR (7-24  $\mu\text{m}$ ) Measurements From the Launch of a Rocketborne Spectrometer into an Aurora (1973), ERP No. 583, AFGL-TR-76-0274, HAES Report No. 51.
2. Stair, A.T., Jr., Ulwick, J.C., Baker, D.J., Wyatt, C.L., and Baker, K.D. (1974) Altitude profiles of infrared radiance of  $\text{O}_3$  (9.6  $\mu\text{m}$ ) and  $\text{CO}_2$  (15  $\mu\text{m}$ ), Geophysical Research Letters, 1, No. 3:117-118.
3. Condron, T.P. (1973) Calibration Data for the HS-1B-2B Radiometer, December 1973 (unpublished report).
4. Perreault, P.D., and Baron, M.J. (1975) ICECAP '74 - Chatanika Radar Results, HAES Report No. 47, Topical Report, DNA3871T, Contract No. DNA 001-74-C-0167, Stanford Research Institute, Menlo Park, California
5. Atmospheric Sciences Laboratory, White Sands Missile Range, New Mexico, private communication.
6. Aspect Report, Rocket No. A18-006-4 (1974) Aspect Report Number 4600, Analysis and Simulation Branch, AFCRL Computation Center.
7. Rogers, J.W. (1975) Instrumentation Analysis and Data Processing for Rocketborne LWIR Spectrometers (With Application to Rocket A18.006-2 of 22 March 1973), ERP No. 539, AFCRL-TR-75-0535, HAES Report No. 23.
8. Baker, D.J., Conley, T.D., and Stair, A.T., Jr. (1977) On the altitude of the OH airglow, ECS Trans. AGU 58:460.

## Appendix A

Instrumentation Analysis for Spectrometer Model  
HS-1B-2B Flown on Rocket A18.006-4

### A1. INTRODUCTION

The purpose of this appendix is to provide in a condensed manner the information on the performance of the spectrometer flown in 1974, as was presented by Rogers<sup>7</sup> for the spectrometer flown in 1973. (These will be referred to as 1973 CVF or 1974 CVF in the rest of this appendix.)

### A2. DIGITIZATION AND SCAN DETERMINATION

Digitization and scan determination were performed as for the 1973 CVF with minor changes. The analog data tape was digitized from 15 to 415 sec after launch, but scan determination was terminated with the cover closing at 395 sec. During this time, 766 consecutive scans were obtained, except for the times of the in-flight voltage calibrations at 20.1, 190.4, and 360.6 sec.

### A3. USABLE SCANS

The d-c zero reset values were determined as for the 1973 CVF, but since the CVF used in 1974 rotated in the opposite direction (from the longer wavelengths to



the shorter wavelengths), the d-c reset mask occurred between reference locations 19 and 20. The zero values obtained for the entire flights are shown in Figure A1.

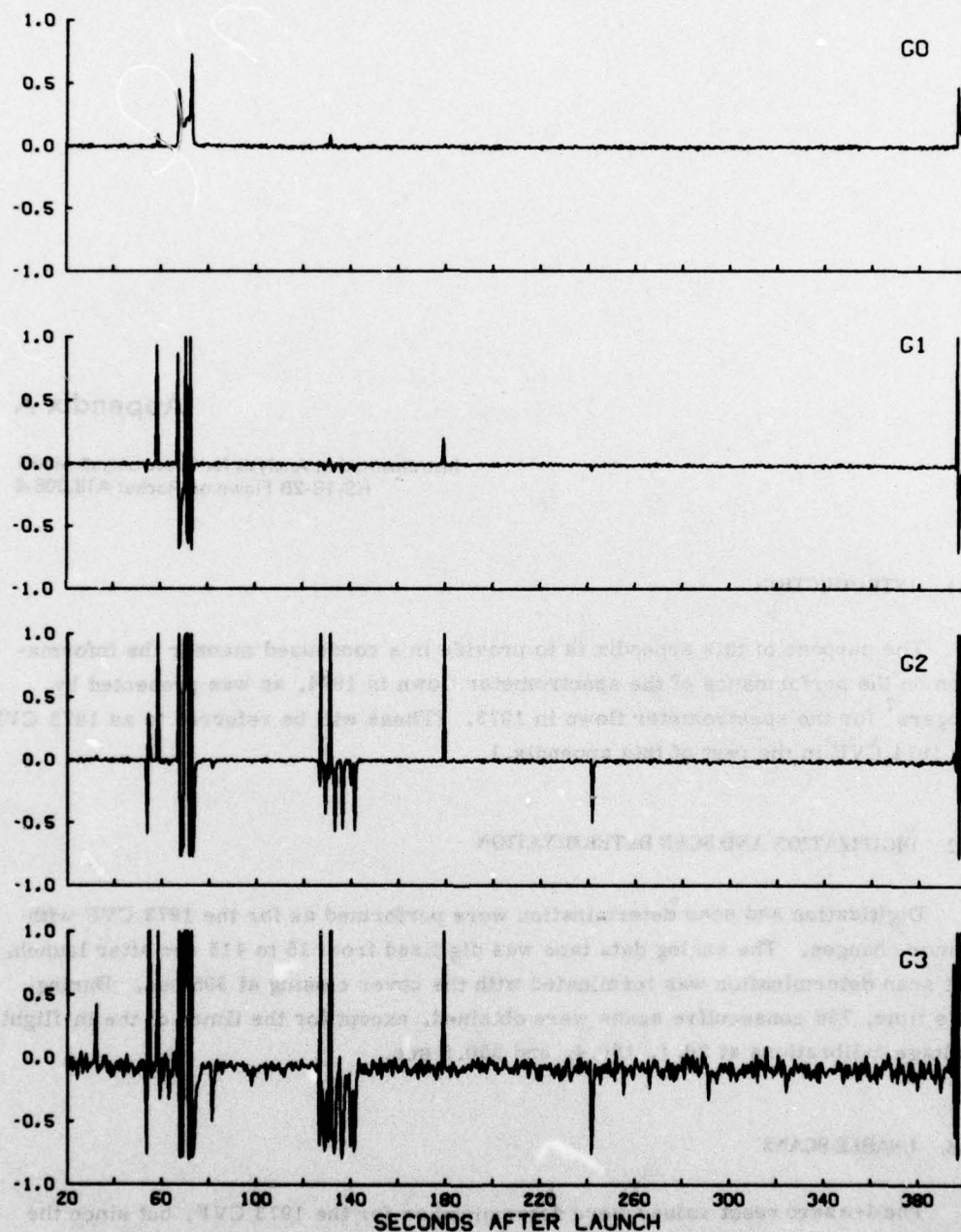


Figure A1. dc Zero Reset Values of Each Data Channel During the Entire Flight

The large deviations in the zero value from zero volts are due to a number of reasons. Before cover opening at 67 sec, rocket motor burn and vehicle orientation maneuvers introduce zero errors. Vacuum cover opening and closing at 67 and 394 sec and an unidentified object in the field of view resulted in additional errors due to a saturation of the spectrometer electronics. Table A1 lists the channels and scans that were not used in the final data calculations, since they were considered to have unreliable zero values. The first useful data scan after cover opening is scan 117, while the last useful scan is 766.

Table A1. List of Channels and Scans With Unreliable Zero Values for Scans 117 through 766

Channel	Upleg Scans	Downleg Scans
G3	< 125 or 77.5 sec	> 763 or 393.7 sec
G2	< 119 or 74.5 sec	> 764 or 394.2 sec
G1	< 118 or 74.0 sec	None
G0	None	None

Certain scans are discarded if the data for the entire scan cannot be recovered and are not included in the final set of flight data used for analysis. A summary of the rejected scans, for reasons explained in more detail in Reference 6, is shown in Table A2. Besides the 6 scans rejected because of intense gamma rays, 25 additional scans had a slight gamma ray disturbance. This usually affected only a single data point that was corrected by an editing procedure.

Table A2. Summary of Discarded and "Good" Data Scans

Before Cover Opening at 67 sec (scans 1-102)		After Cover Opening (Scans 103-766)	
Scans obtained	102	Scans obtained	664
Calibration scans	10	Calibration scans	63
Vehicle noise	34	Saturated scans	13
"Good" background scans	58	Gamma ray disturbance	6
		Object in field of view	40



#### A4. BACKGROUND LEVELS AND ERRORS

As with the 73 CVF, the absolute background level of the spectrometer when there was no signal falling on the detector, was obtained after launch but prior to cover opening. A total of 48 "good" background scans was obtained; however, no scans were obtained after data taking, because the cover temperature had risen well above 4°K due to aerodynamic heating by the atmosphere. The averages of the background voltage levels for all four data channels are shown in Figure A2, with the G2 and G3 channels exhibiting apparent coherent signals as a function of wavelength. As explained in Reference 6, the coherent noise can come from a number of sources in the spectrometer payload. These average values of background voltage are subtracted from the voltage obtained for each channel before the instrument response is applied. This should give an accurate value for the signal levels seen by the spectrometer, which are actually increased above the inherent background levels.

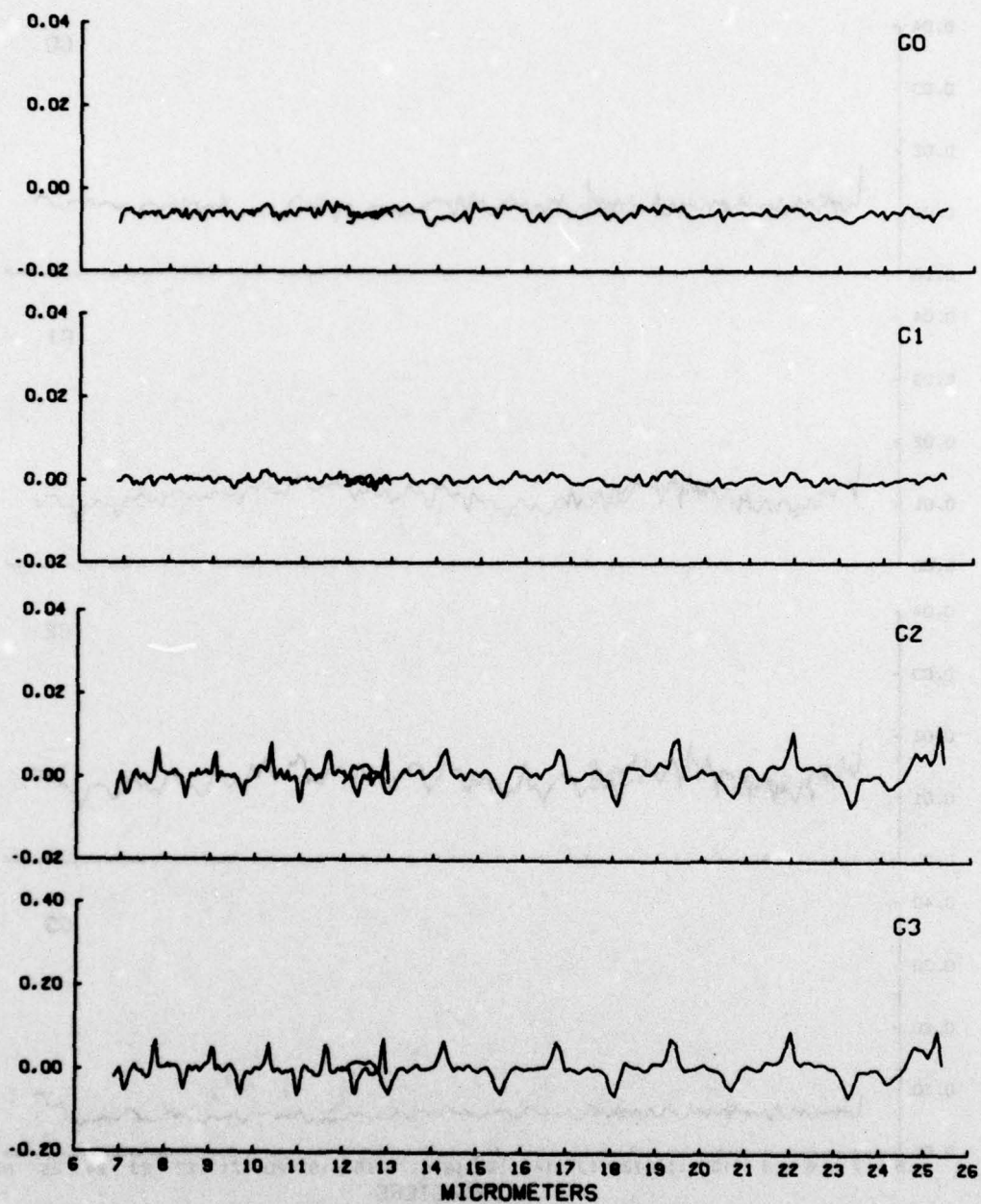
#### A5. RADIANCE VALUES

Figure A3 shows the standard deviations of the background signal for the 58 scans shown averaged in Figure A2. Errors associated with the spectral radiance values are assigned from these background standard deviation calculations using statistical methods for the propagation of errors.

Spectral scans are formed by combining voltage signals from the four gain channels using the criteria described in Reference 6. Examples of the resulting spectra are shown in the main text by Figures 7 and 8 for scans 432 and 736, and Figure 9 illustrates the result of averaging over 36 scans at apogee.

Table A2. Summary of Background and Gain Data

Parameter	Before Cover Opening at 87 sec (Scans 1-101)	After Cover Opening (Scans 102-451)
Scans obtained	101	350
Collection scans	10	340
Vehicle noise	18	322
Ground and atmospheric noise	34	306
Gain in 10% intervals	10	340



**Figure A2. Averages of 58 Background Scans Before Cover Opening of the CVF Spectrometer**



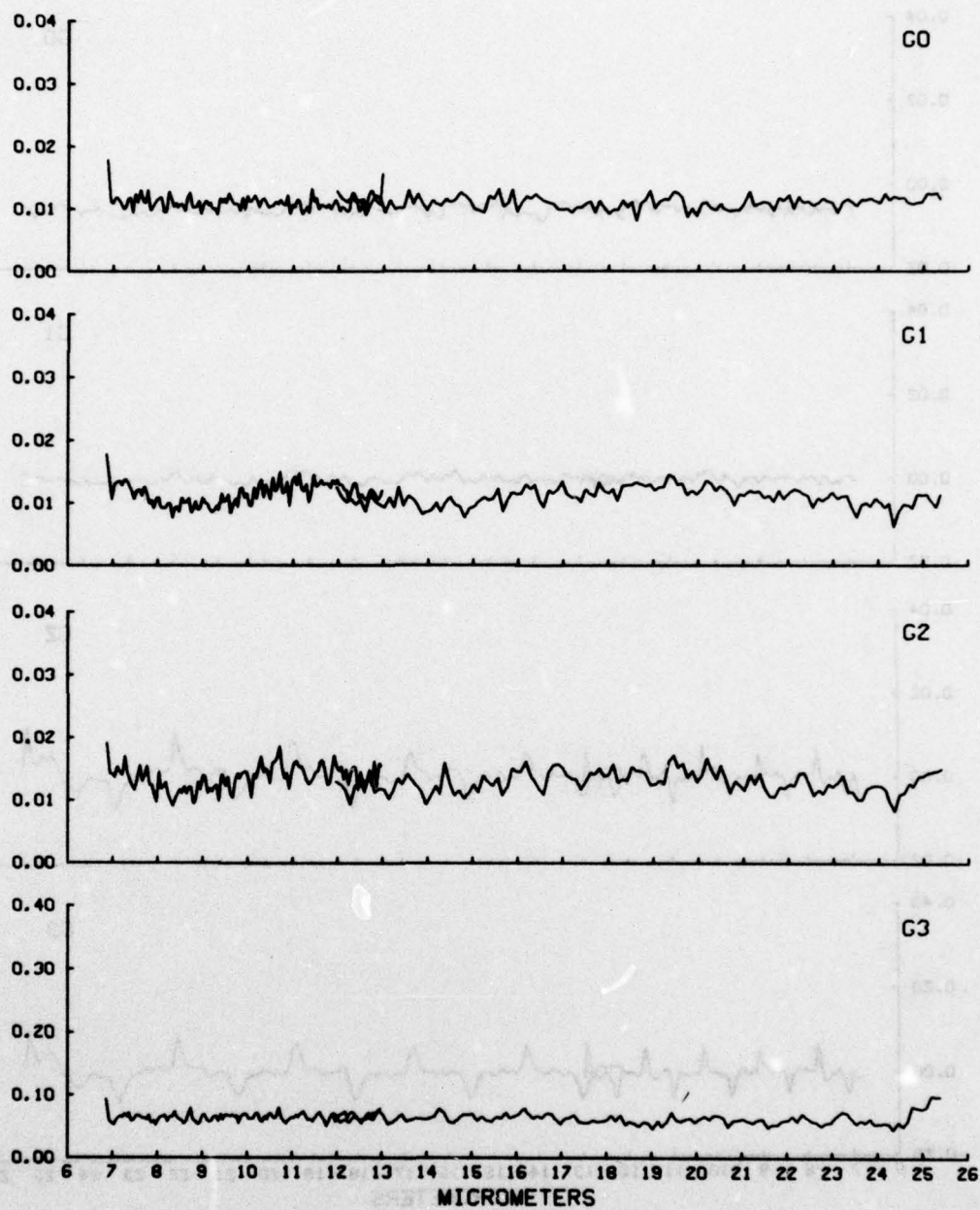


Figure A3. Standard Deviations of the 58 Averaged Background Scans for Each Data Channel

## Appendix B

### Ascent Intensity Correction

The high detector temperatures mentioned in Section 4.1 and shown in Figure 3 resulted in erroneous spectrometer signal levels for a portion of the rocket ascent. A drop in sensitivity was immediately apparent from the low output of the first internal calibration signal after cover opening. Eight seconds later, the calibration signal started to recover, but remained below normal until 29 sec after the detector had returned to its operational temperature. In addition to the sensitivity drop, another error in the signal level was observed between 95 and 105 sec. The zero voltage level exhibited a severe negative drift during the scans in this time period, which was the time of the maximum recovery rate of the detector temperature.

It should be pointed out that absolute corrections to the signal levels received during this portion of the ascent cannot be obtained, but approximate corrections to the data can be performed. The voltage drift occurring during the scan was corrected by adding to the signal at each filter position a voltage that starts at zero and linearly increases during the scan. The dc reset electronics returns the signal to zero volts at the beginning of the scan, and the slope of the added linear voltage is determined from the measured signal level at the end of the scan. The results of this drift correction and the uncorrected ascent altitude profiles are shown in Figure B1 for the  $15\text{ }\mu\text{m}$   $\text{CO}_2$  emission and in Figure B2 for the unidentified emission at  $9.3\text{ }\mu\text{m}$ . The altitude profiles are only changed between 120 and 132 km (95–105 sec) during the maximum recovery rate of the detector temperature. Since the filter rotation is from longer to shorter wavelengths, there is a larger correction at  $9.3\text{ }\mu\text{m}$  than at  $15\text{ }\mu\text{m}$ .



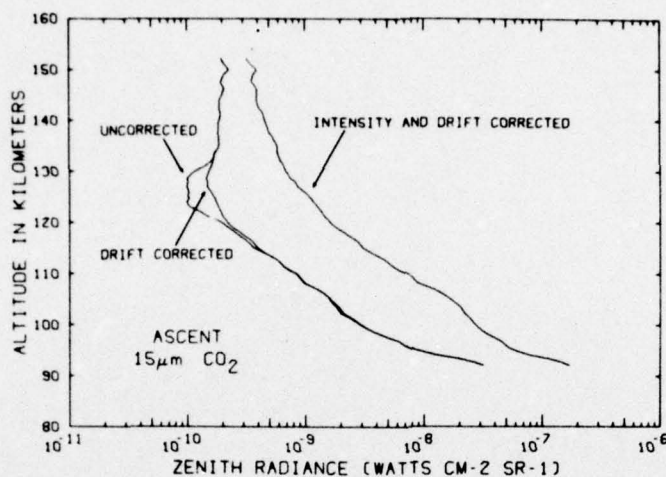


Figure B1. Ascent Intensity Corrections to the CO<sub>2</sub> Zenith Radiance Altitude Profile at 15  $\mu\text{m}$

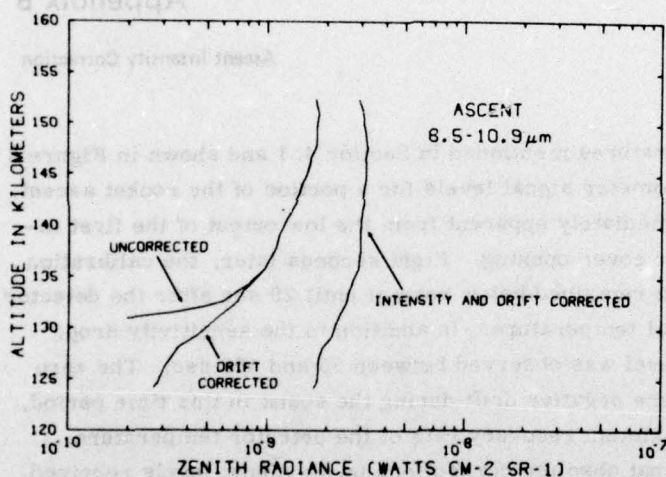


Figure B2. Ascent Intensity Corrections to the Zenith Radiance Altitude Profile of the Unidentified Emission at 9.3  $\mu\text{m}$

The decrease in sensitivity was corrected using the signal from the internal calibration source. This source is insufficiently stable to provide an absolute in-flight calibration of the spectrometer, but can be used to perform approximate corrections to the data. The average value of the internal calibration source signal before cover opening and after the detector temperature had fully recovered was used as the standard for correcting the intensity. The results of this correction are also shown in Figures B1 and B2. The correction factor used was 5.2 for the first good data scan at 92 km (73.6 sec) with a maximum factor of 11.3 at 103 km (91.4 sec). The sensitivity was fully recovered at 167 km (142 sec). The data shown in Figures B1 and B2 terminate at 153 km (125 sec), because of the loss of data due to the anomalous spectrometer signals described in Section 4.3. This

loss of data lasted until 168 km (143 sec) at which time the spectrometer was operating with the correct sensitivity.

The agreement between the  $15\text{ }\mu\text{m CO}_2$  ascent and descent data shown by Figure 14 in Section 5.3 indicates that an approximate correction has indeed been achieved. However, the uncertainties involved in the correction would necessitate using only descent measurements for data analysis.



## Appendix C

### Spectral Data Scans Obtained During The Flight

This appendix contains all the usable data obtained during the flight. Individual scans are shown at altitudes below 104 km in Figures C1 through C16 (92.1 to 103.7 km) during ascent and in Figures C89 through C128 (103.6 to 73.9 km) during descent. At the higher altitudes, scans averaged over 2.5 km increments are shown in Figures C17 through C49 during ascent and Figures C50 through C88 during descent.

Ascent data between 153 and 168 km is not shown due to the anomalous spectrometer signals described in Section 4.3. Figures C1 through C28 show extremely noisy spectra as a result of the intensity correction described in Appendix B. Since the loss in sensitivity was corrected by a multiplicative factor, the spectrometer and telemetry noise were amplified along with the infrared signals.

For individual scans, the scan number, time, and altitude are shown at the top of the figures. The inclusive scan numbers, times, and altitudes are shown for the averaged scans. The numbers in parentheses indicate the number of usable scans and the total number of scans in the 2.5 km increment being averaged. The spectral intensity values are in  $\text{W}/\text{cm}^{-2}/\text{sr}^{-2}/\mu\text{m}^{-1}$ , with the exponent shown in the upper-right-hand corner of the figure.

SCAN 117

73.5 SECS

92.1 KM

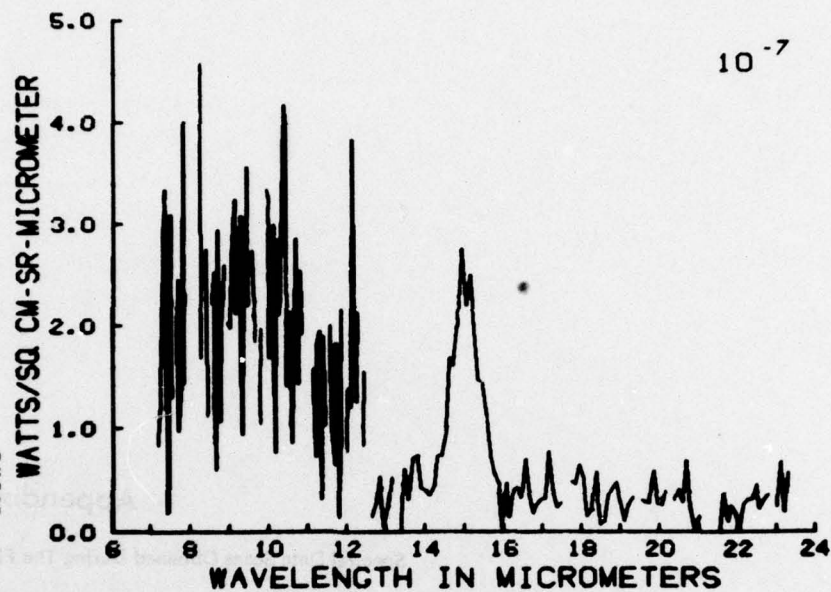


Figure C1

SCAN 118

74.0 SECS

92.9 KM

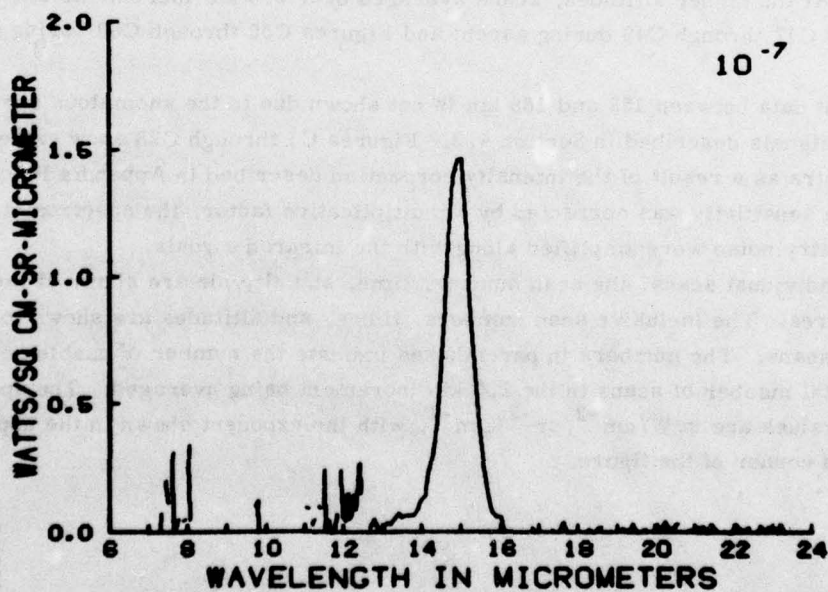


Figure C2



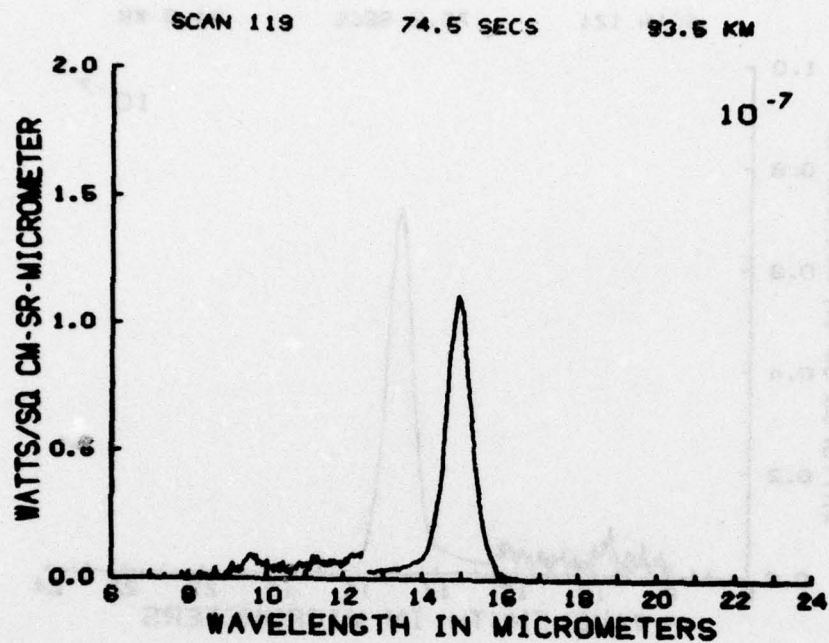


Figure C3

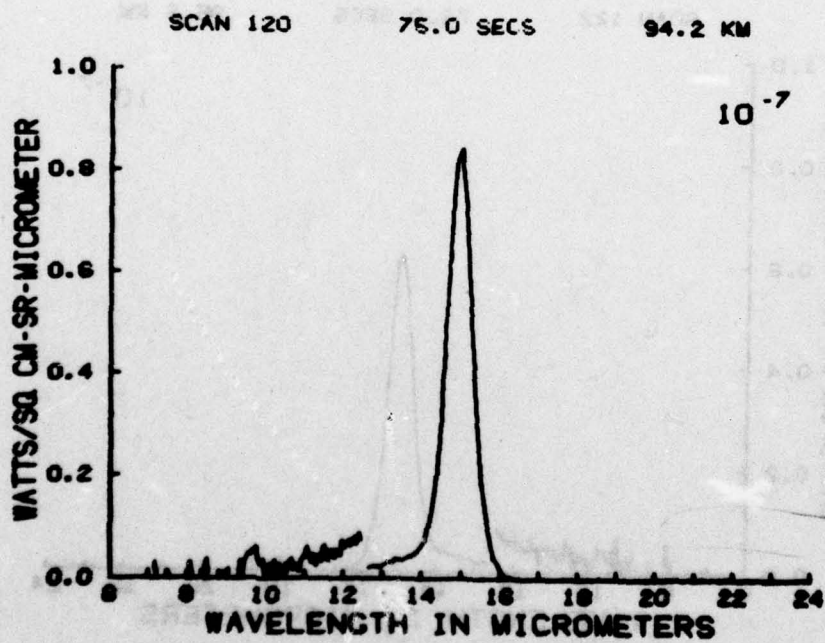


Figure C4

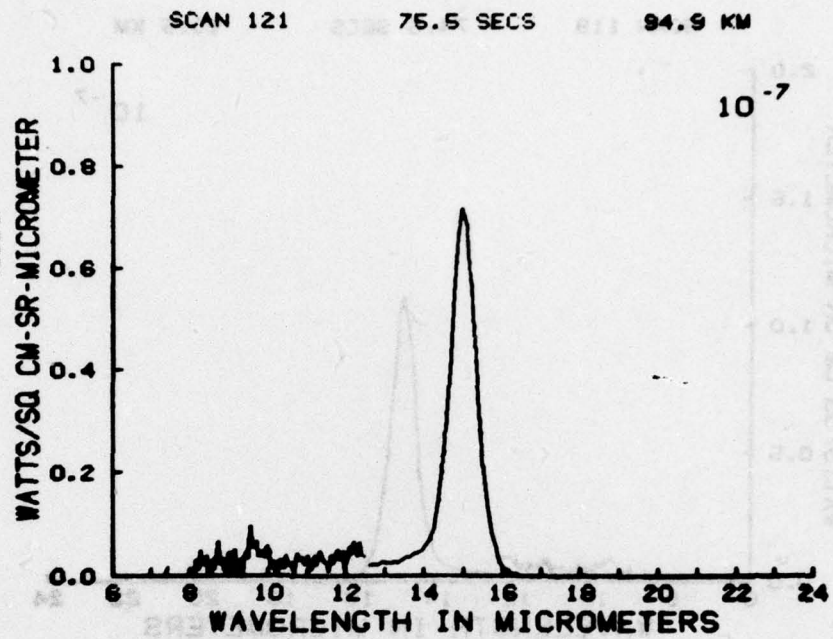


Figure C5

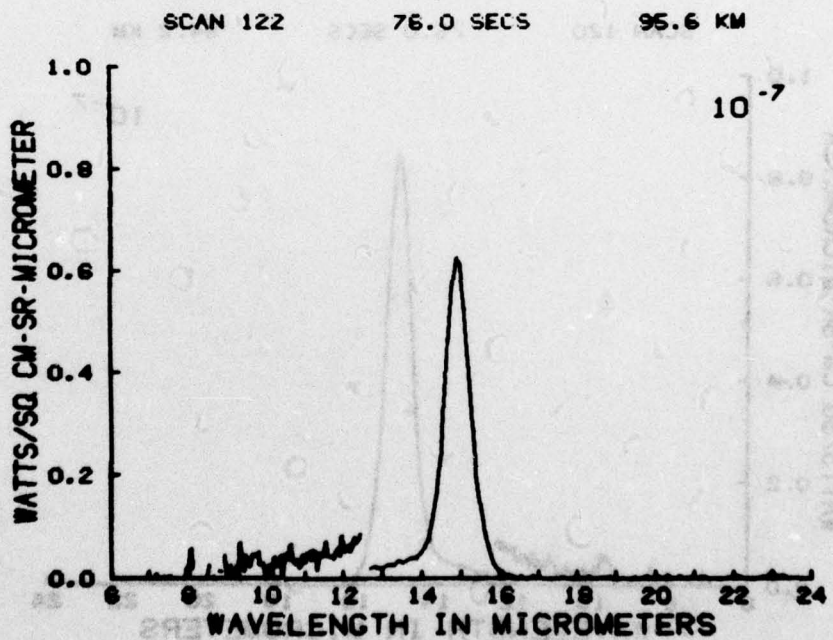


Figure C6



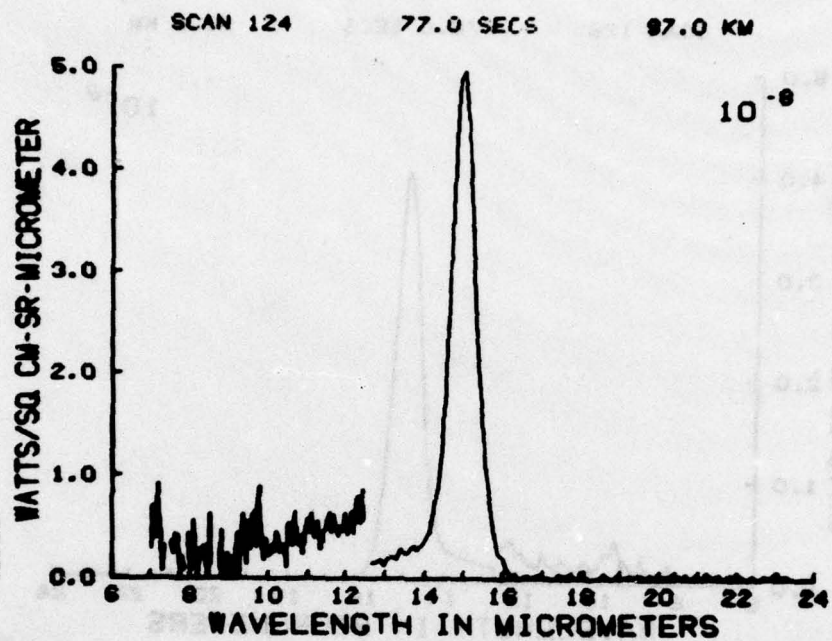


Figure C7

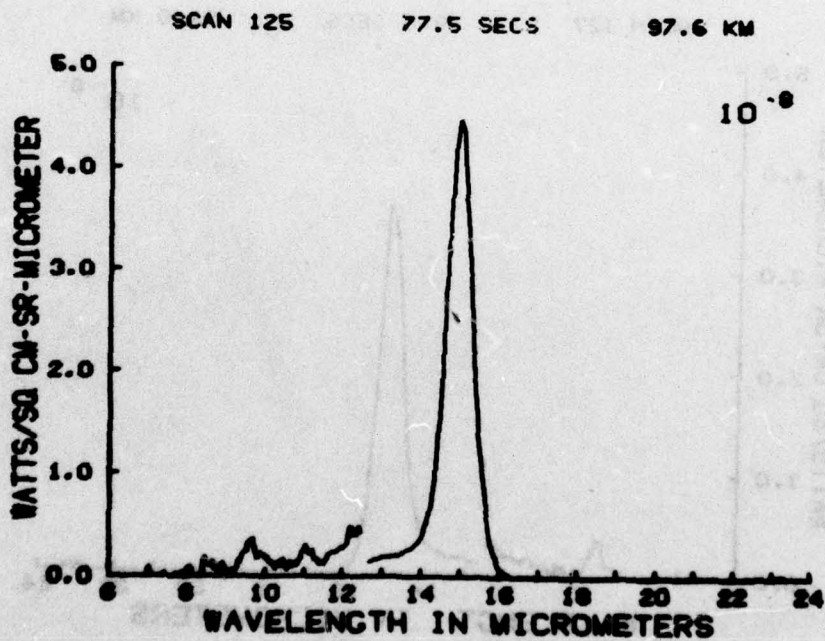


Figure C8

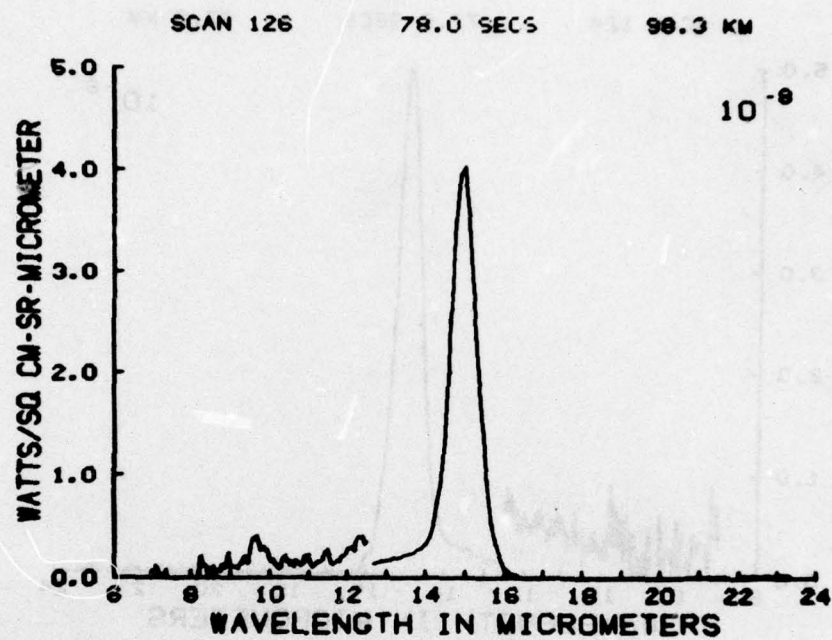


Figure C9

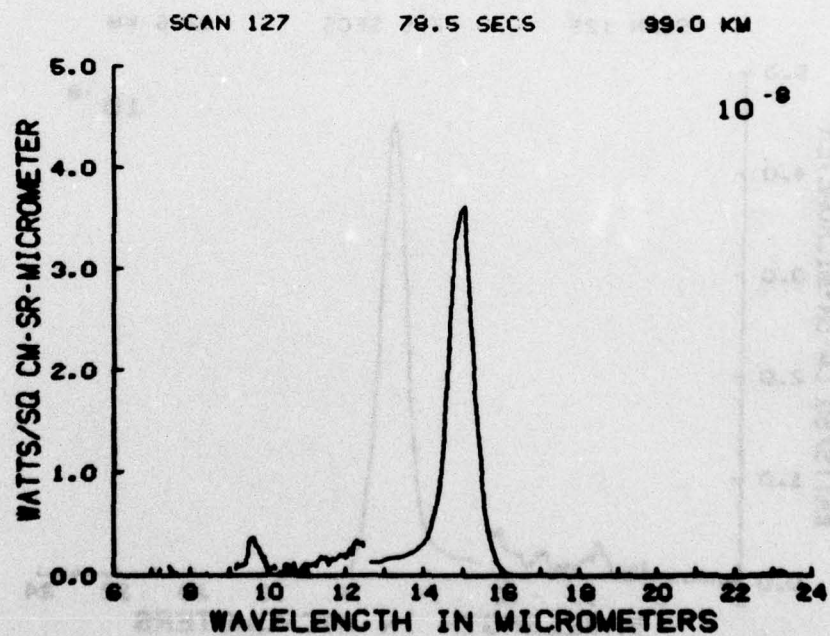


Figure C10



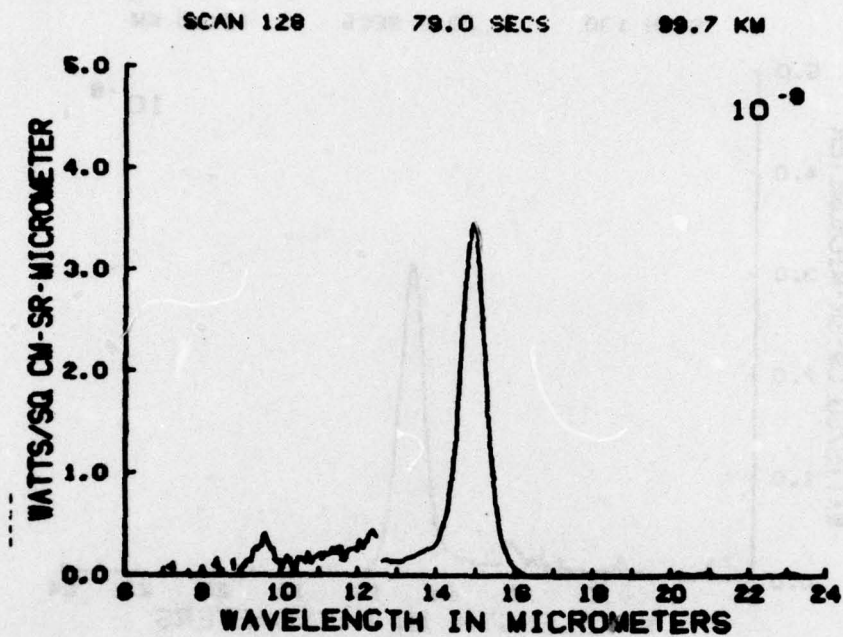


Figure C11

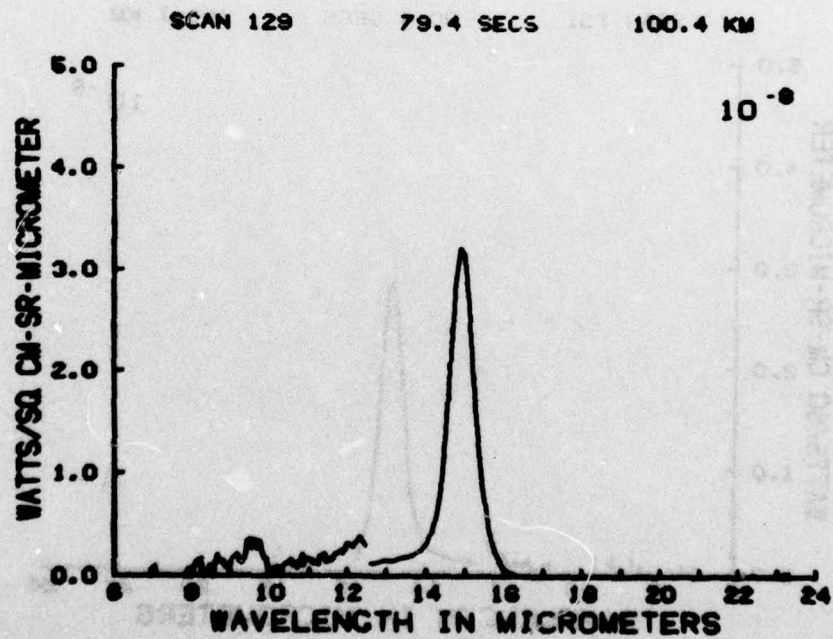


Figure C12

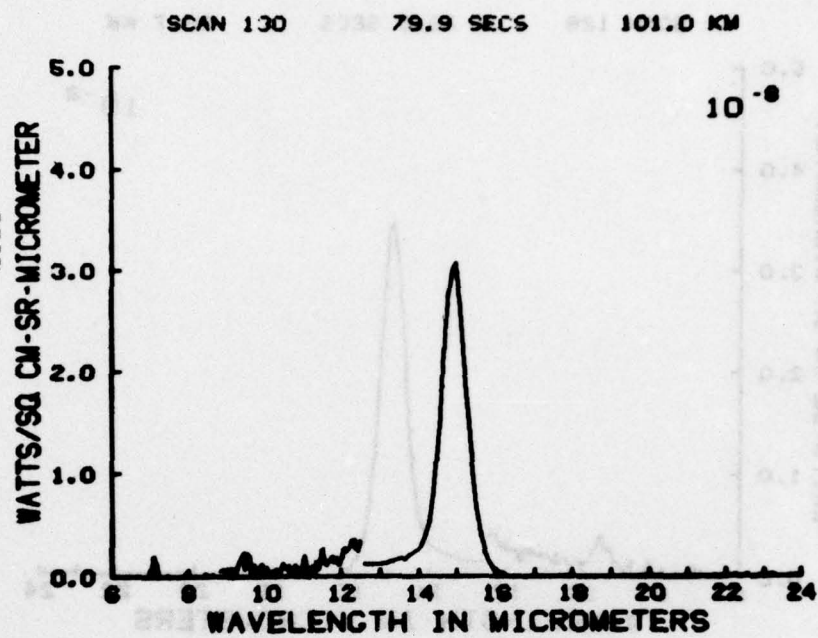


Figure C13

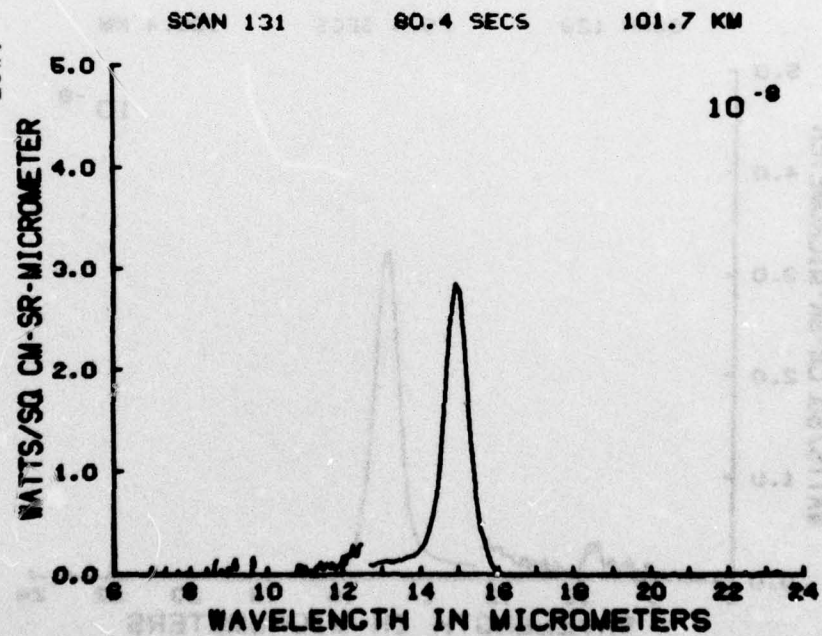


Figure C14



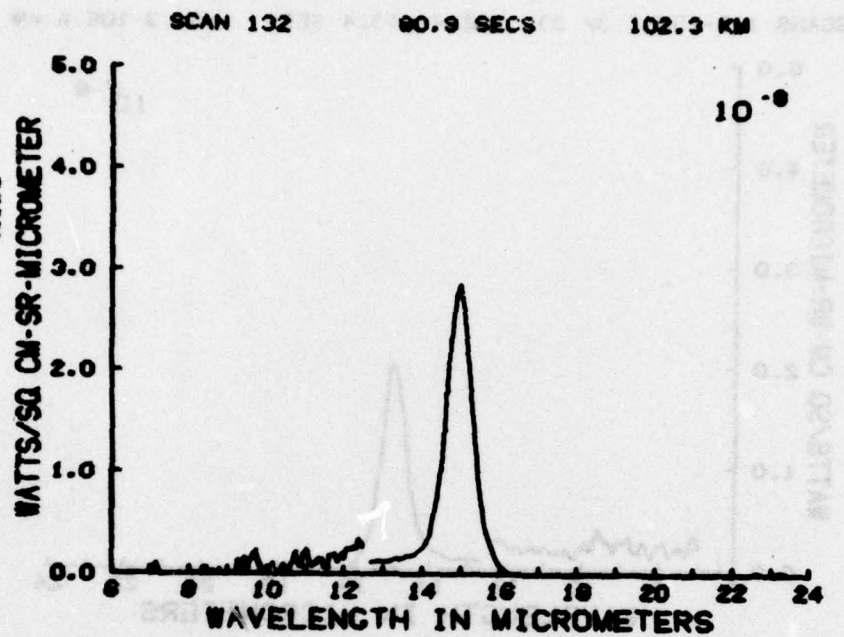


Figure C15

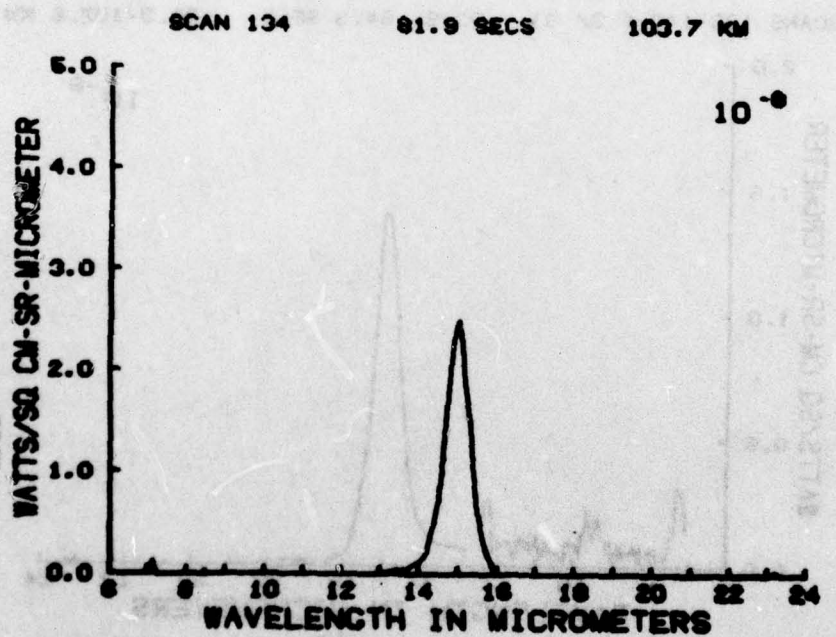


Figure C16

SCANS 135-137 ( 3/ 3) 82.4- 83.4 SECS 104.3-105.6 KM

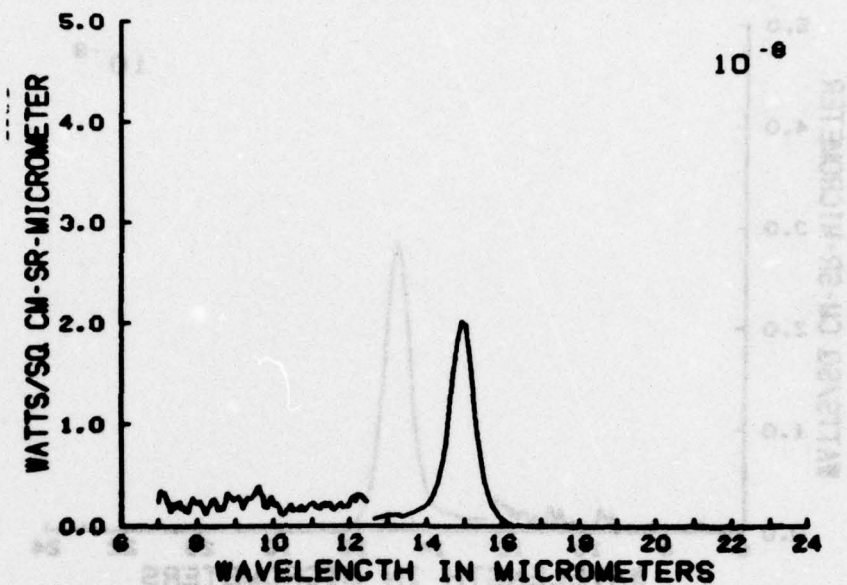


Figure C17

SCANS 138-140 ( 3/ 3) 83.9- 84.9 SECS 106.3-107.6 KM

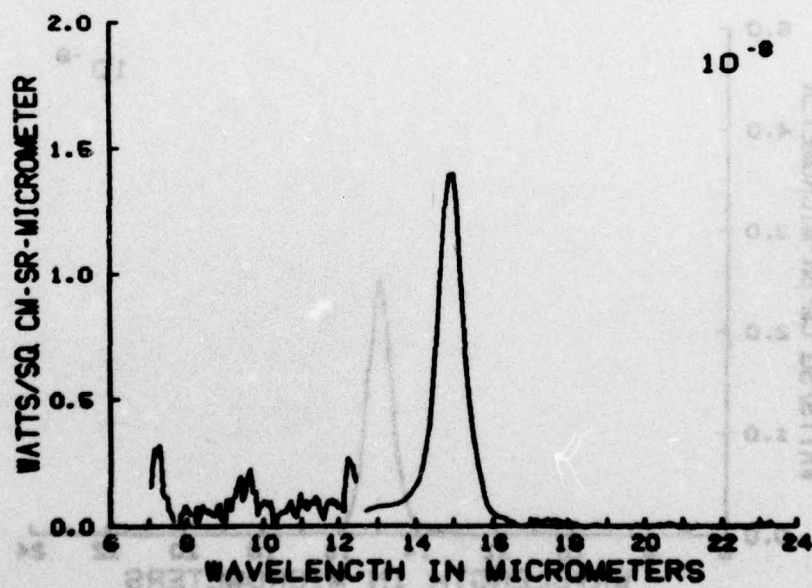


Figure C18



SCANS 141-145 ( 3 / 5 ) 85.4- 87.3 SECS 106.2-110.6 KM

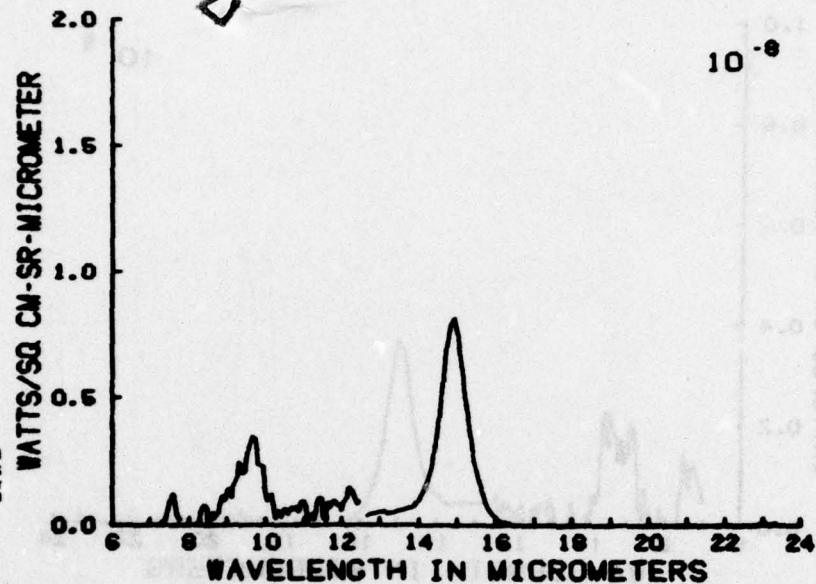
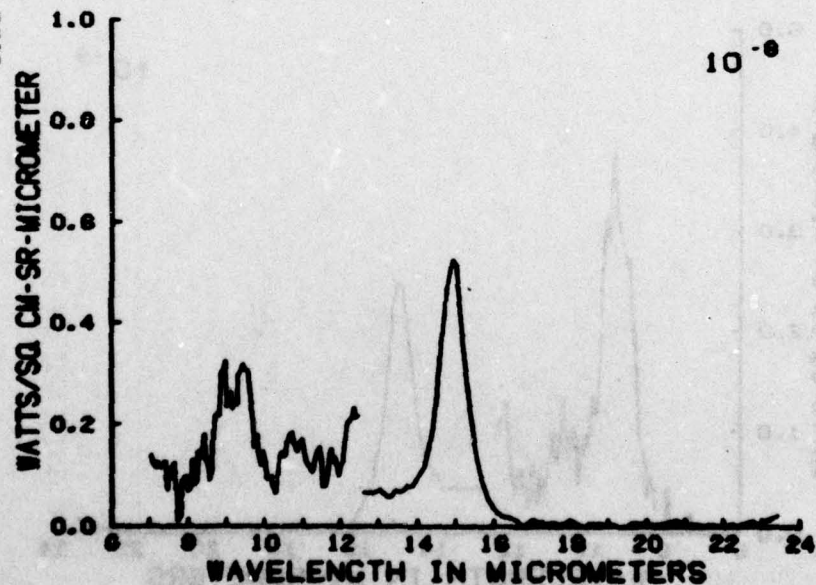


Figure C19

SCANS 146-149 ( 4 / 4 ) 87.8- 89.3 SECS 111.4-113.3 KM



Figurs C20

SCANS 150-152 ( 3/ 3) 89.8- 90.8 SECS 114.0-116.2 KM

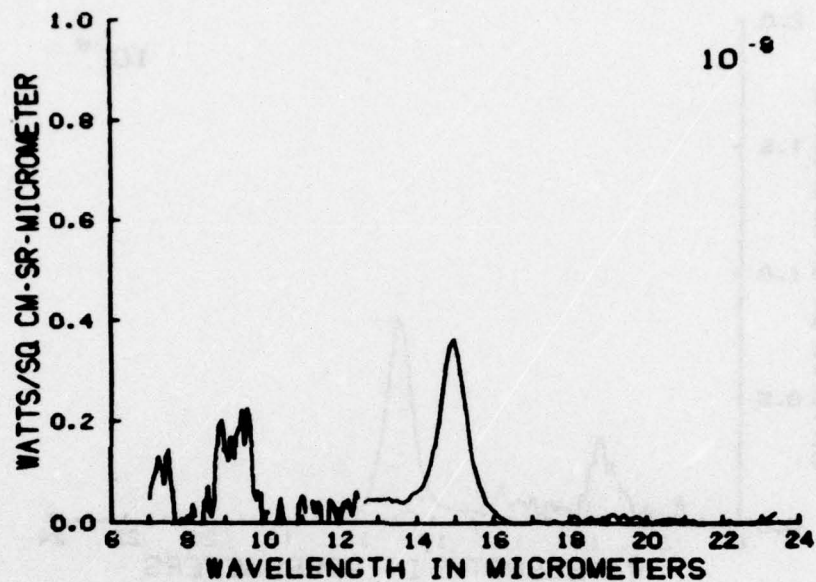


Figure C21

SCANS 154-157 ( 4/ 4) 91.7- 93.2 SECS 116.4-118.2 KM

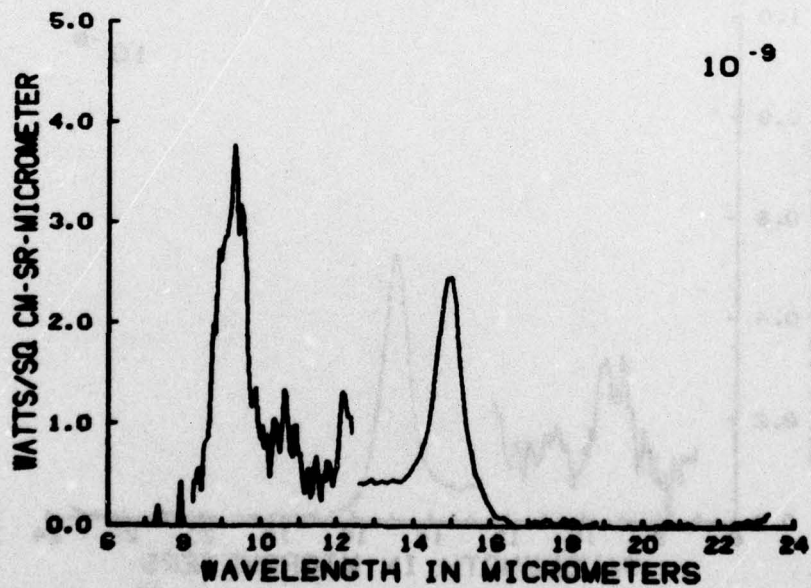


Figure C22



SCANS 158-161 ( 4/ 4 ) 93.7- 95.2 SECS 118.8-120.7 KM

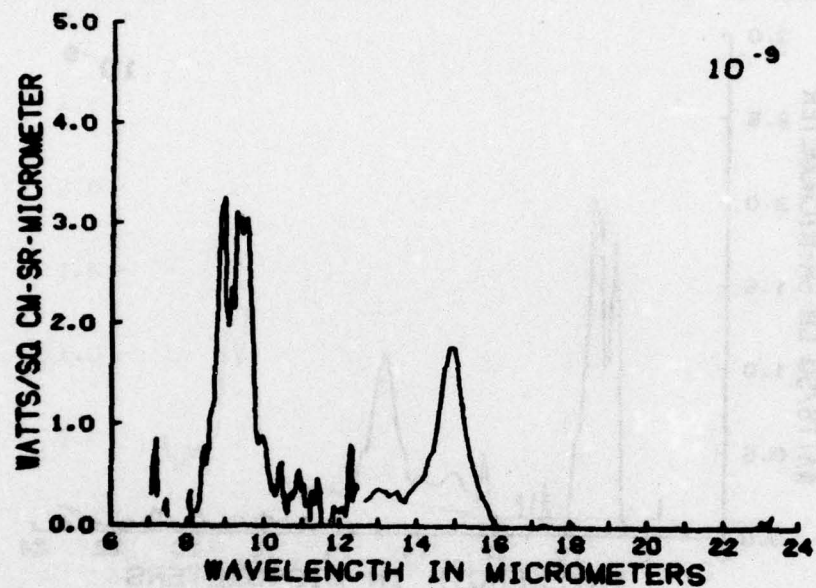


Figure C23

SCANS 162-166 ( 4/ 5 ) 96.7- 97.6 SECS 121.2-123.6 KM

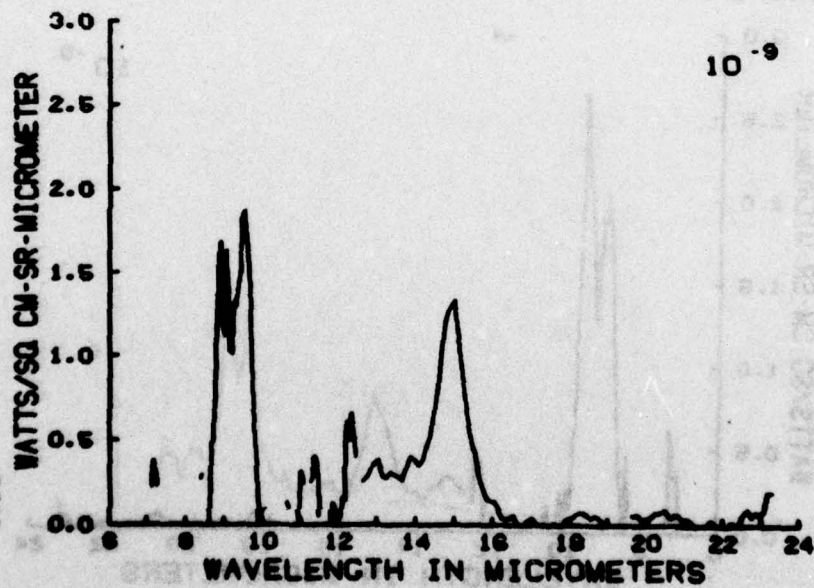


Figure C24

SCANS 167-170 ( 4/ 4) 98.1- 99.6 SECS 124.2-125.9 KM

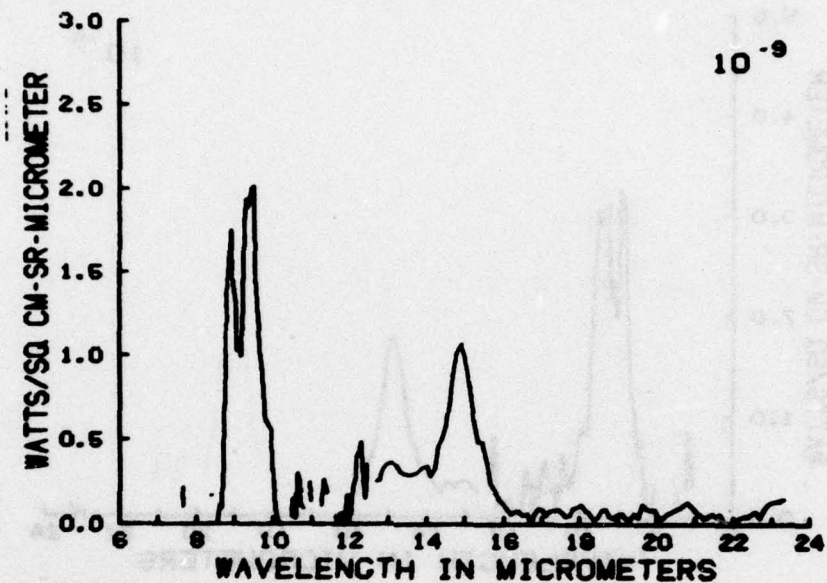


Figure C25

SCANS 171-175 ( 4/ 5) 100.1-102.1 SECS 126.5-128.9 KM

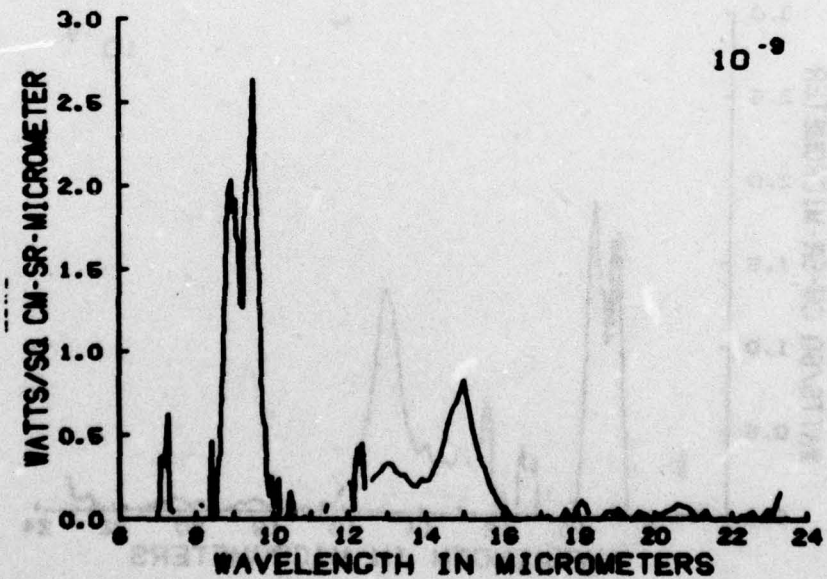


Figure C26

SCANS 176-179 ( 4/ 4) 102.6-104.0 SECS 129.3-131.0 KM

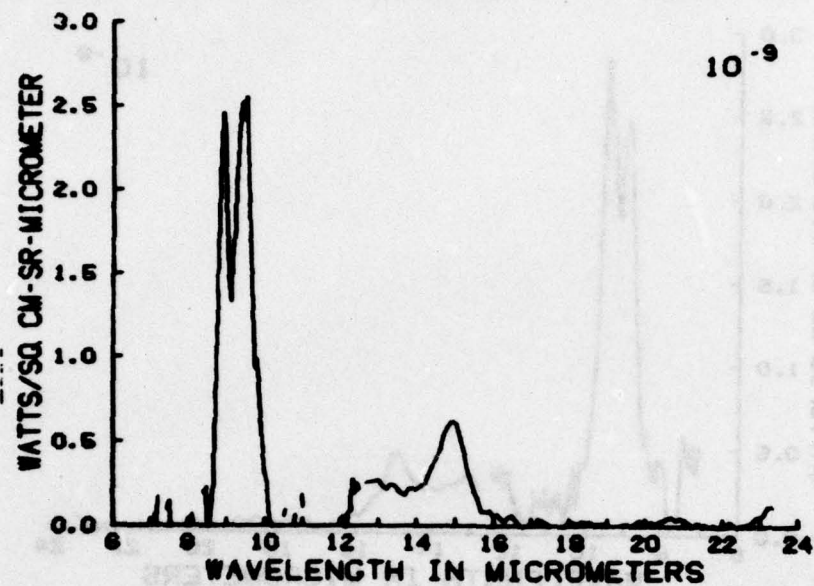


Figure C27

SCANS 180-184 ( 4/ 5) 104.5-106.5 SECS 131.6-133.8 KM

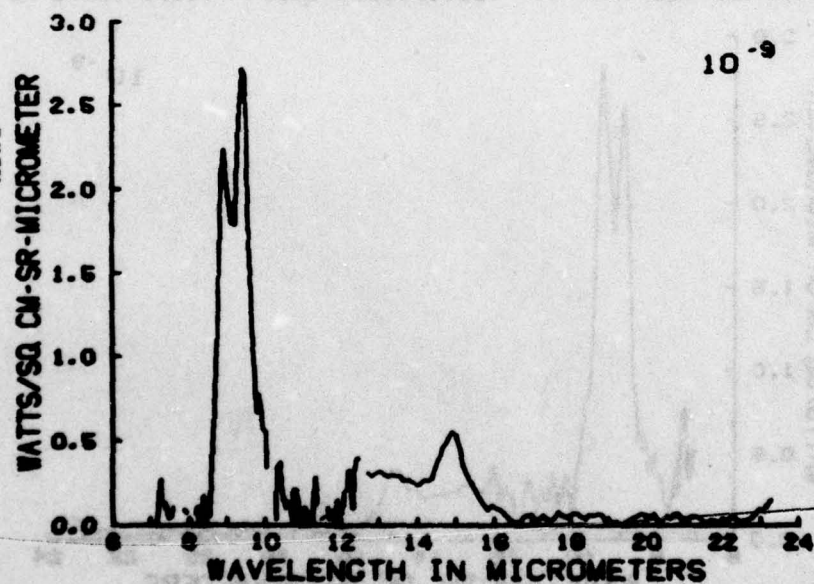


Figure C28



SCANS 185-188 ( 4/ 4 ) 107.0-108.5 SECS 134.3-136.0 KM

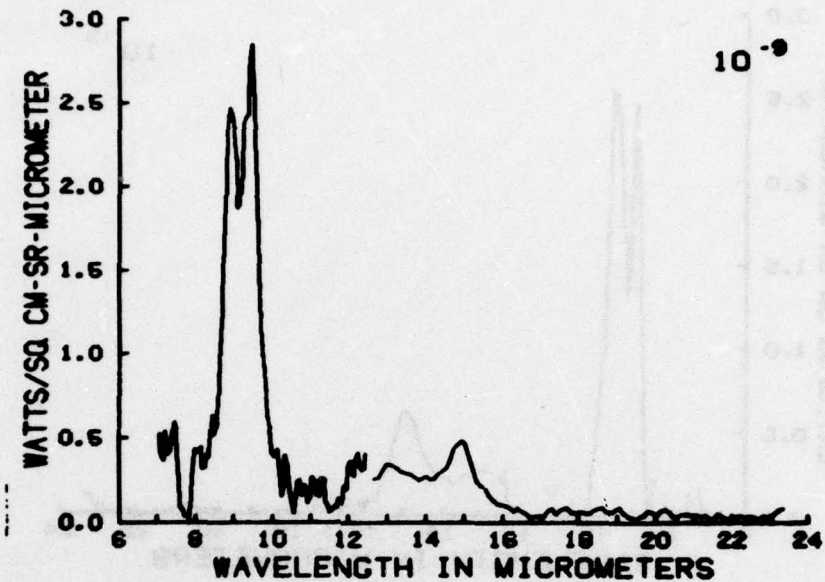


Figure C29

SCANS 189-192 ( 4/ 4 ) 109.0-110.4 SECS 136.5-138.1 KM

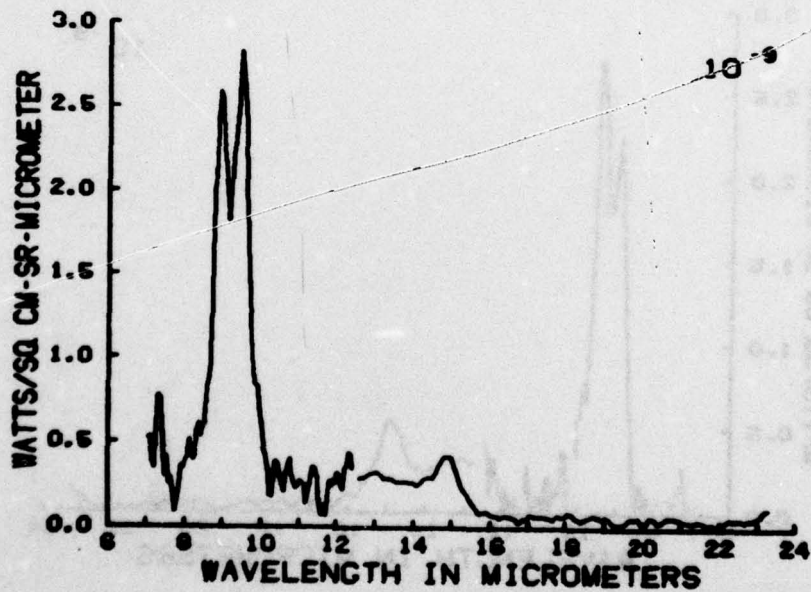


Figure C30

SCANS 194-199 ( 5/ 5) 111.4-113.4 SECS 139.1-141.2 KM

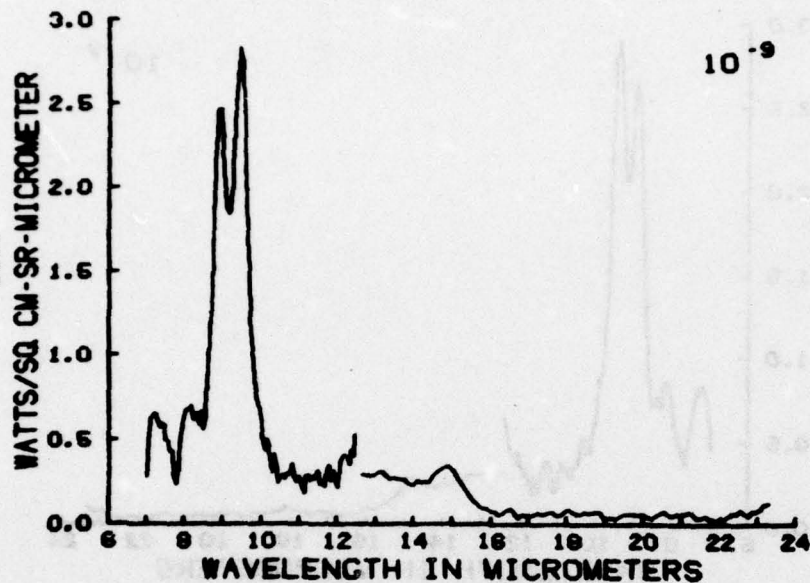


Figure C31

SCANS 199-202 ( 4/ 4) 113.9-115.3 SECS 141.7-143.3 KM

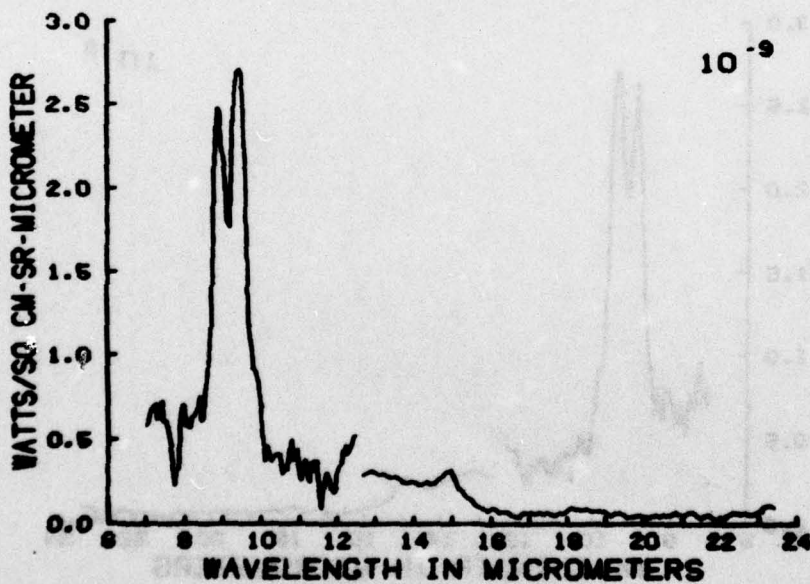


Figure C32

SCANS 204-208 ( 5/ 5) 116.3-118.3 SECS 144.3-146.2 KM

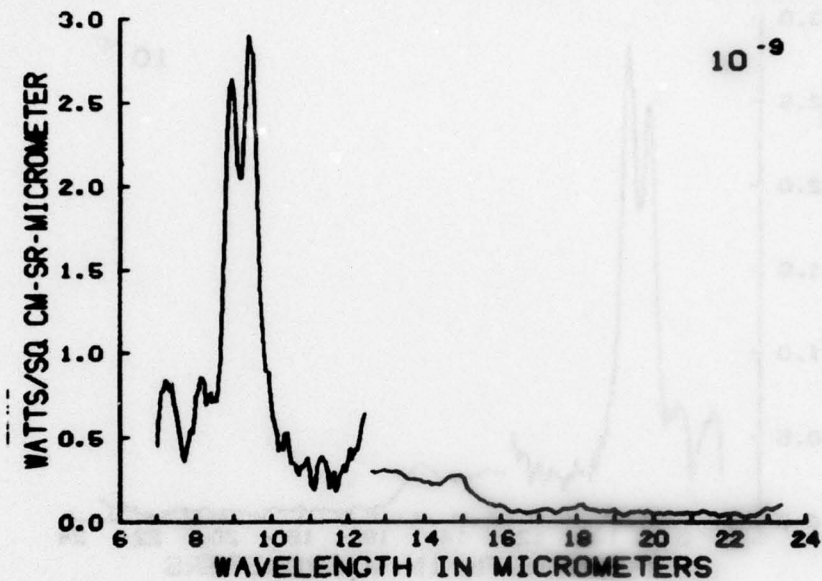


Figure C33

SCANS 209-212 ( 4/ 4) 118.8-120.3 SECS 148.7-148.2 KM

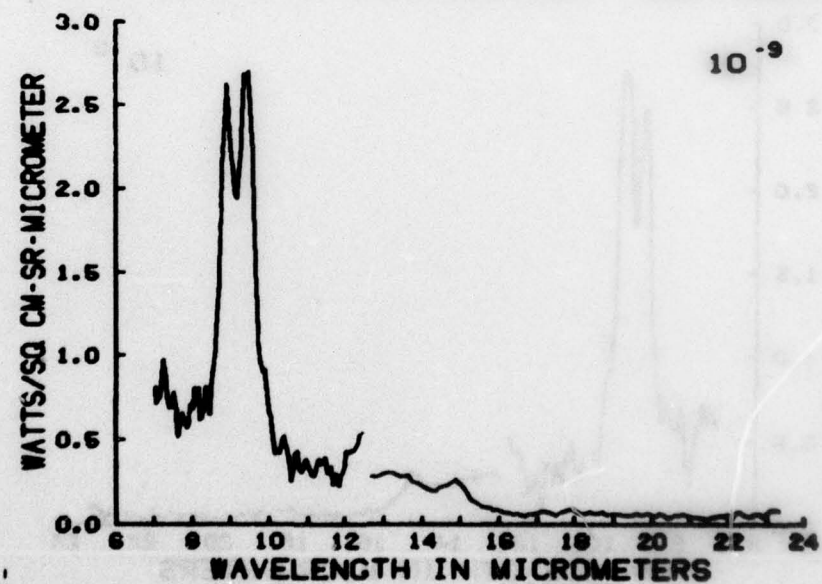


Figure C34



SCANS 214-218 ( 5/ 5) 121.3-123.2 SECS 149.2-151.0 KM

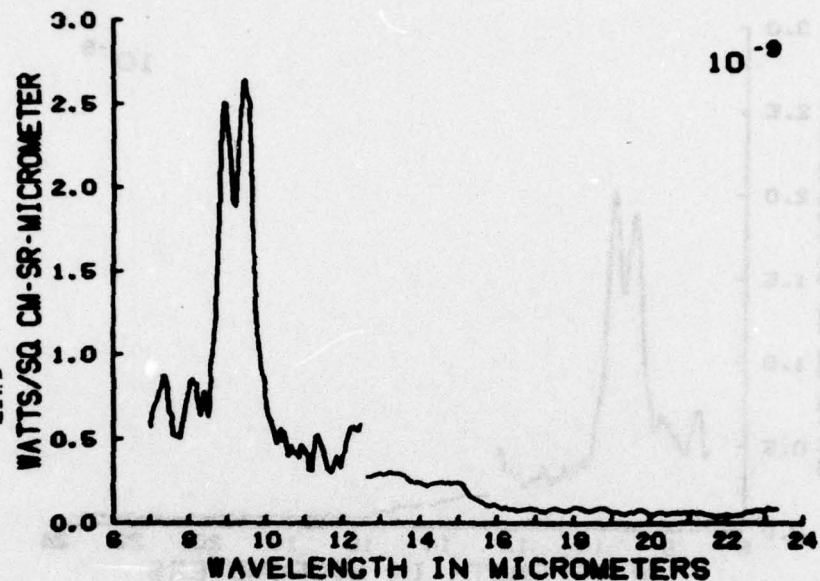


Figure C35

SCANS 219-222 ( 4/ 4) 123.7-125.2 SECS 161.6-162.9 KM

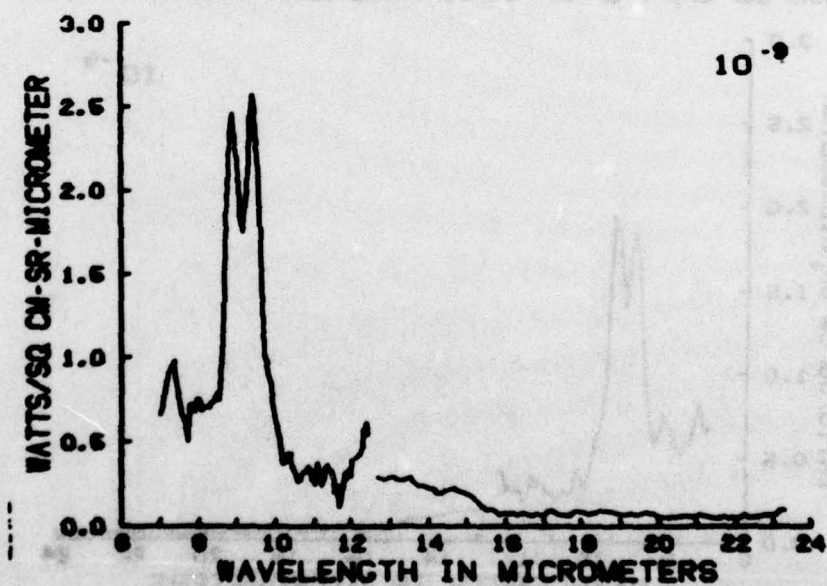


Figure C36

SCANS 258-266 ( 5/ 9) 142.9-146.8 SECS 160.0-171.0 KM

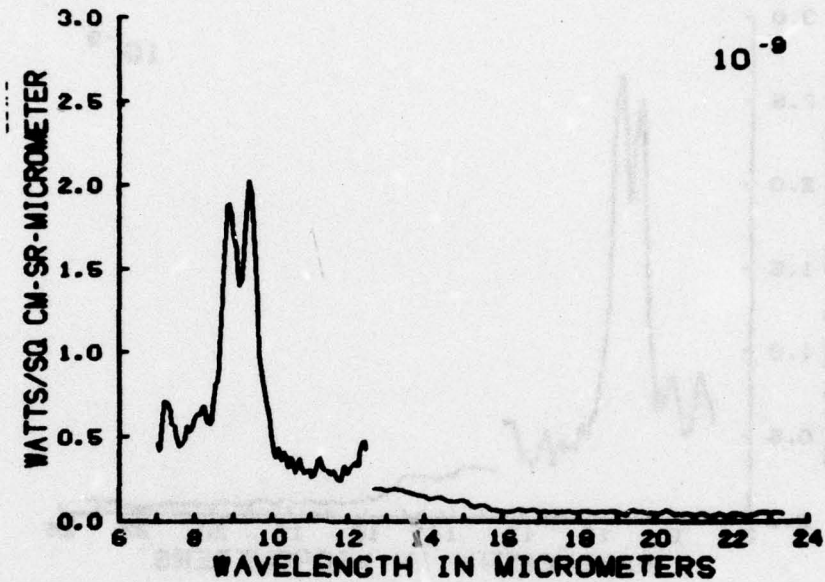


Figure C37

SCANS 267-272 ( 6/ 6) 147.3-149.8 SECS 171.3-173.1 KM

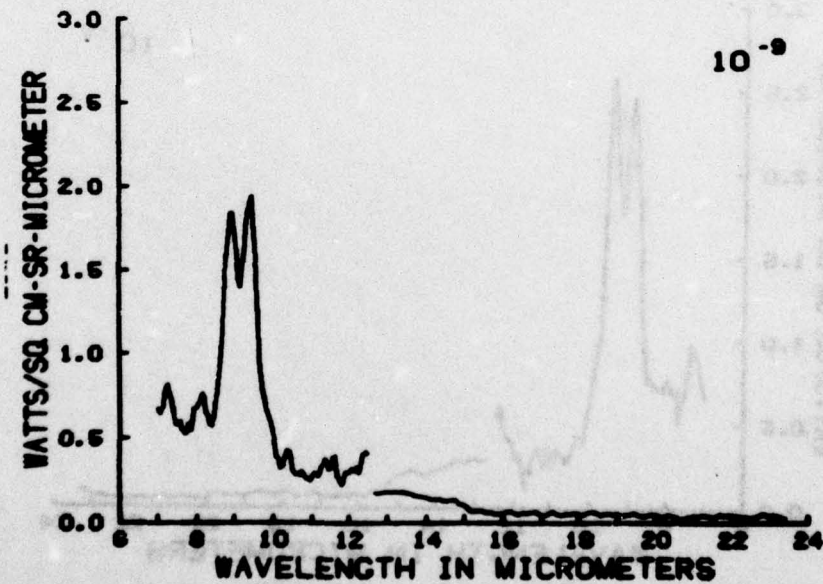


Figure C38

SCANS 274-280 ( 7 / 7 ) 150.8-153.7 SECS 173.8-176.8 KM

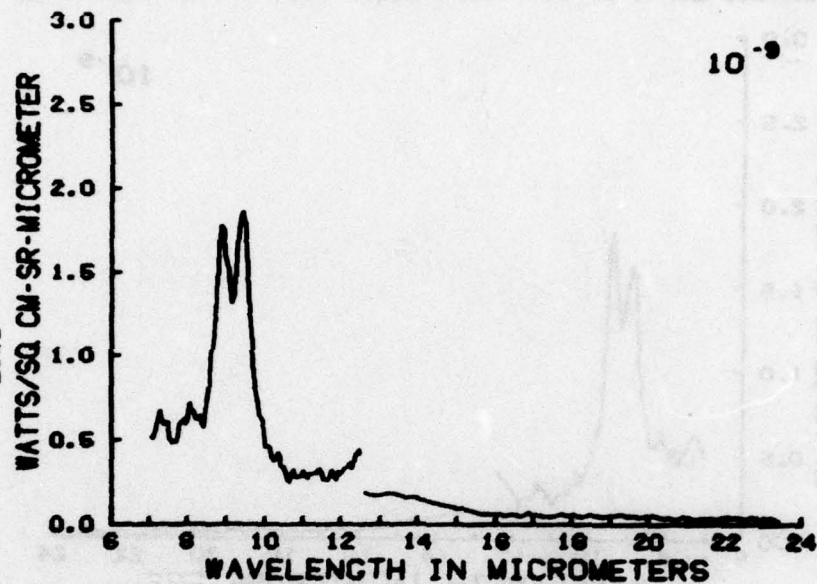


Figure C39

SCANS 291-298 ( 6 / 8 ) 154.2-157.6 SECS 176.2-176.4 KM

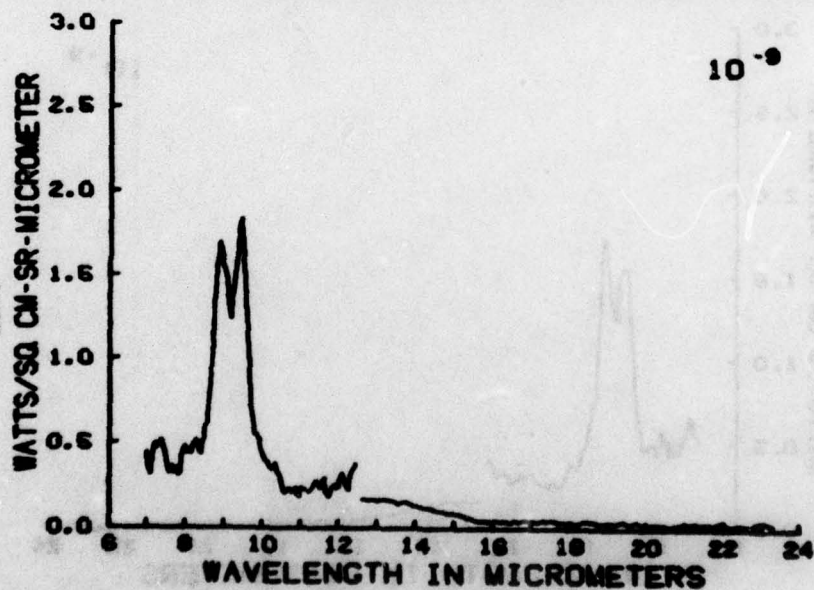


Figure C40



SCANS 289-297 ( 8/ 9) 158.1-162.1 SECS 178.7-181.1 KM

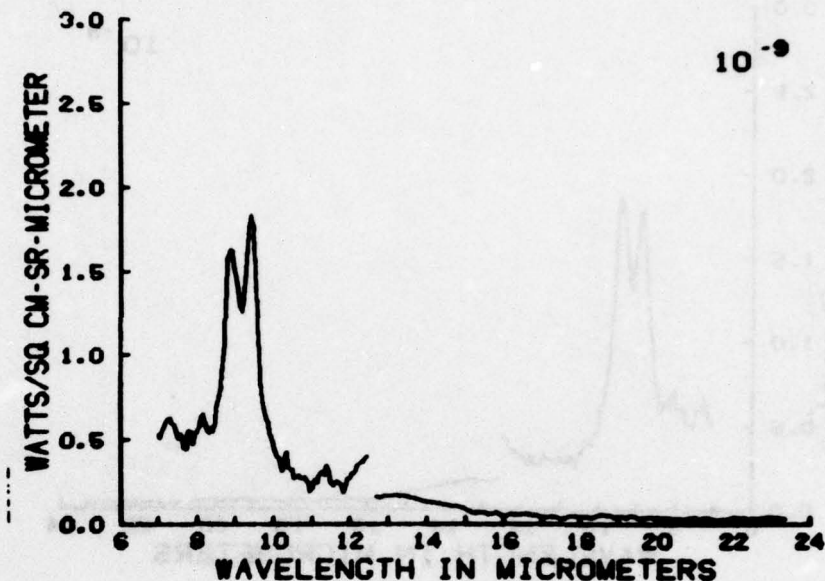


Figure C41

SCANS 298-306 ( 8/ 9) 162.6-166.5 SECS 181.4-183.7 KM

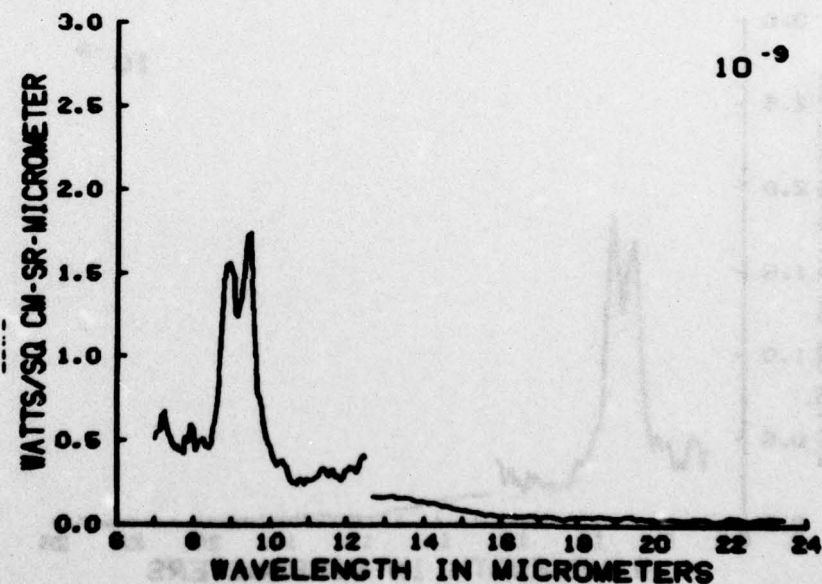


Figure C42

SCANS 307-315 ( 8/ 9) 167.0-170.9 SECS 183.9-186.1 KM

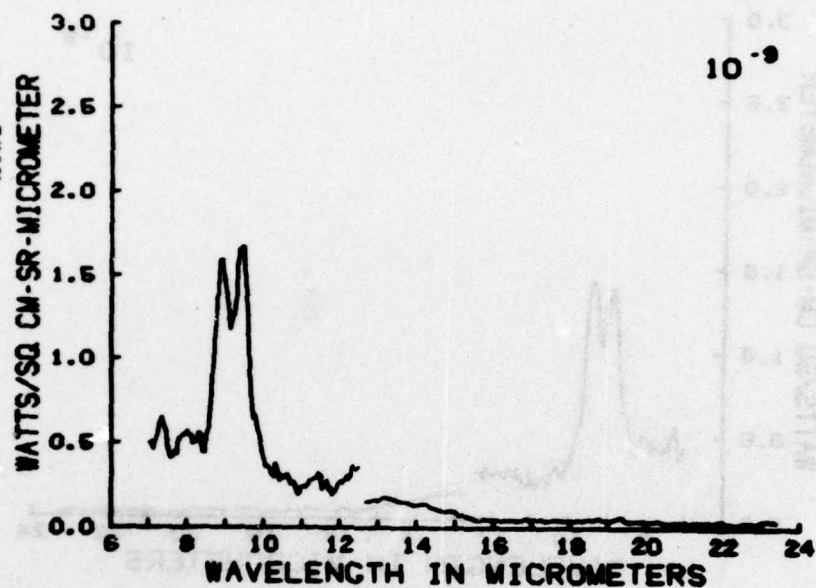


Figure C43

SCANS 316-326 (10/11) 171.4-176.3 SECS 186.3-188.7 KM

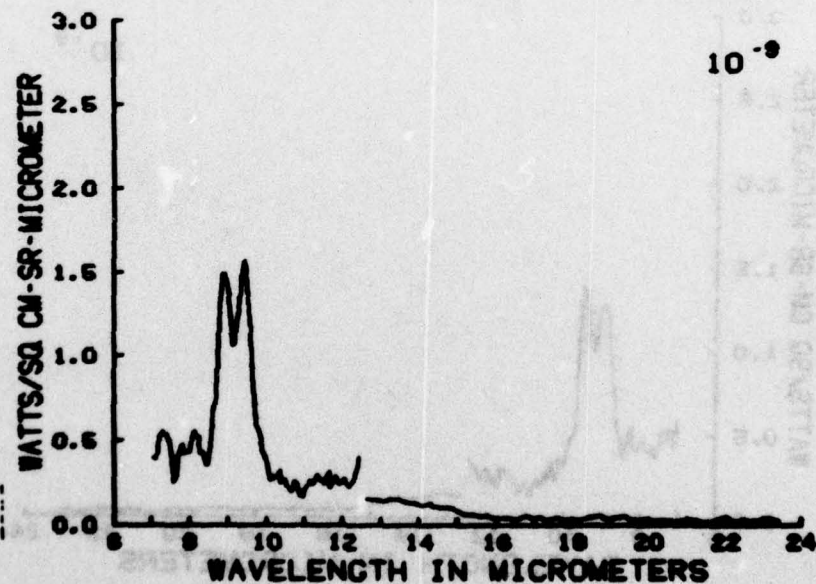


Figure C44

SCANS 327-337 ( 9/11) 176.8-181.7 SECS 188.9-191.1 KM

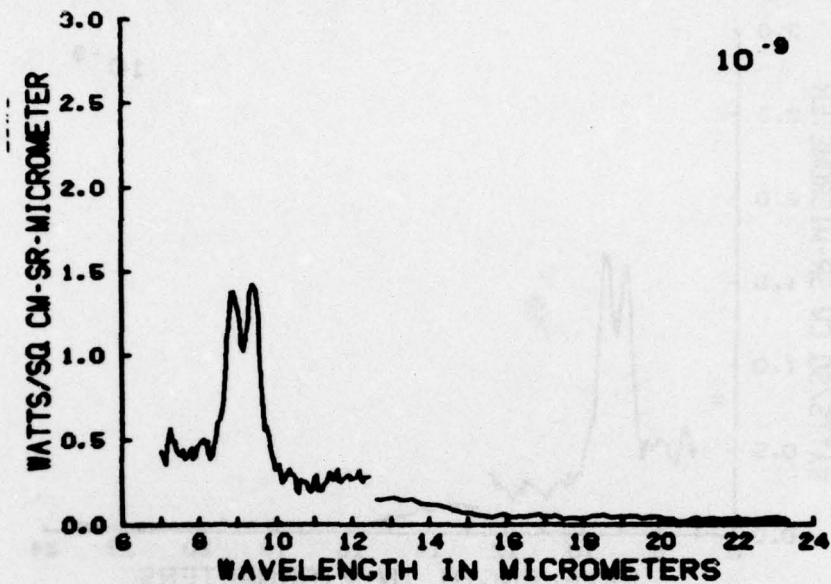


Figure C45

SCANS 338-350 (10/13) 182.2-188.1 SECS 191.3-193.6 KM

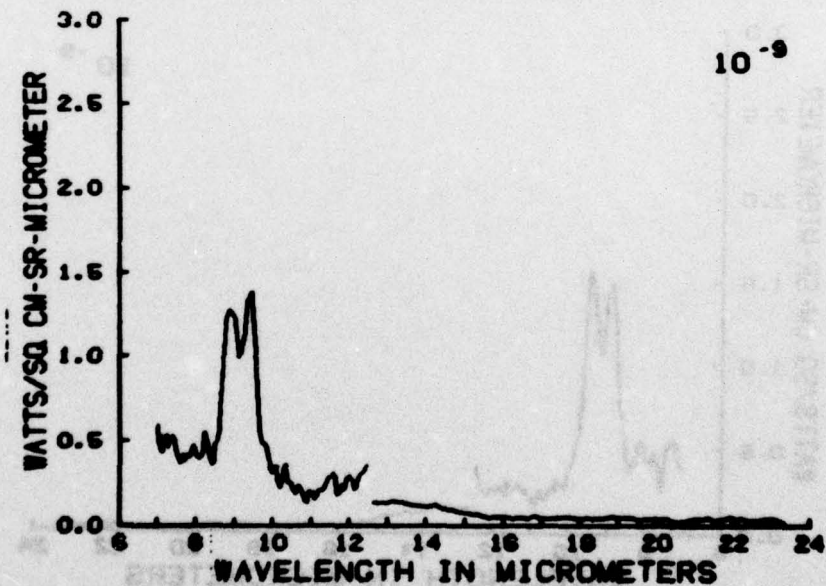


Figure C46



SCANS 351-365 (10/15) 189.6-196.5 SECS 193.7-196.2 KM

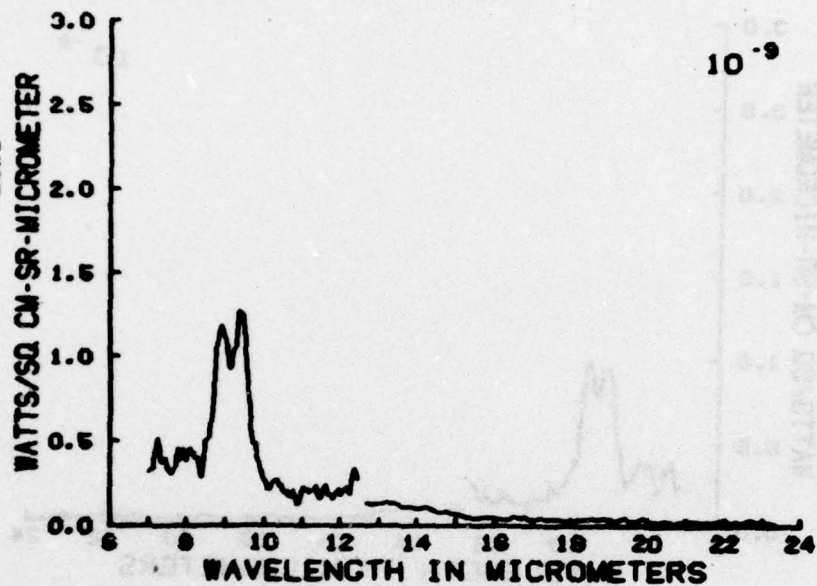


Figure C47

SCANS 387-397 (17/21) 197.5-207.3 SECS 196.5-199.7 KM

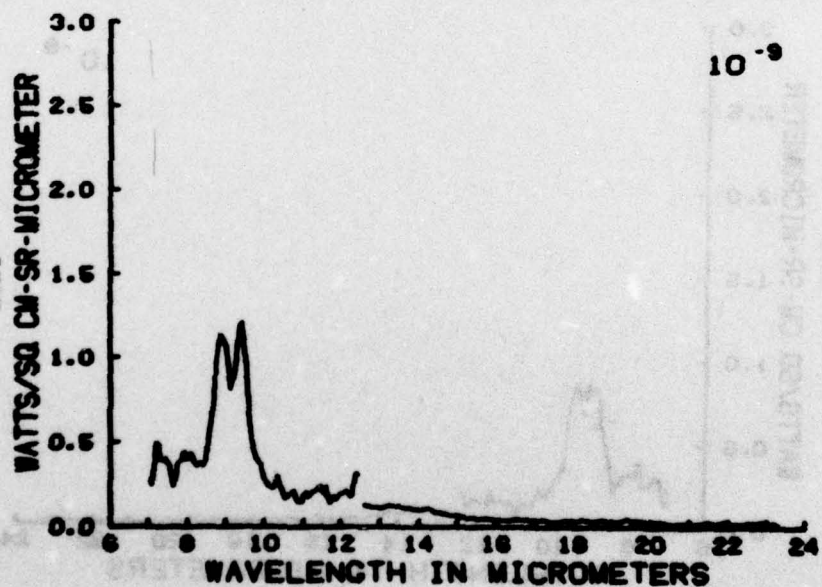


Figure C48

SCANS 388-427 (36/40) 207.8-227.0 SECS 198.8-200.6 KM

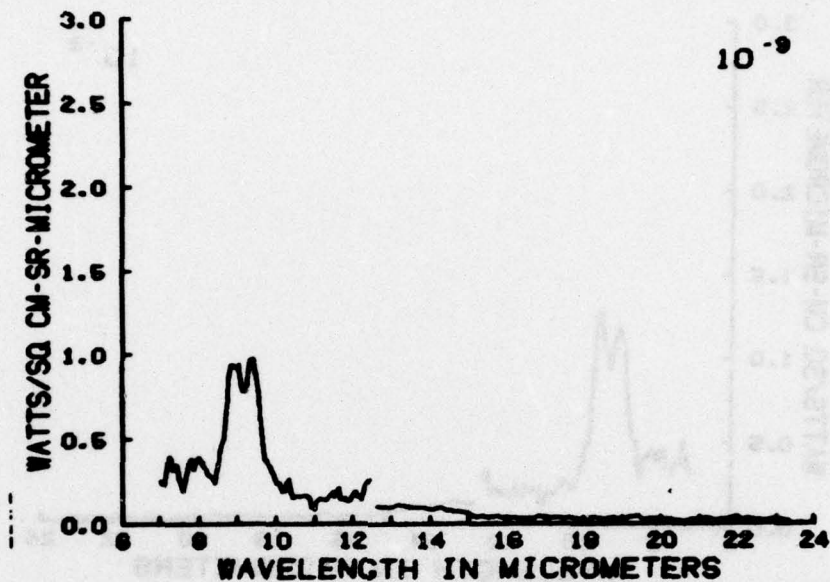


Figure C49

SCANS 428-468 (36/41) 227.5-247.2 SECS 200.6-198.8 KM

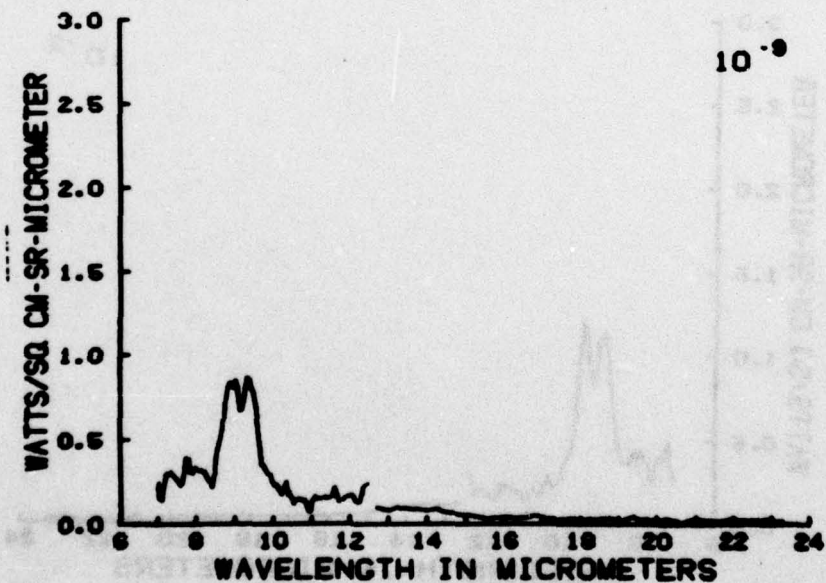


Figure C50

SCANS 469-490 (20/22) 247.6-258.0 SECS 198.7-196.4 KM

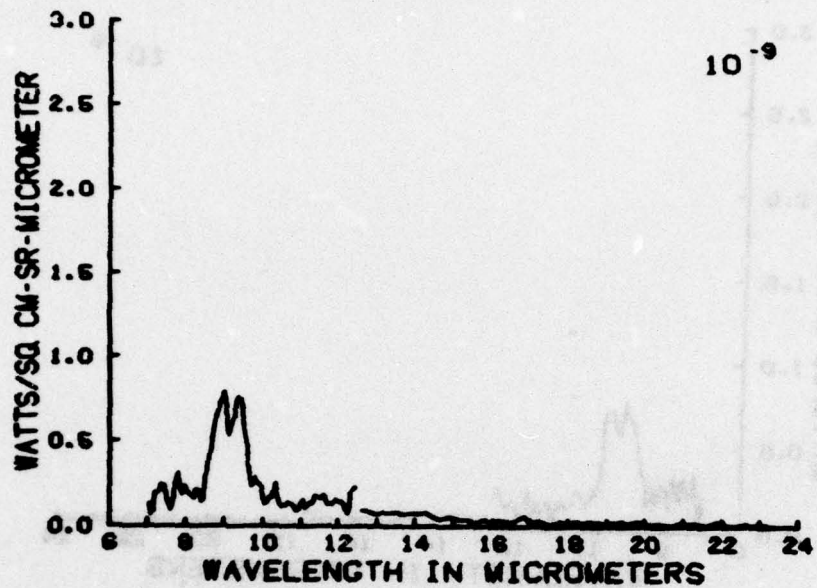


Figure C51

SCANS 492-506 (14/15) 259.0-266.4 SECS 196.1-193.8 KM

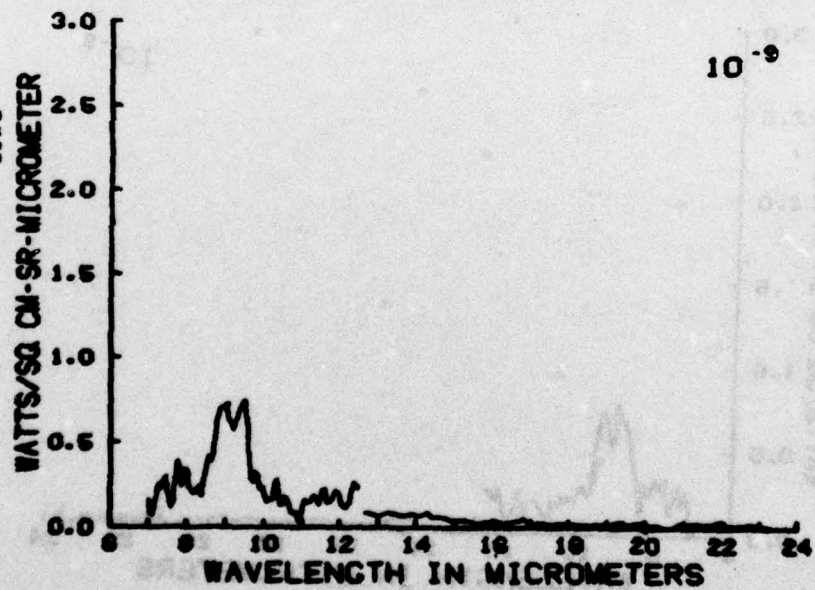


Figure C52



SCANS 507-519 (11/13) 266.8-272.8 SECS 193.6-191.3 KM

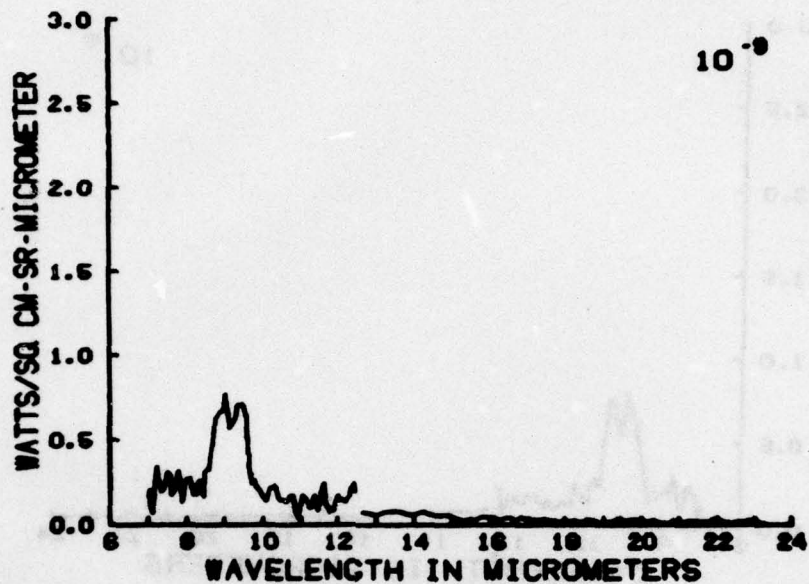


Figure C53

SCANS 521-529 ( 9/ 9) 273.7-277.7 SECS 190.9-188.2 KM

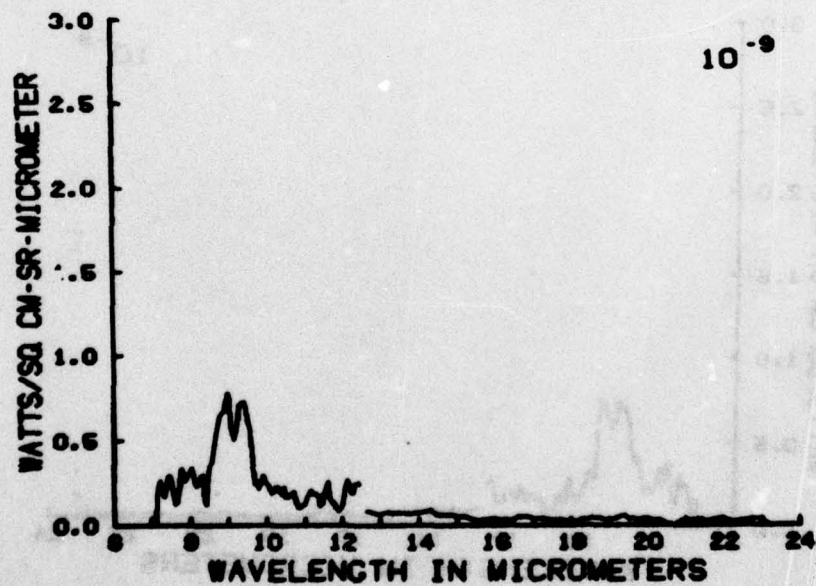


Figure C54

SCANS 531-541 (10/11) 279.7-283.6 SECS 106.7-106.4 KM

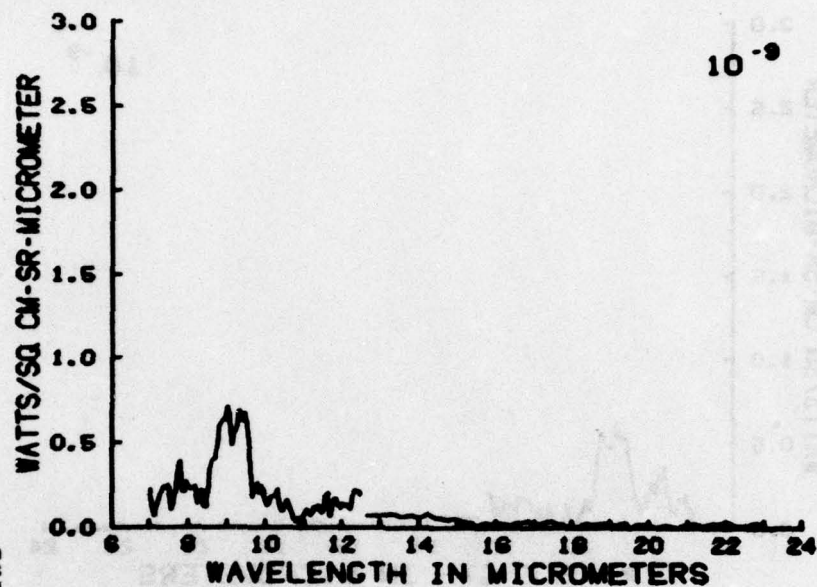


Figure C55

SCANS 542-549 ( 8/ 8) 284.1-287.5 SECS 106.1-104.3 KM

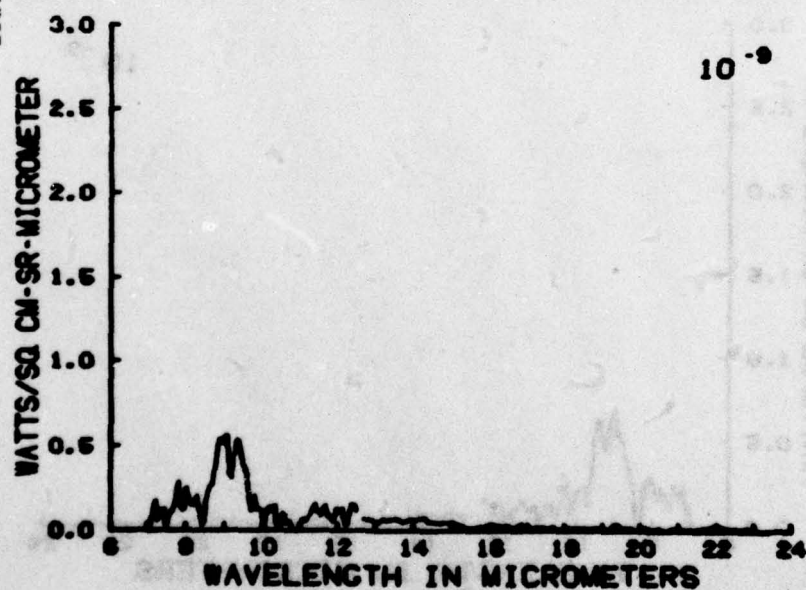


Figure C56

SCANS 551-559 ( 9/ 9) 288.5-292.4 SECS 183.7-181.5 KM

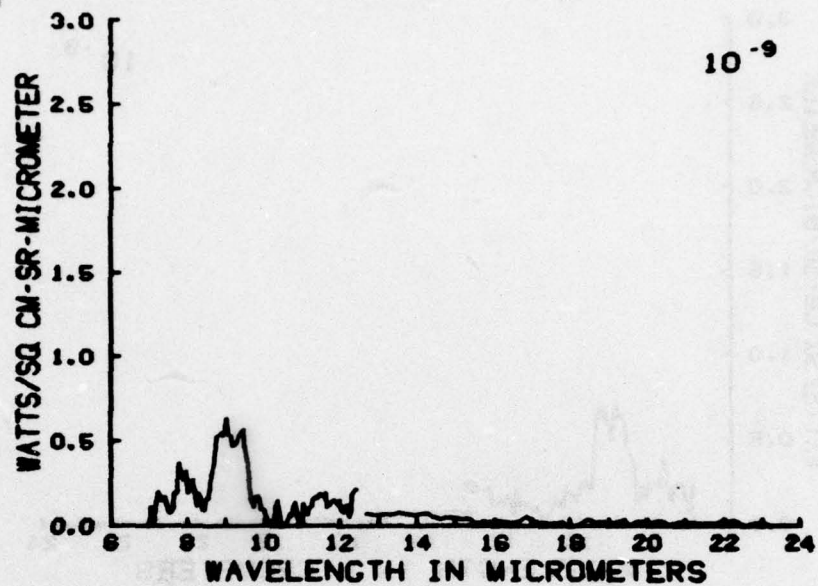


Figure C57

SCANS 561-569 ( 8/ 8) 293.4-296.9 SECS 180.9-178.8 KM

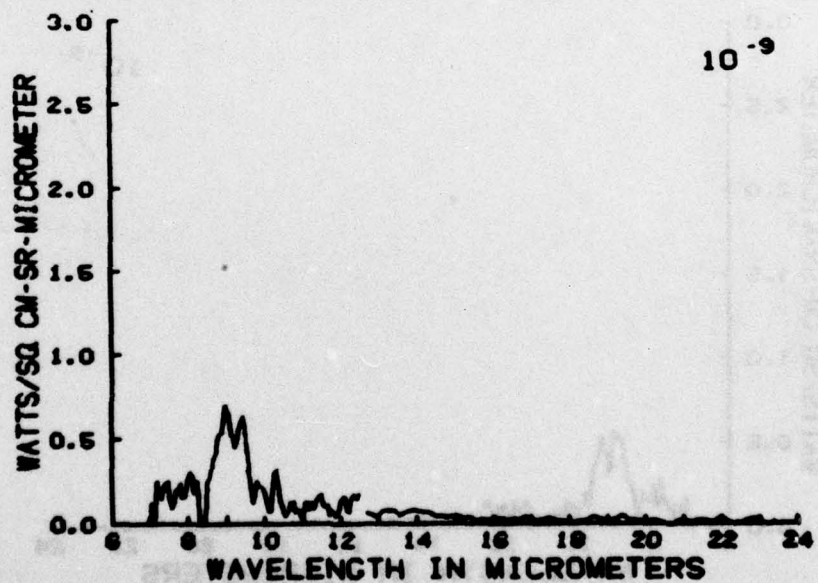


Figure C58



SCANS 569-576 ( 7 / 8 ) 297.3-300.8 SECS 176.5-176.3 KM

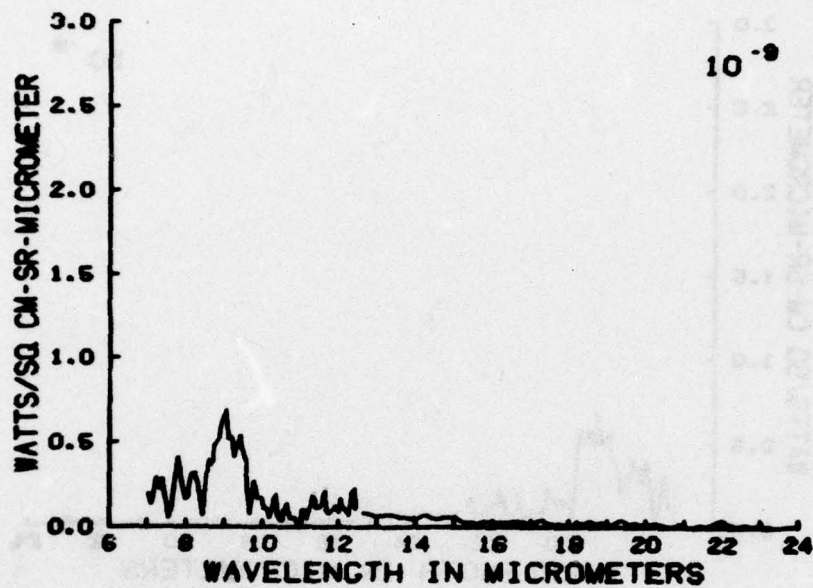


Figure C59

SCANS 577-584 ( 7 / 8 ) 301.3-304.7 SECS 176.0-174.0 KM

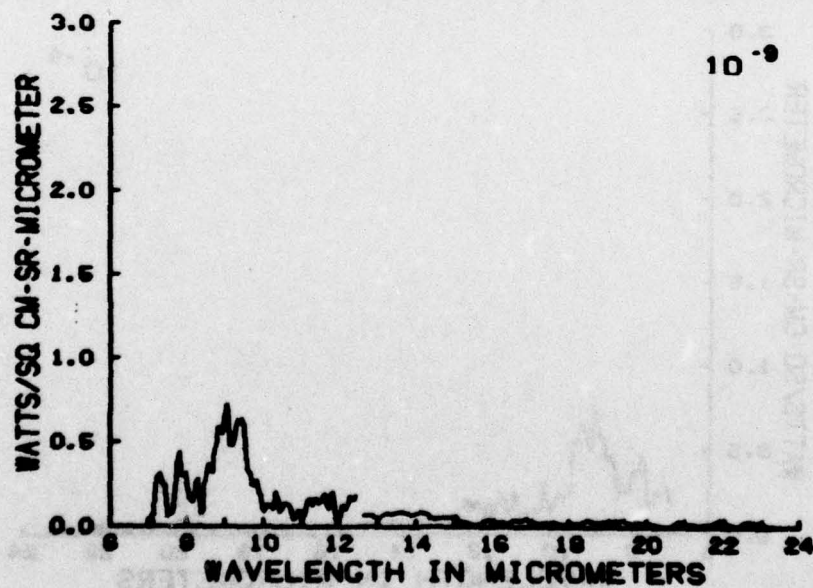


Figure C60

SCANS 585-591 ( 6/ 7) 305.2-308.2 SECS 173.7-171.3 KM

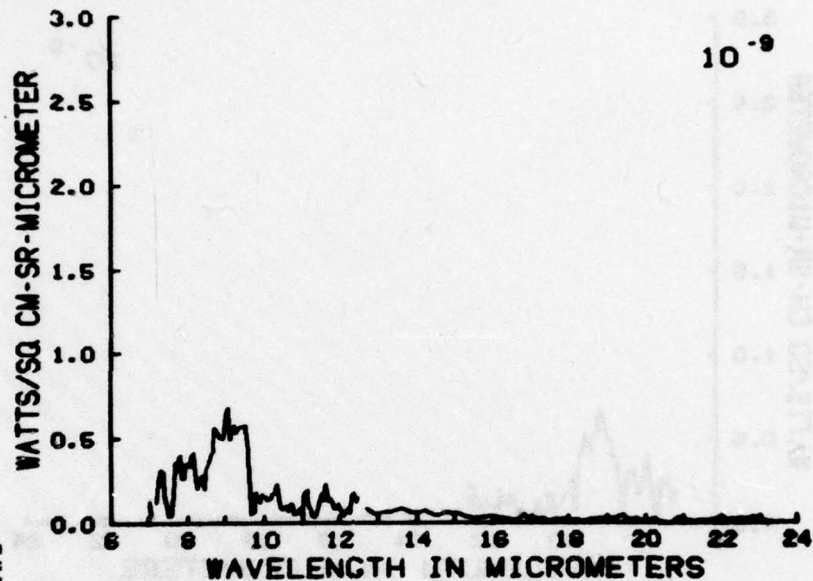


Figure C61

SCANS 592-597 ( 6/ 6) 308.7-311.1 SECS 170.9-168.9 KM

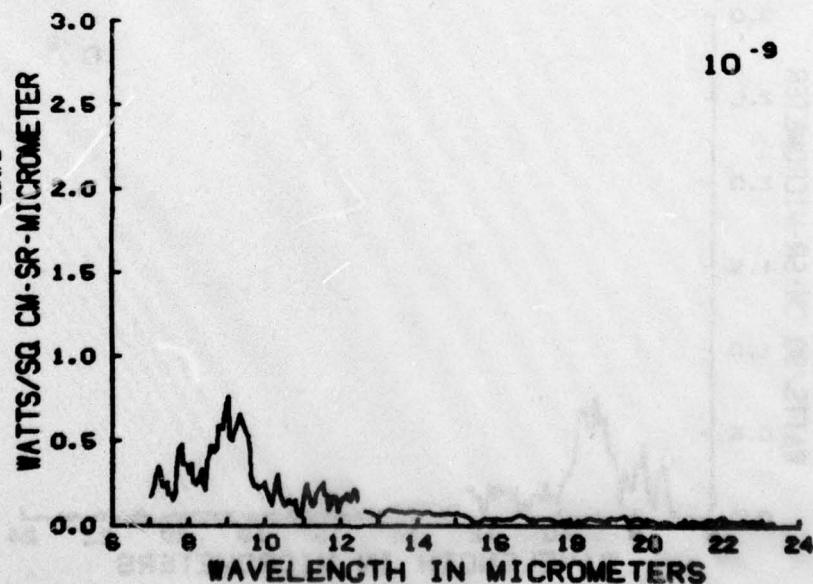


Figure C62

SCANS 598-603 ( 5/ 6 ) 311.6-314.1 SECS 168.5-166.6 KM

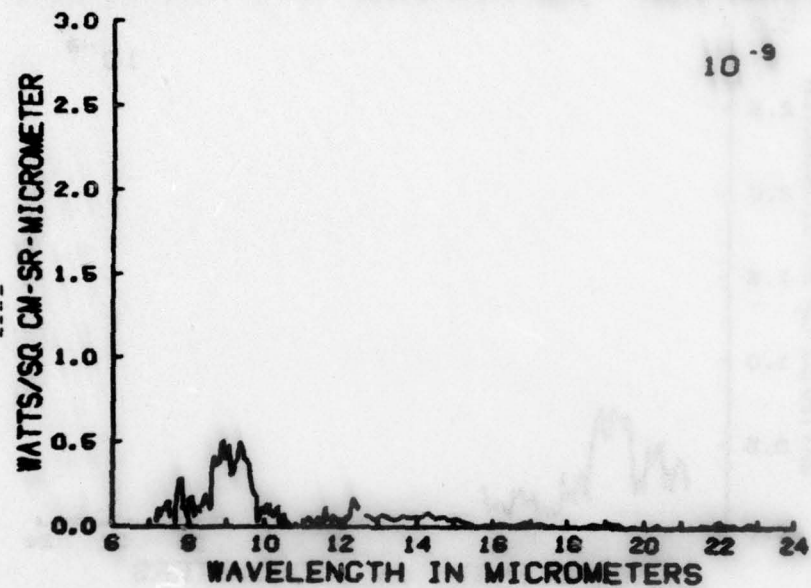


Figure C63

SCANS 604-609 ( 6/ 6 ) 314.6-317.0 SECS 166.2-164.3 KM

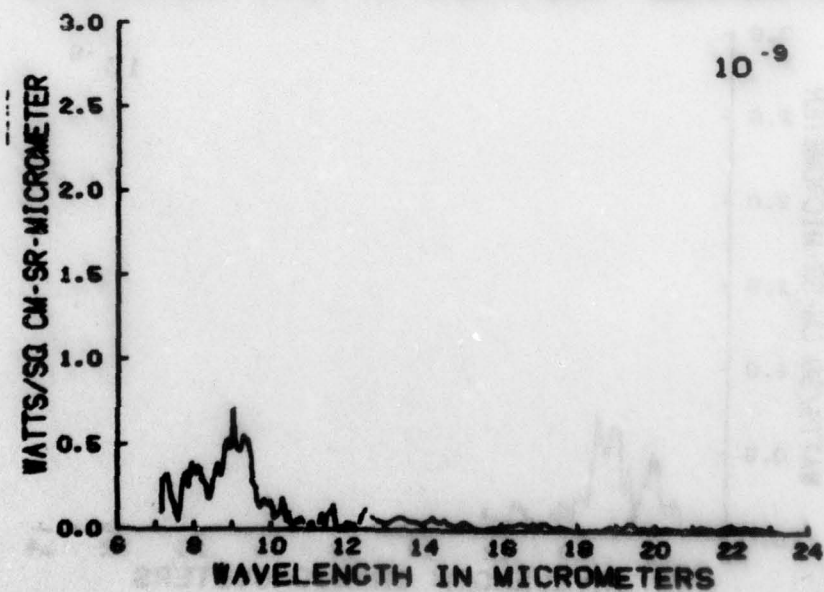


Figure C64



SCANS 611-616 ( 6/ 6 ) 319.0-320.5 SECS 163.6-161.4 KM

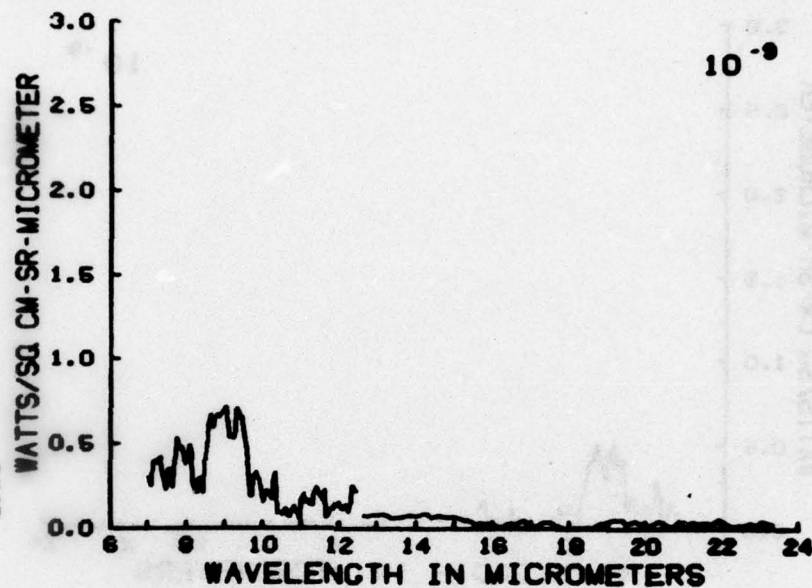


Figure C65

SCANS 617-622 ( 5/ 6 ) 321.0-323.4 SECS 161.0-160.9 KM

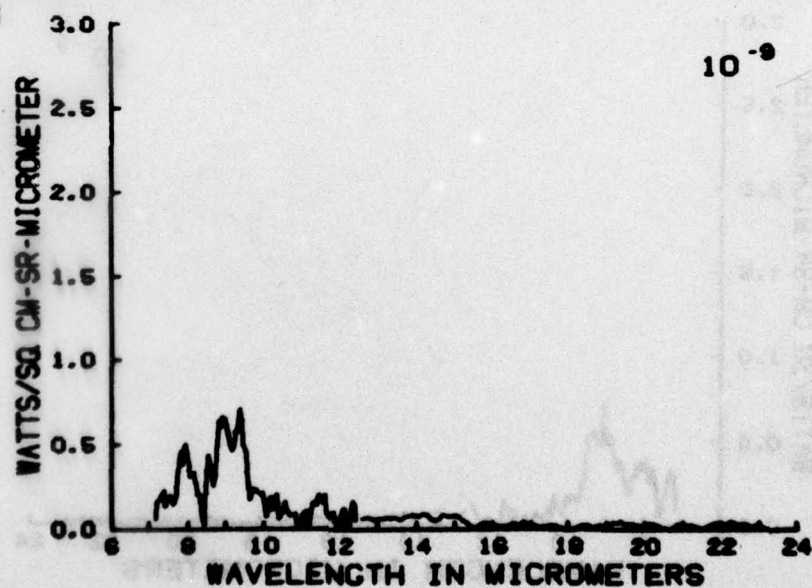


Figure C66

SCANS 623-628 ( 6/ 6 ) 323.9-326.4 SECS 158.5-156.3 KM

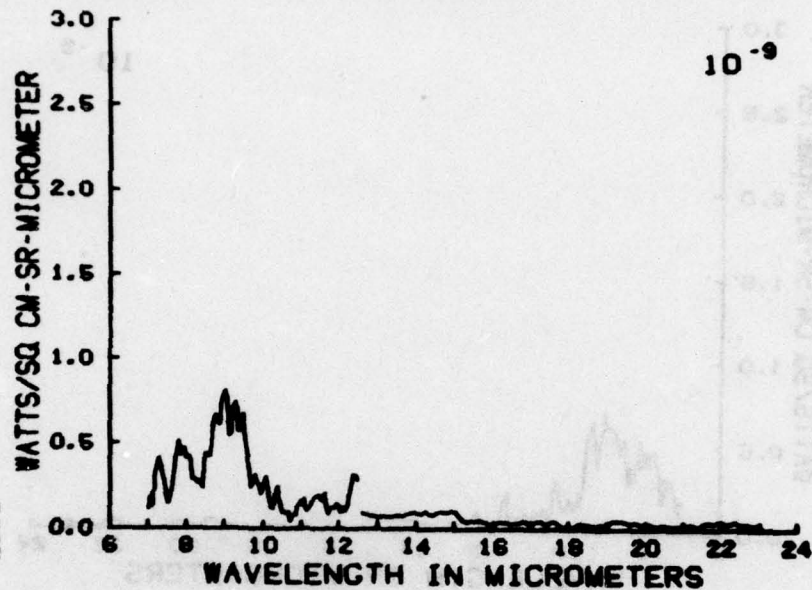


Figure C67

SCANS 629-634 ( 5/ 6 ) 326.9-329.3 SECS 155.8-153.6 KM

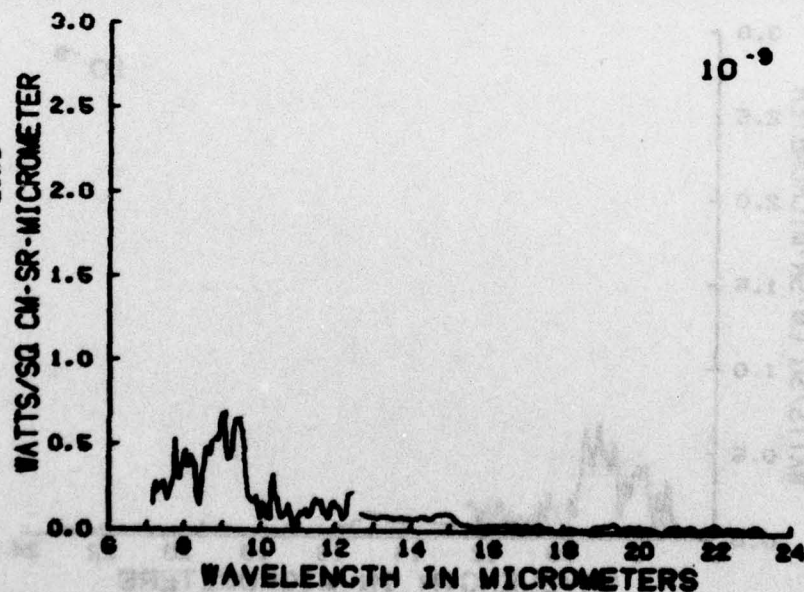


Figure C68

SCANS 636-639 ( 5/ 5) 329.8-331.8 SECS 153.2-151.3 KM

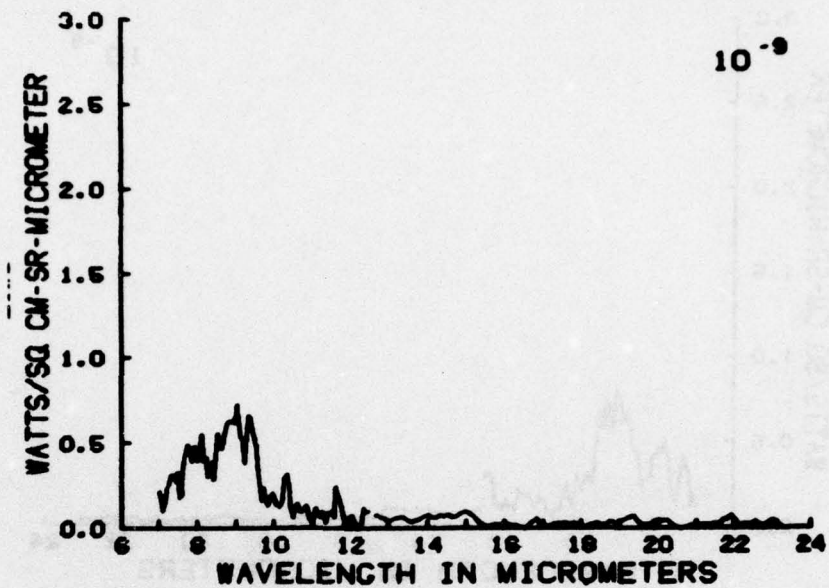


Figure C69

SCANS 641-644 ( 4/ 4) 332.8-334.2 SECS 150.4-149.0 KM

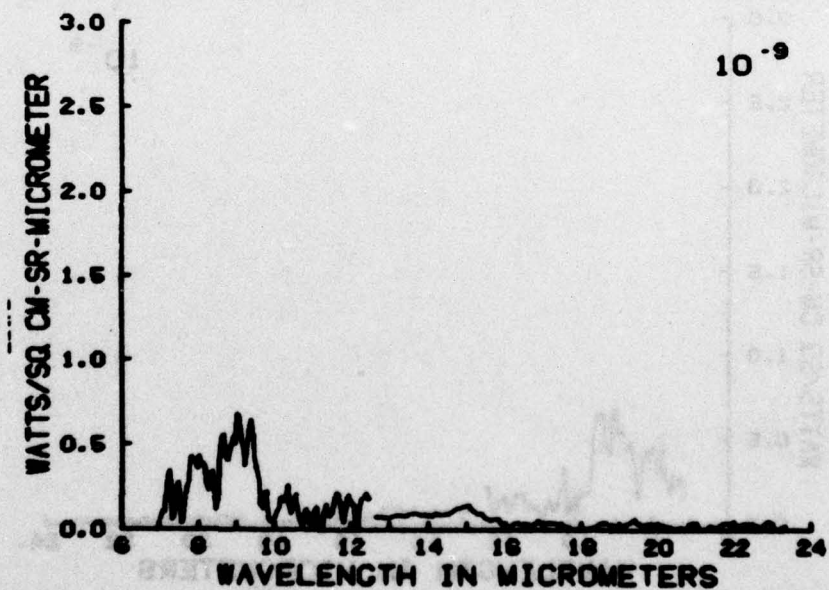


Figure C70



SCANS 645-649 ( 5/ 5) 334.7-336.7 SECS 148.6-146.6 KM

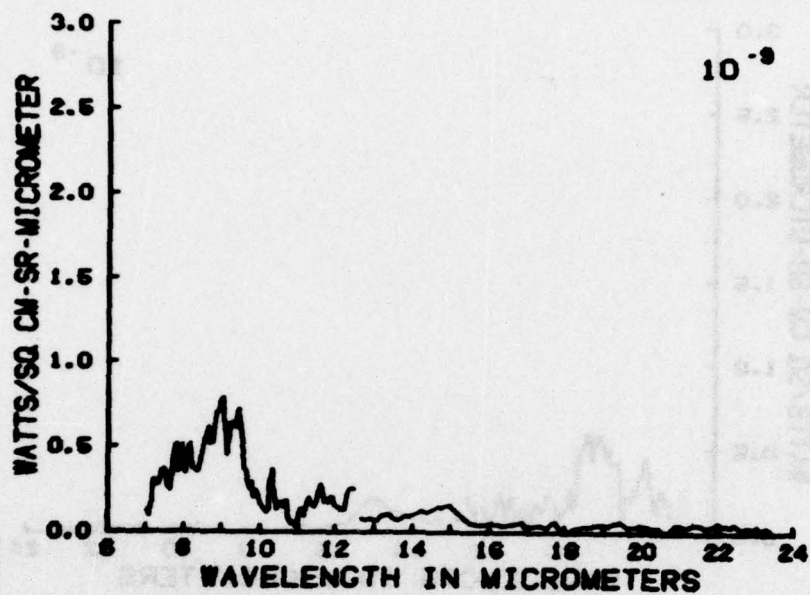


Figure C71

SCANS 651-654 ( 4/ 4) 337.7-339.2 SECS 145.8-144.1 KM

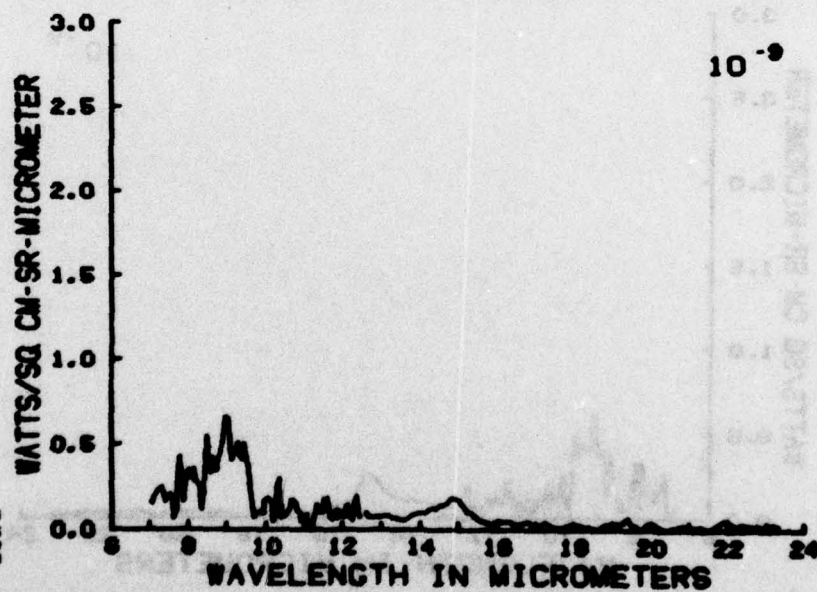


Figure C72

SCANS 655-659 ( 5/ 5 ) 339.6-341.6 SECS 143.6-141.6 KM

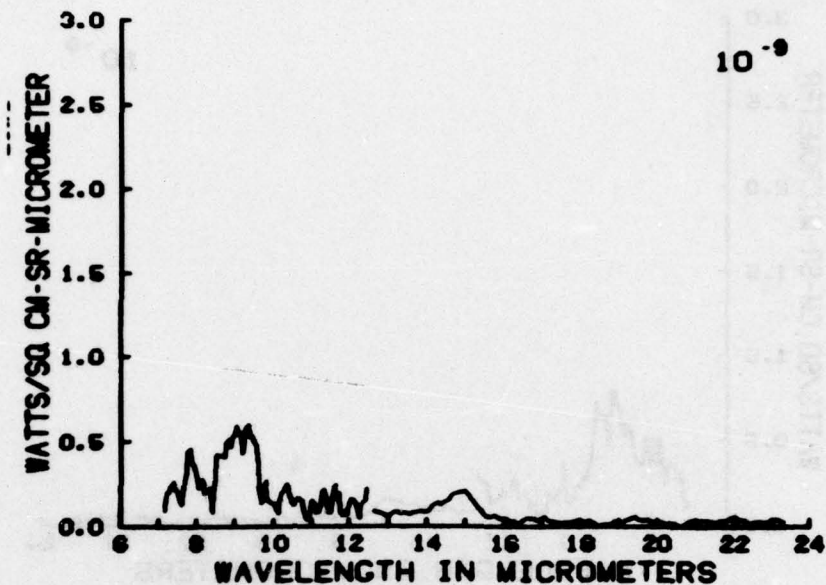


Figure C73

SCANS 661-664 ( 4/ 4 ) 342.6-344.1 SECS 140.6-138.1 KM

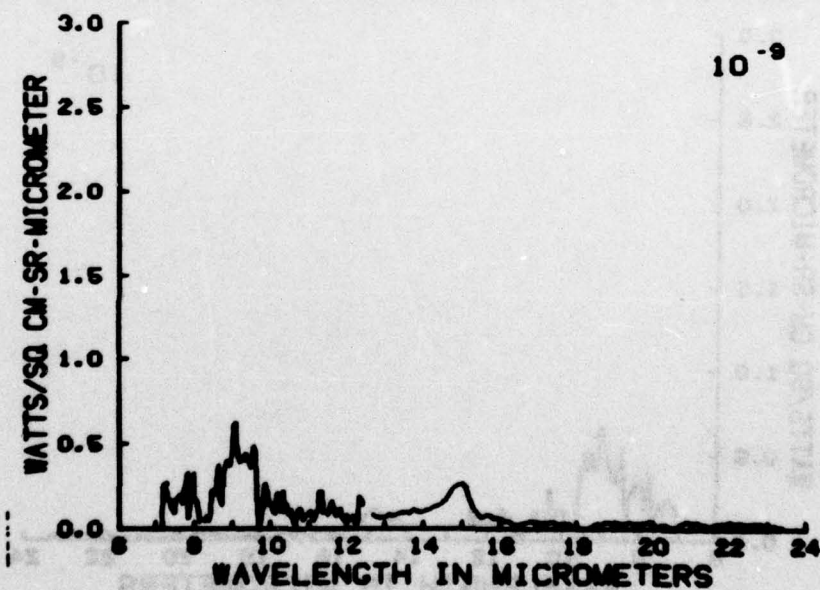


Figure C74

SCANS 665-669 ( 5/ 5 ) 344.6-346.5 SECS 136.6-136.6 KM

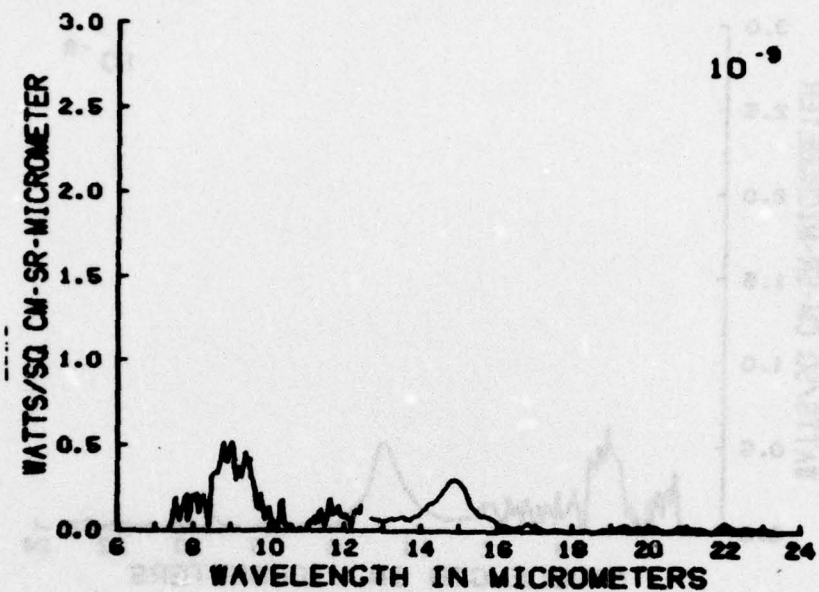


Figure C75

SCANS 671-674 ( 4/ 4 ) 347.5-349.0 SECS 136.4-136.6 KM

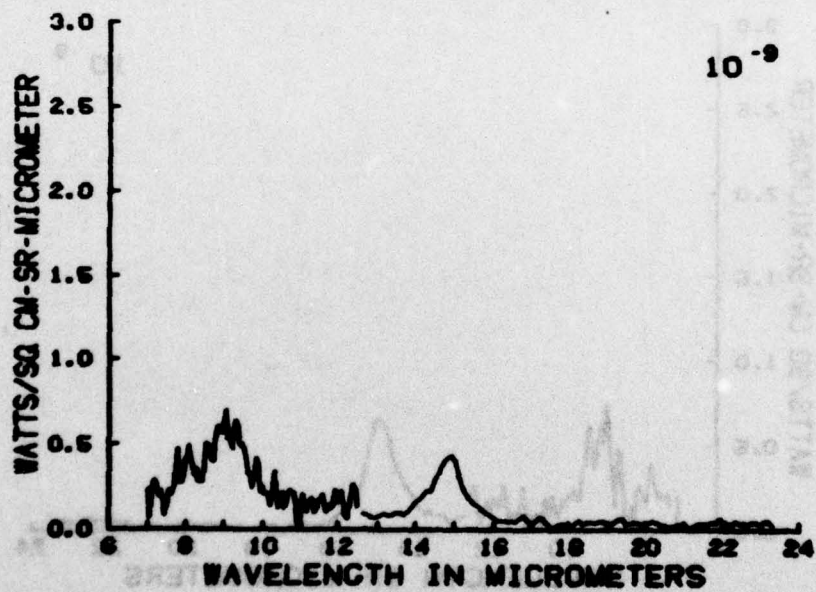


Figure C76



SCANS 675-678 ( 4/ 4) 349.5-351.0 SECS 133.3-131.6 KM

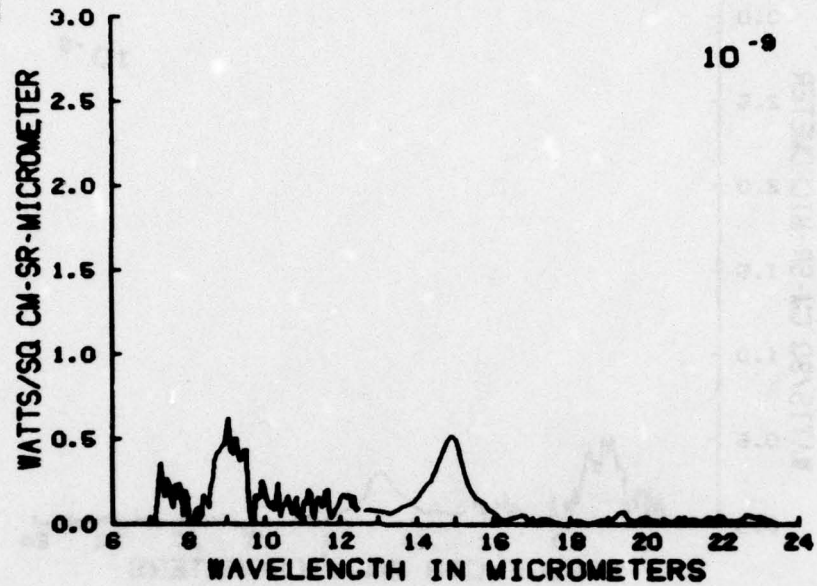


Figure C77

SCANS 679-683 ( 4/ 5) 351.5-353.4 SECS 131.1-128.8 KM

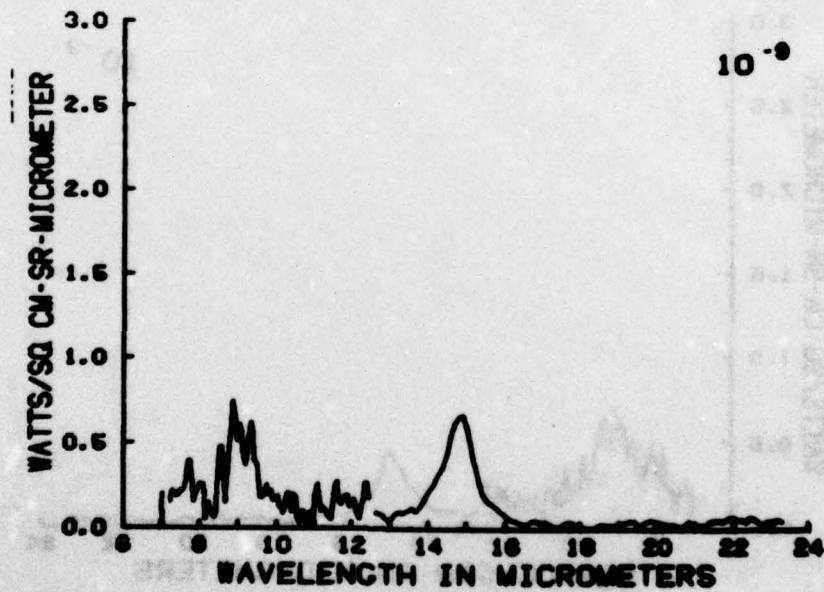


Figure C78

SCANS 694-697 ( 4/ 4) 353.9-355.4 SECS 128.3-128.6 KM

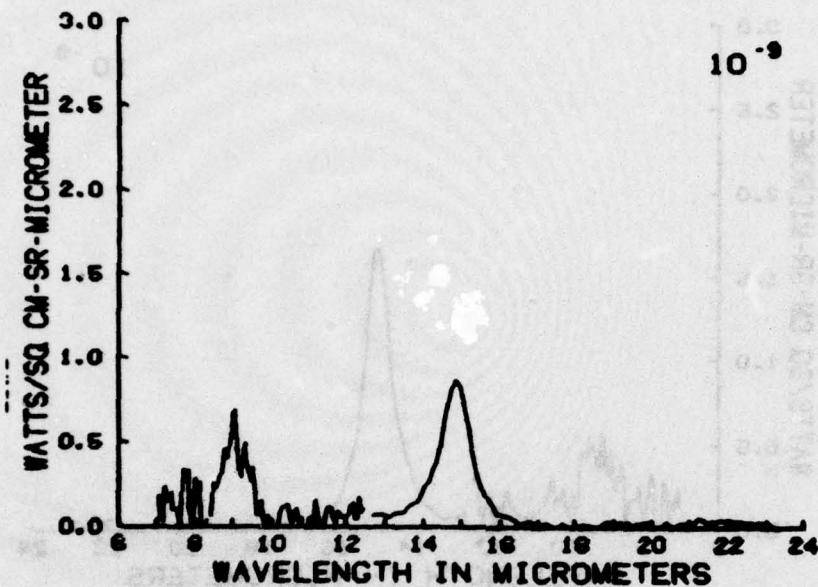


Figure C79

SCANS 698-692 ( 4/ 5) 355.9-357.8 SECS 128.1-128.8 KM

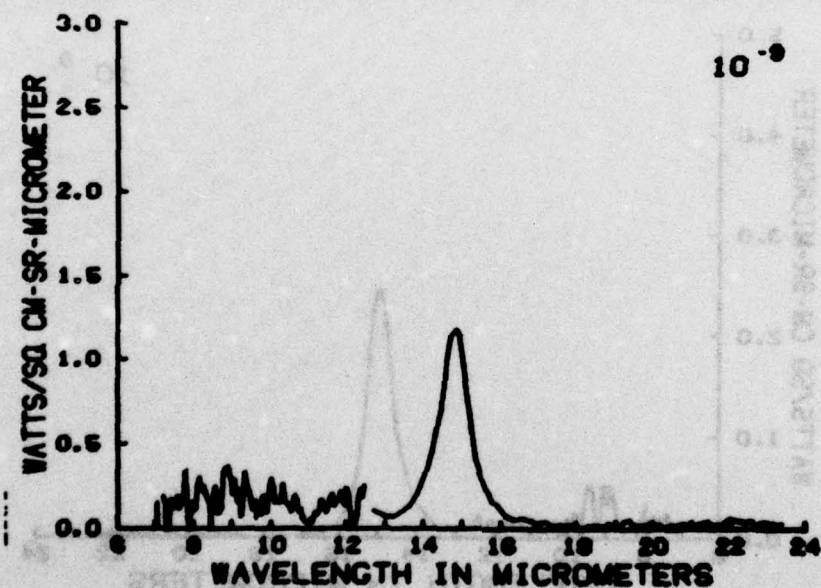


Figure C80

SCANS 693-696 ( 3/ 3) 358.3-359.3 SECS 123.2-122.0 KM

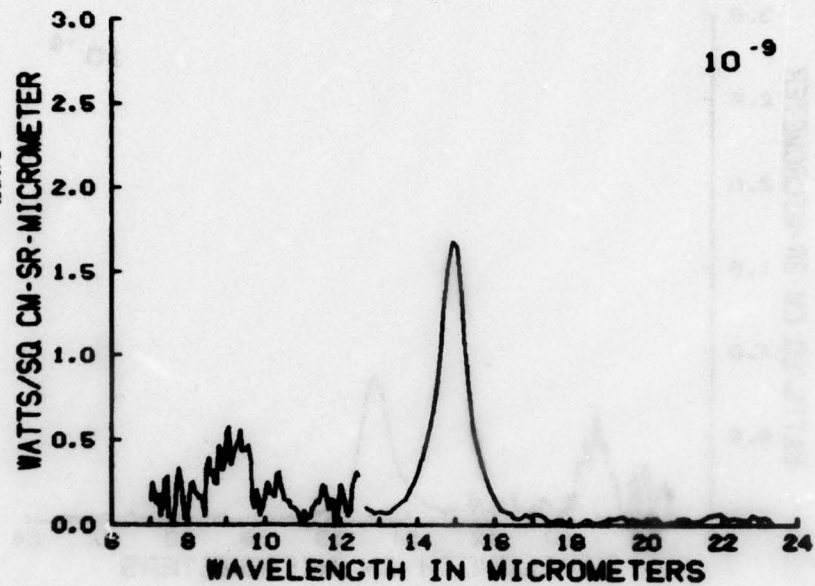


Figure C81

SCANS 696-699 ( 3/ 4) 359.8-362.3 SECS 121.5-118.5 KM

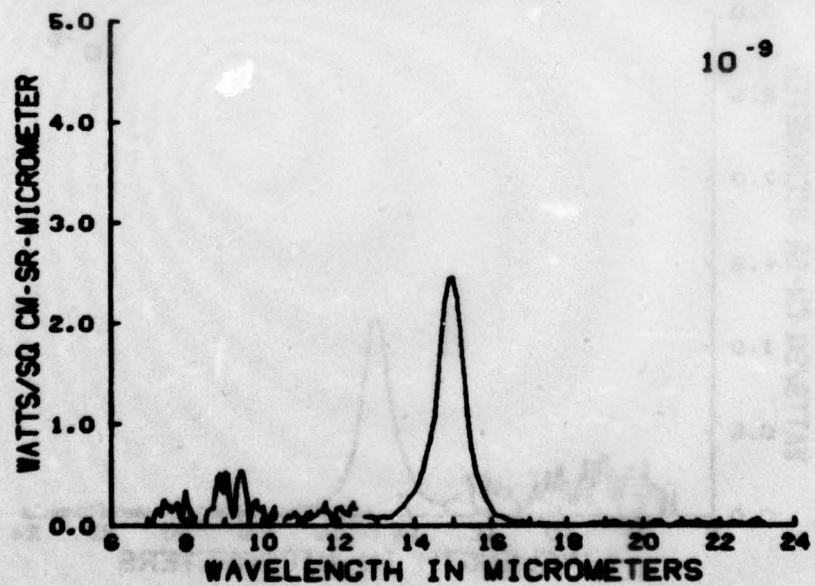


Figure C82



SCANS 700-702 ( 3/ 3 ) 362.8-363.7 SECS 117.9-118.7 KM

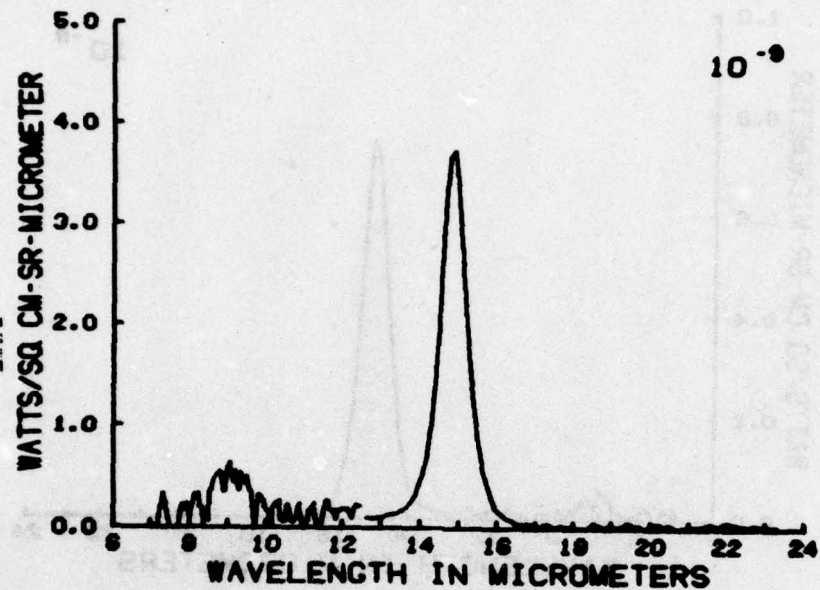


Figure C83

SCANS 703-706 ( 4/ 4 ) 364.2-365.7 SECS 116.1-114.3 KM

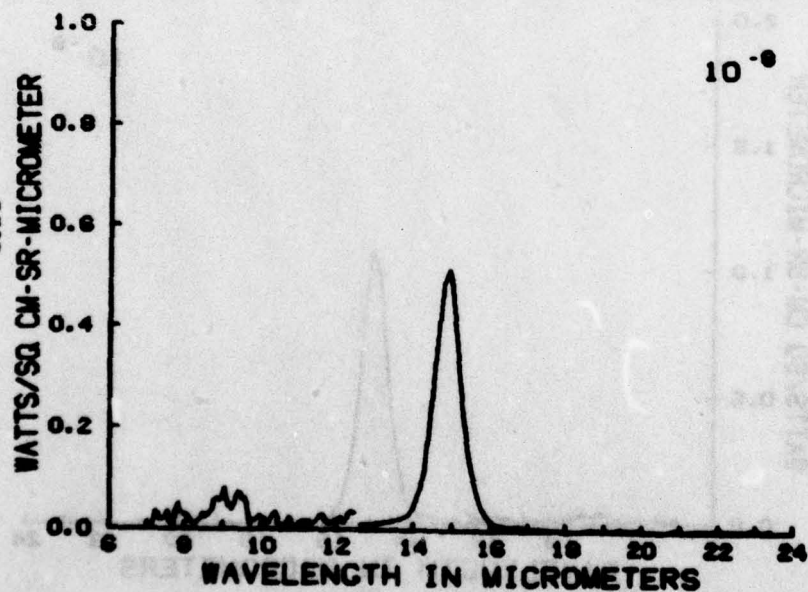


Figure C84

SCANS 707-710 ( 3/ 4 ) 366.2-367.7 SECS 113.7-111.8 KM

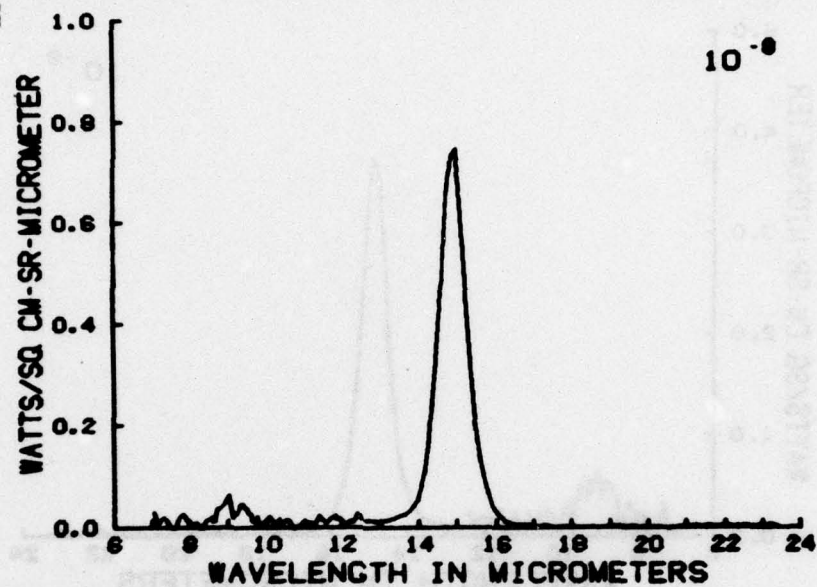


Figure C85

SCANS 711-714 ( 4/ 4 ) 368.2-369.7 SECS 111.2-108.4 KM

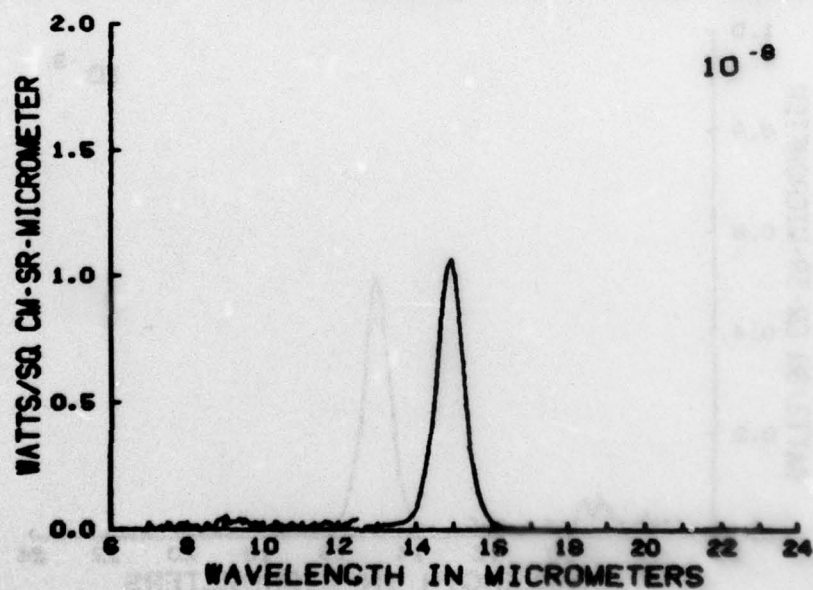


Figure C86

SCANS 715-717 ( 3/ 3) 370.1-371.1 SECS 106.7-107.6 KM

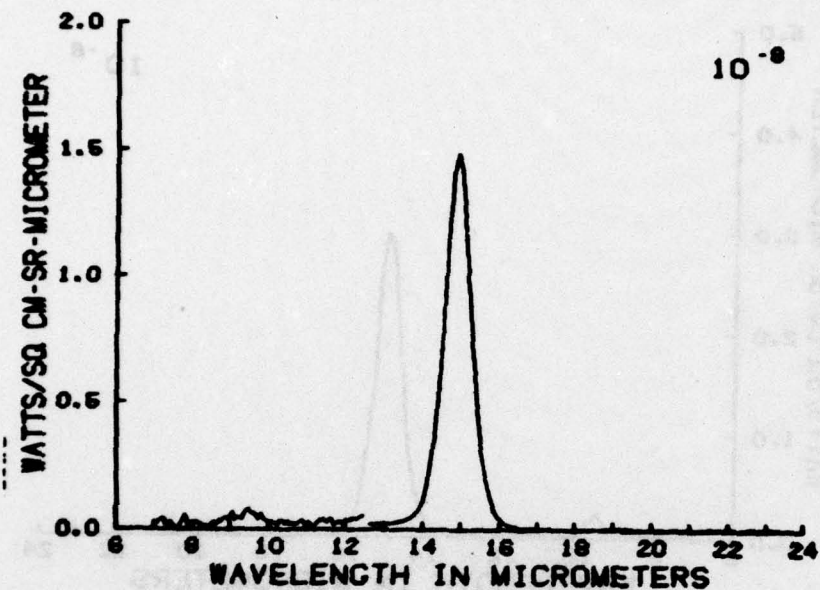


Figure C87

SCANS 719-722 ( 4/ 4) 372.1-373.6 SECS 106.2-104.3 KM

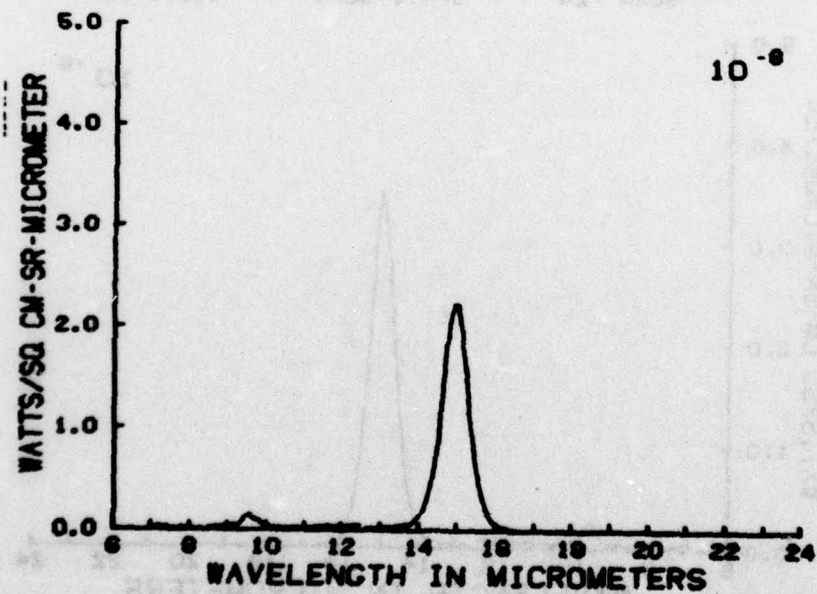


Figure C88



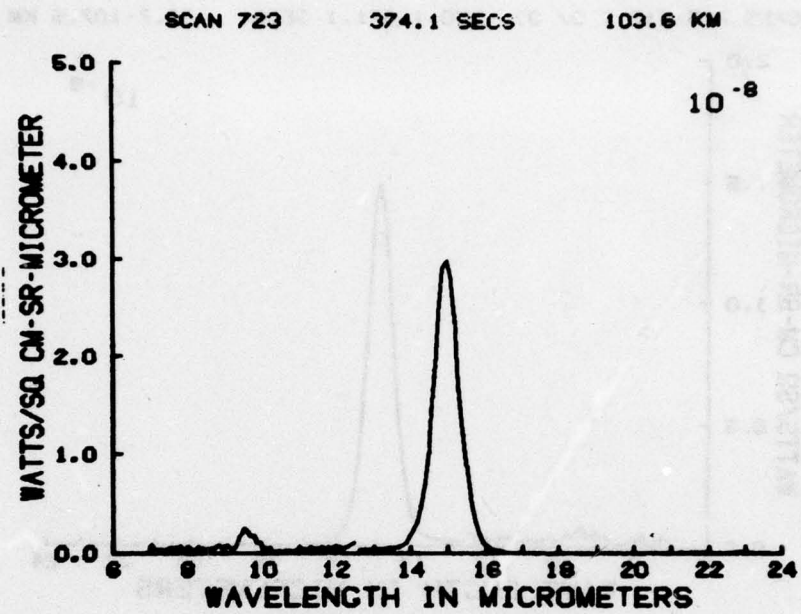


Figure C89

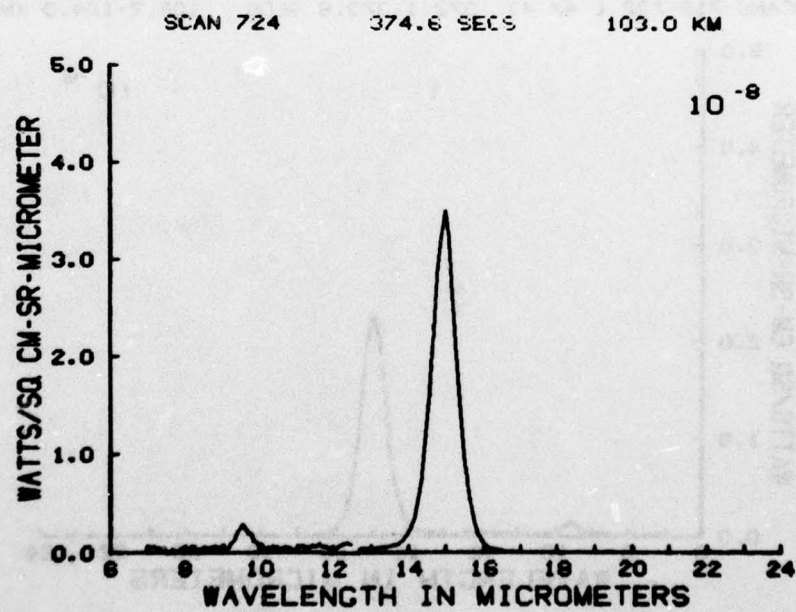


Figure C90

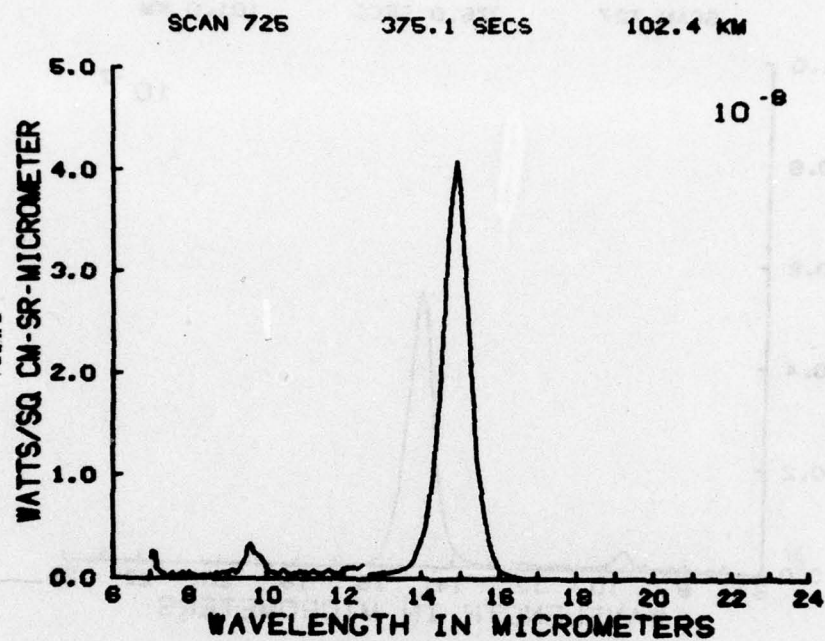


Figure C91

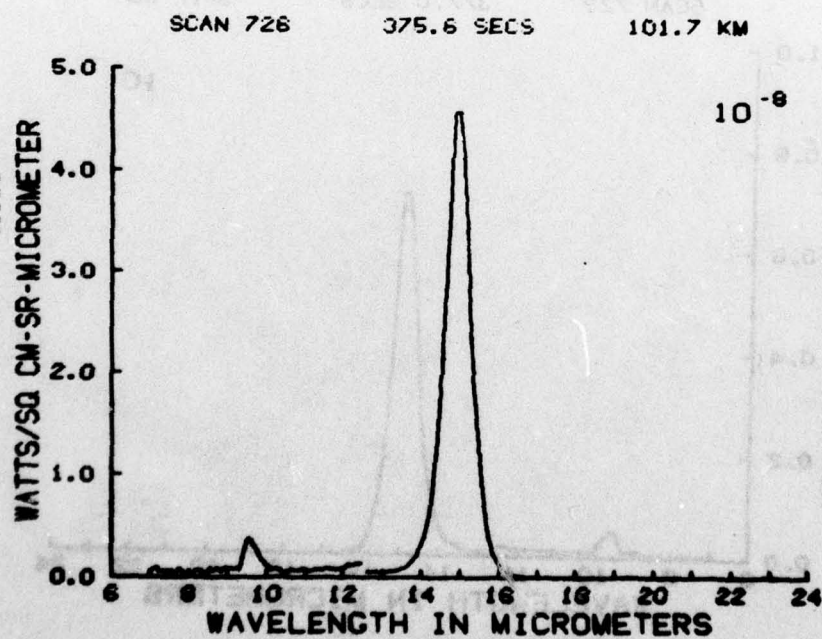


Figure C92

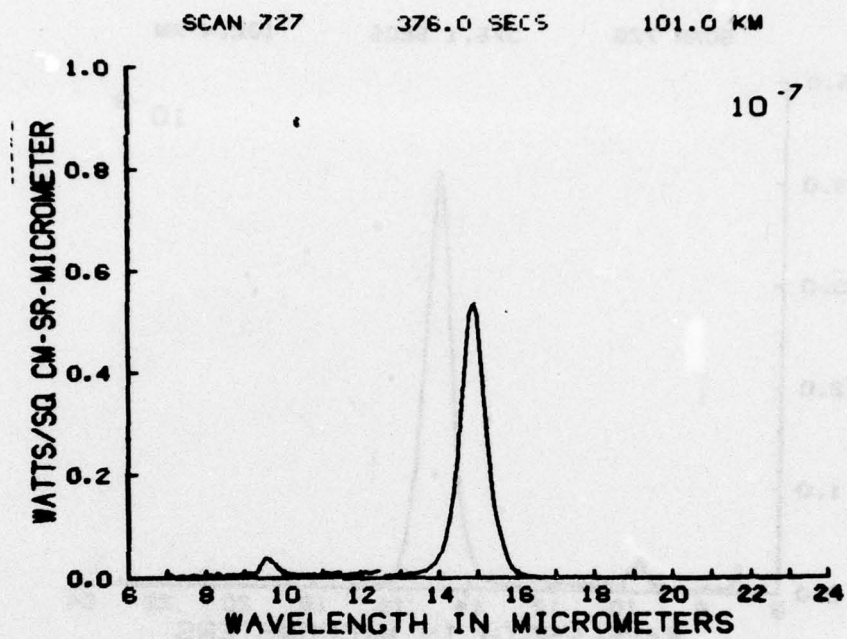


Figure C93

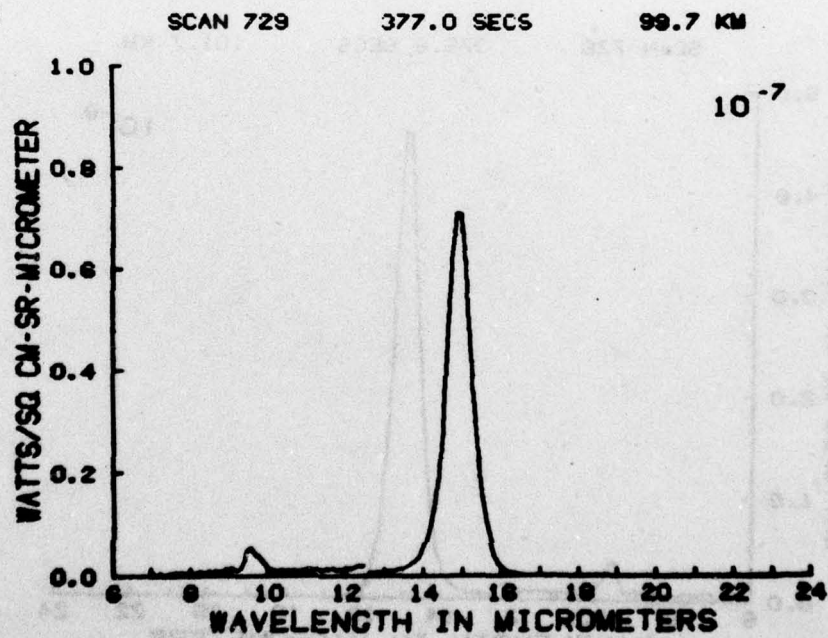


Figure C94



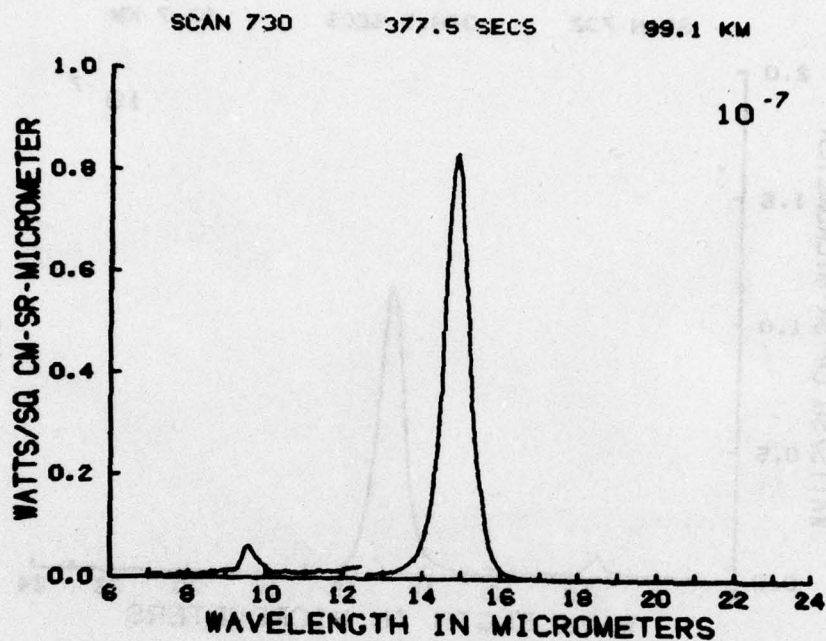


Figure C95

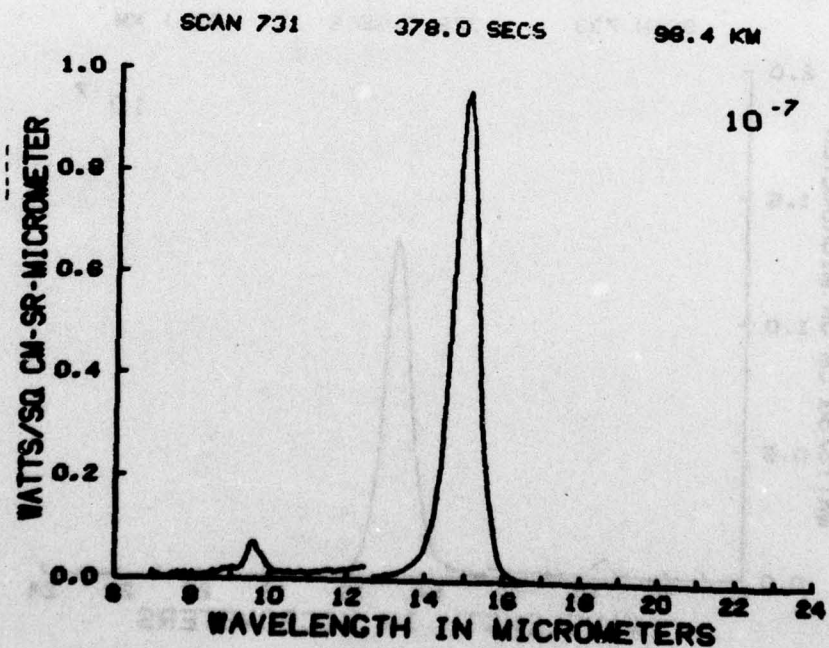


Figure C96

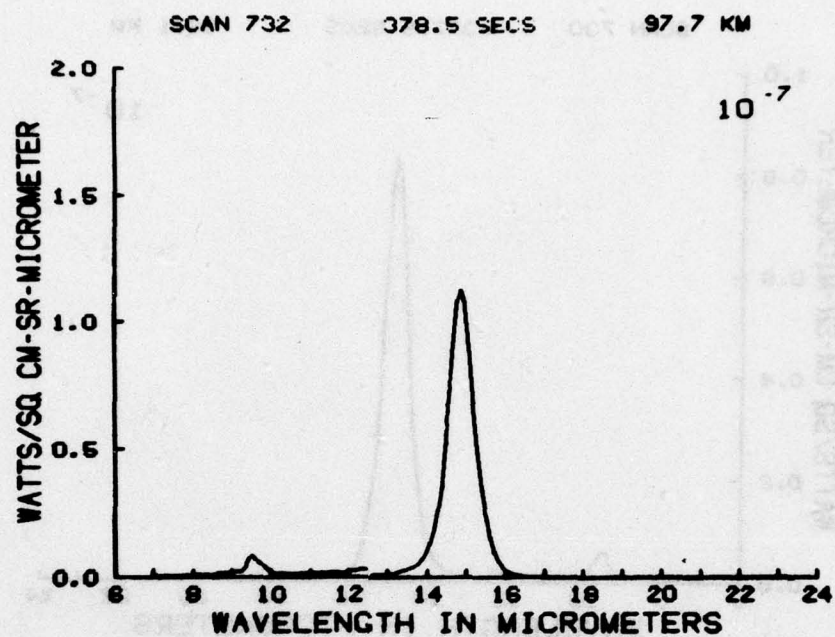


Figure C97

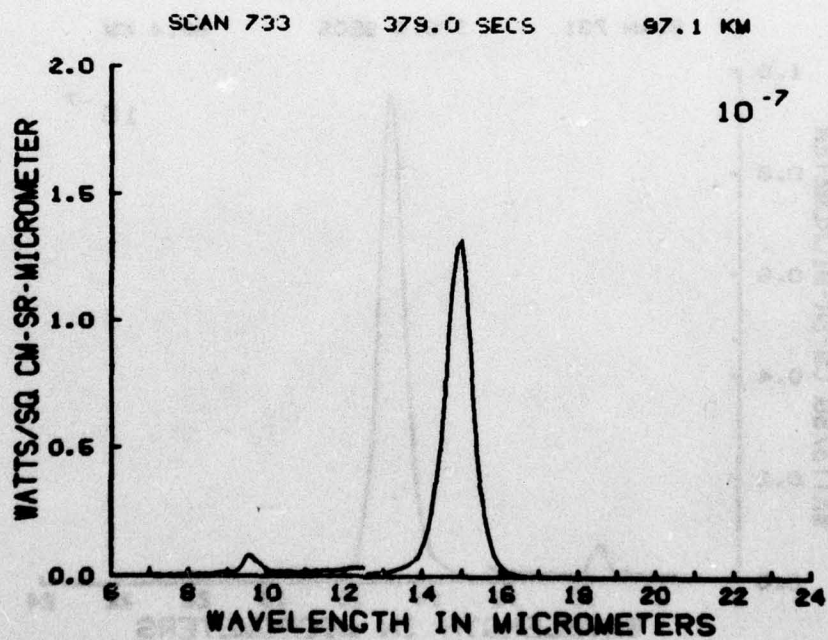


Figure C98

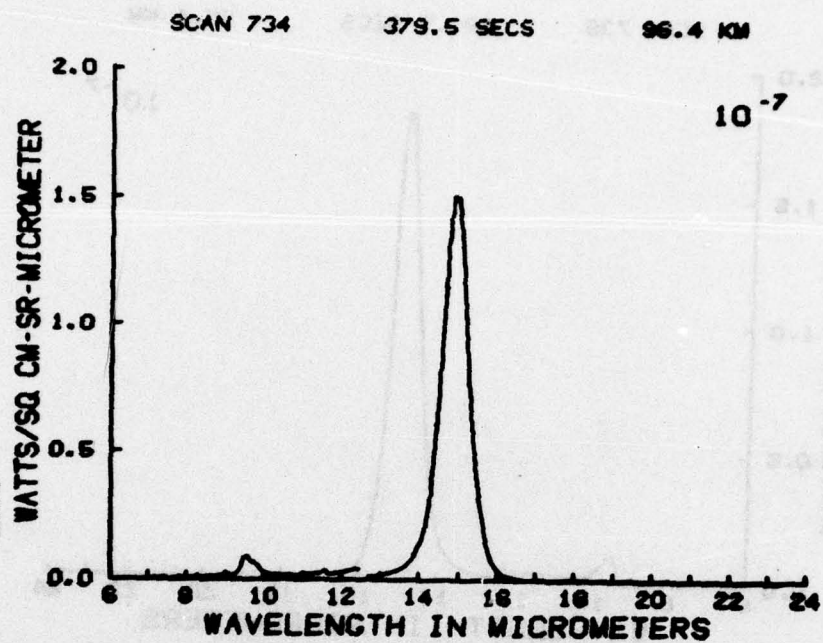


Figure C99

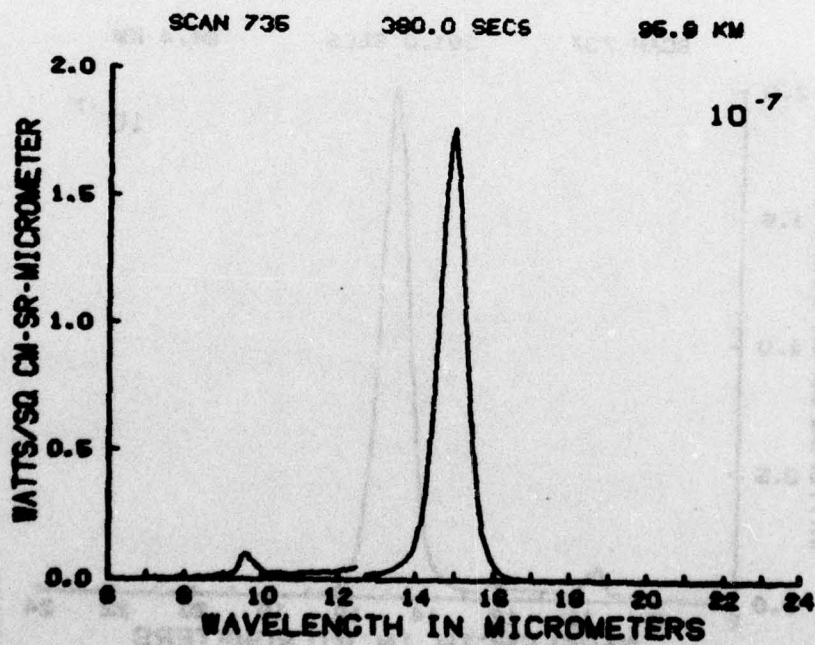


Figure C100



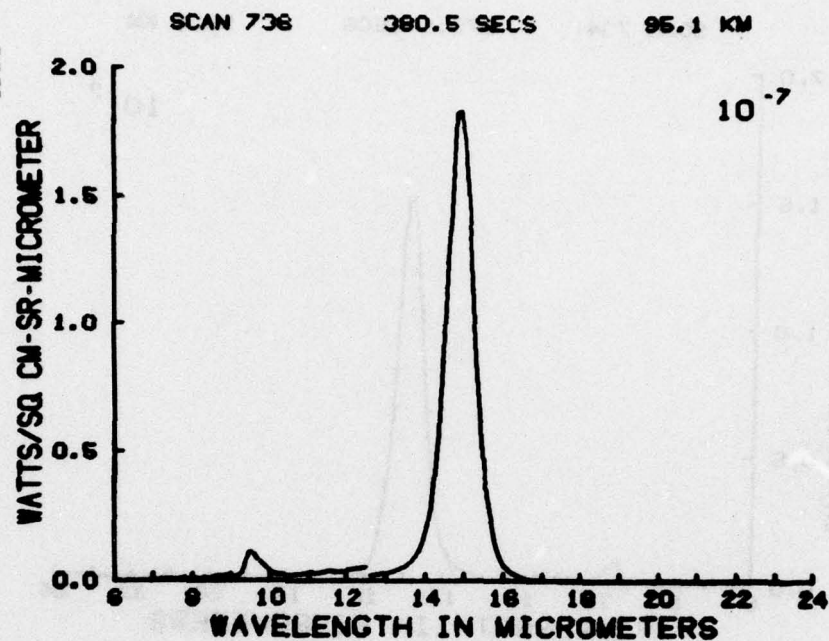


Figure C101

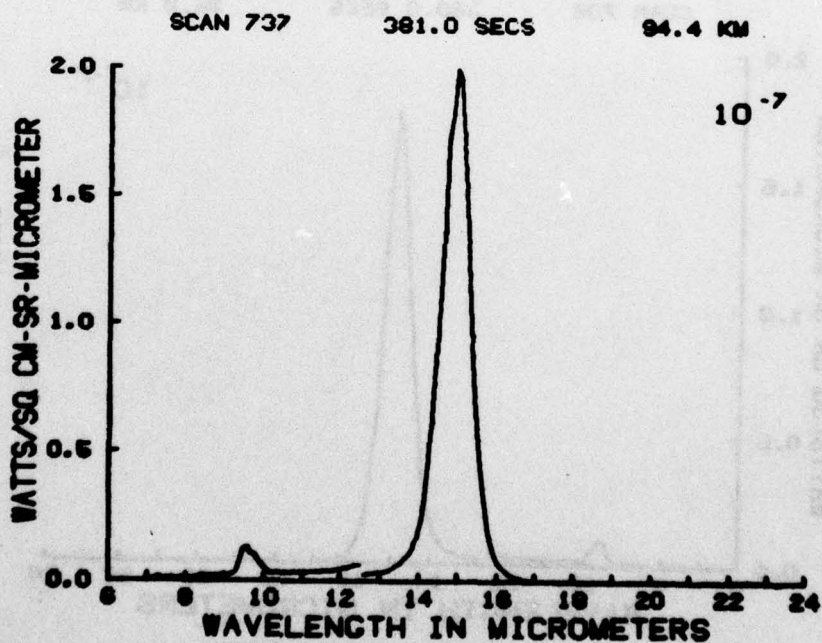


Figure C102

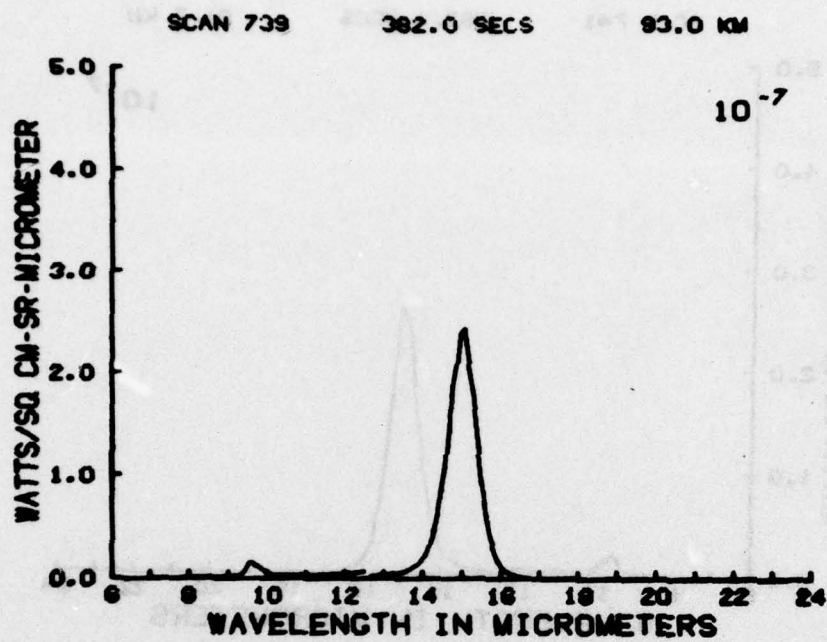


Figure C103

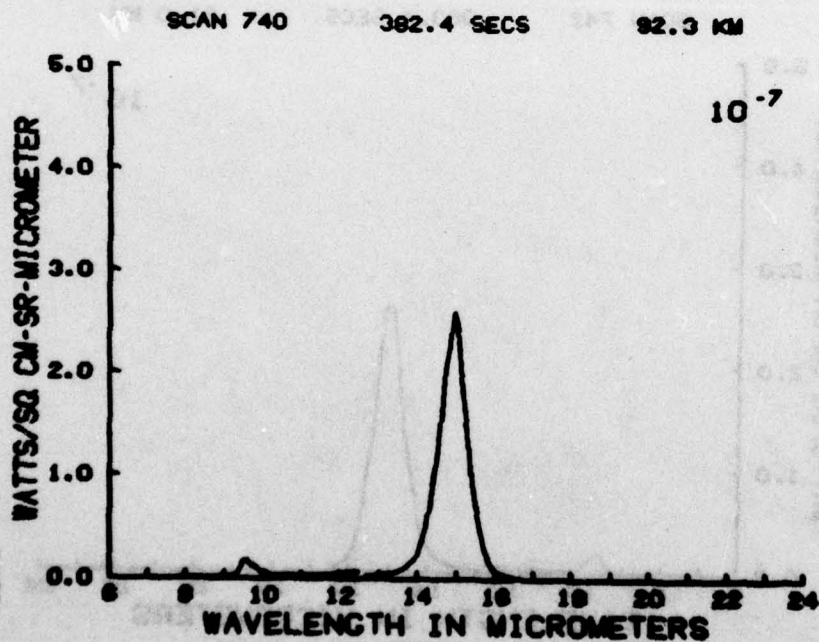


Figure C104

SCAN 741

382.9 SECS

91.7 KM

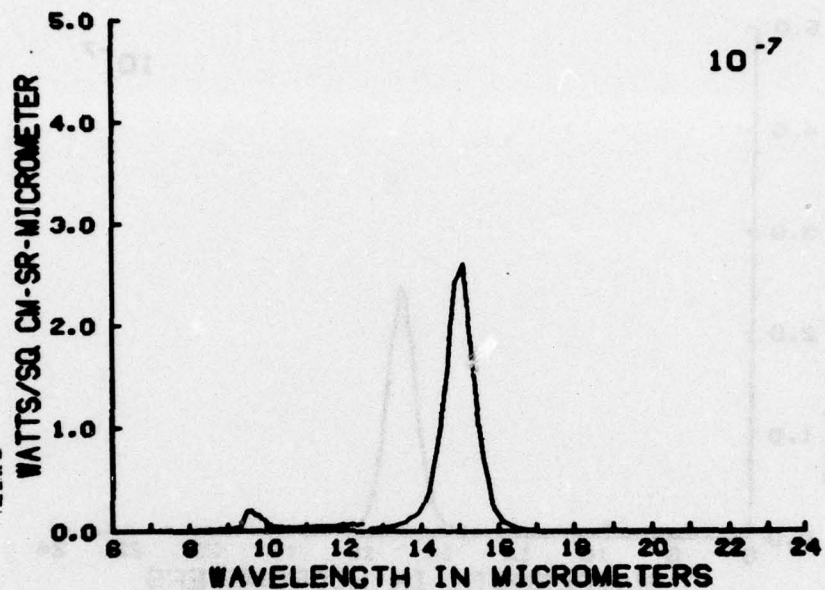


Figure C105

SCAN 742

383.4 SECS

91.0 KM

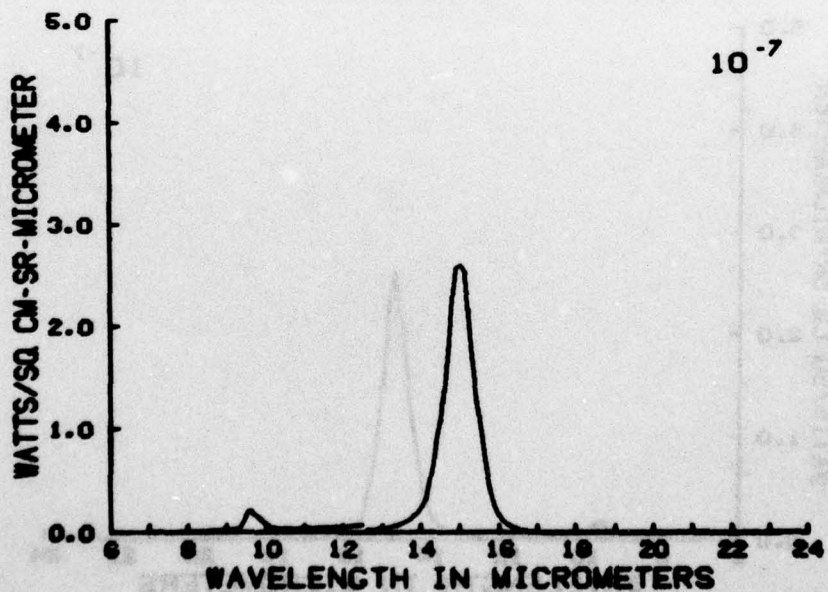


Figure C106



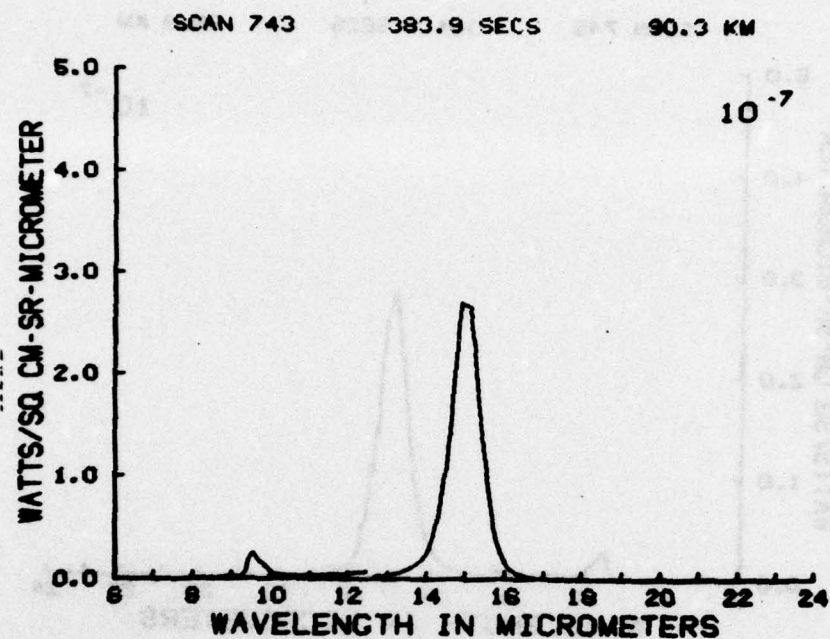


Figure C107

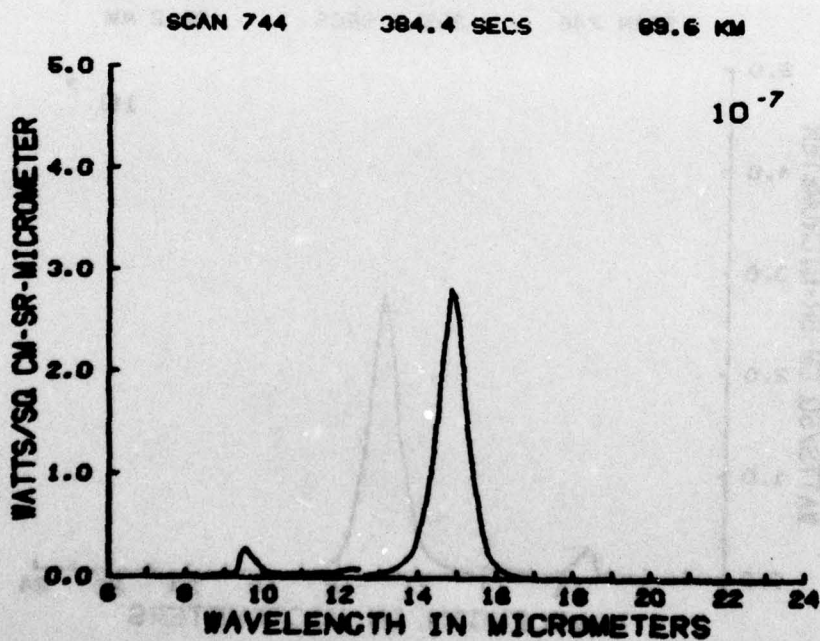


Figure C108

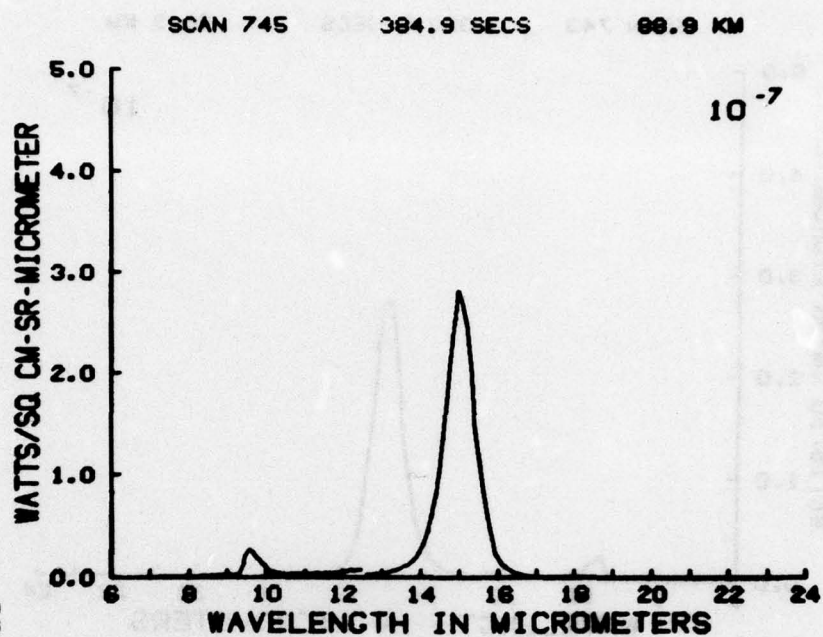


Figure C109

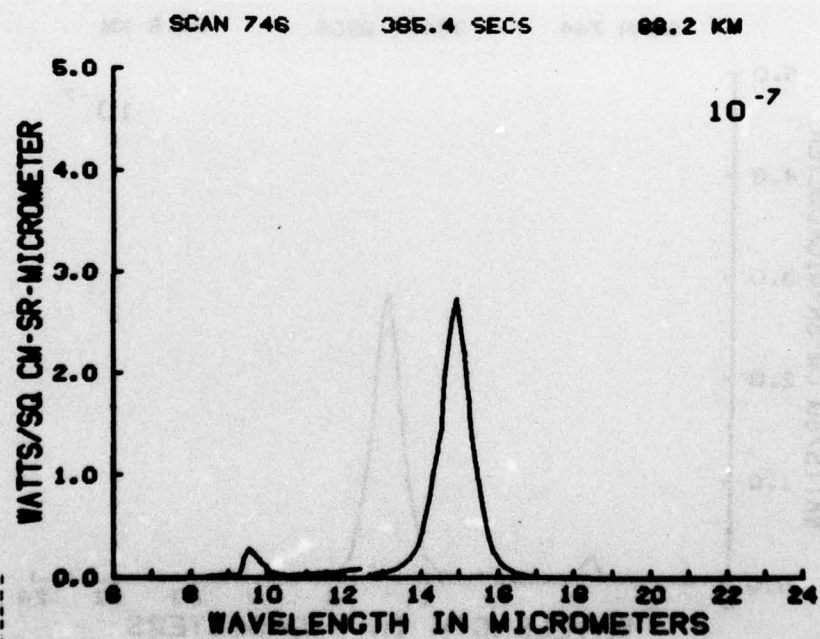


Figure C110

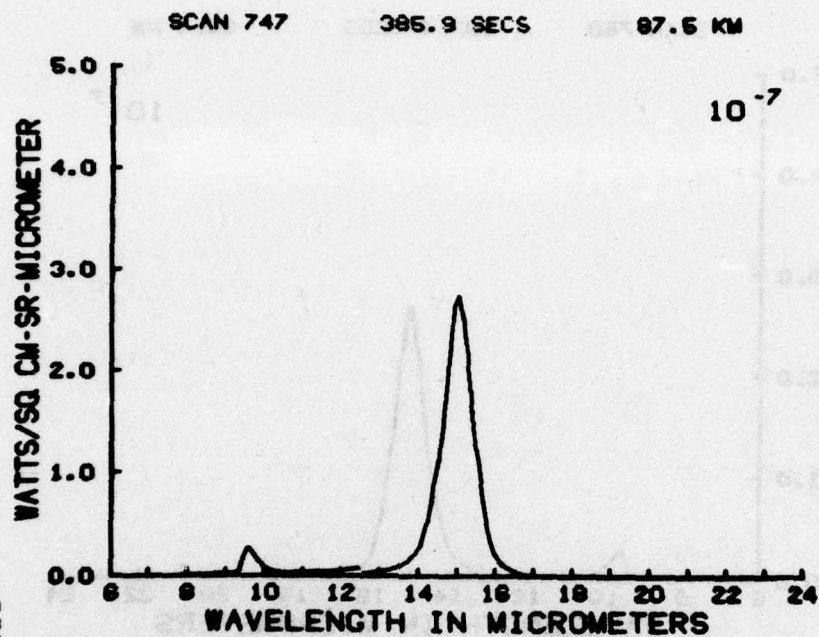


Figure C111

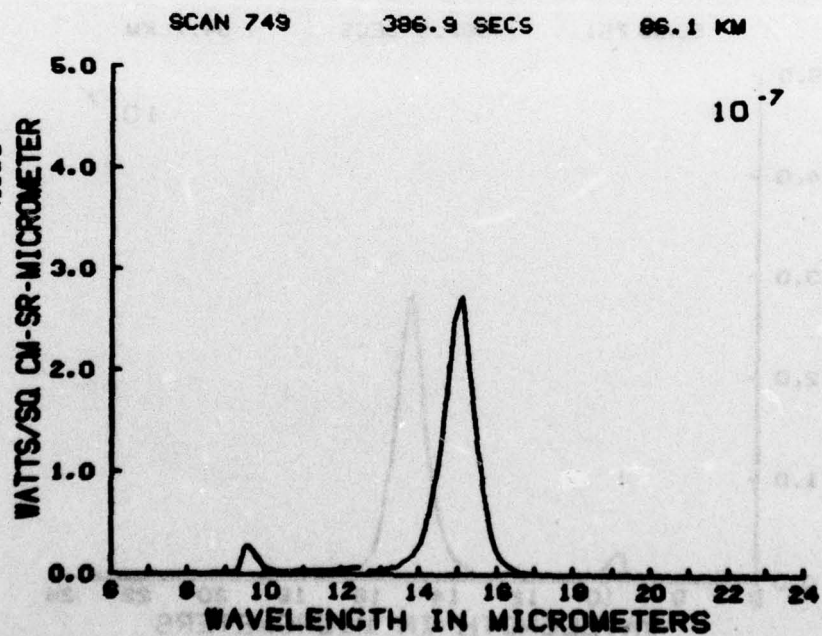


Figure C112



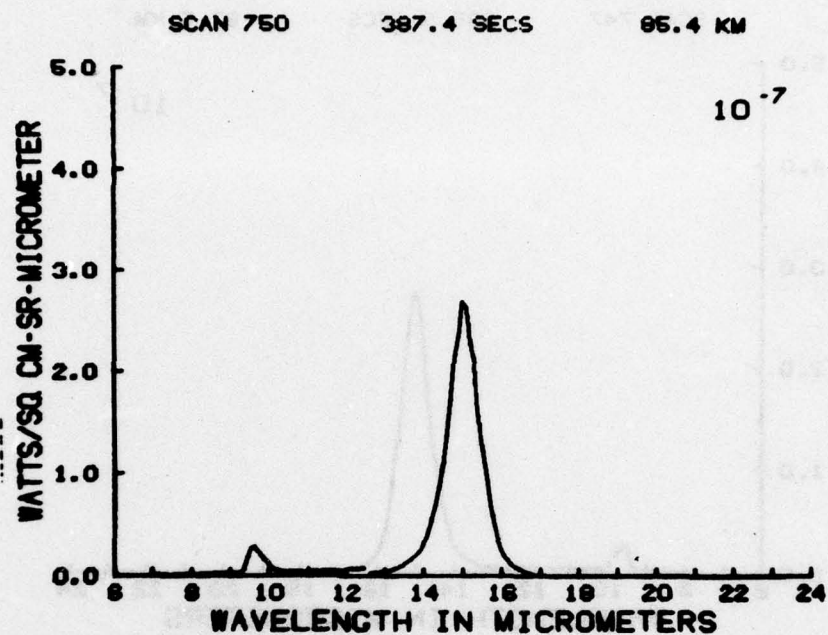


Figure C113

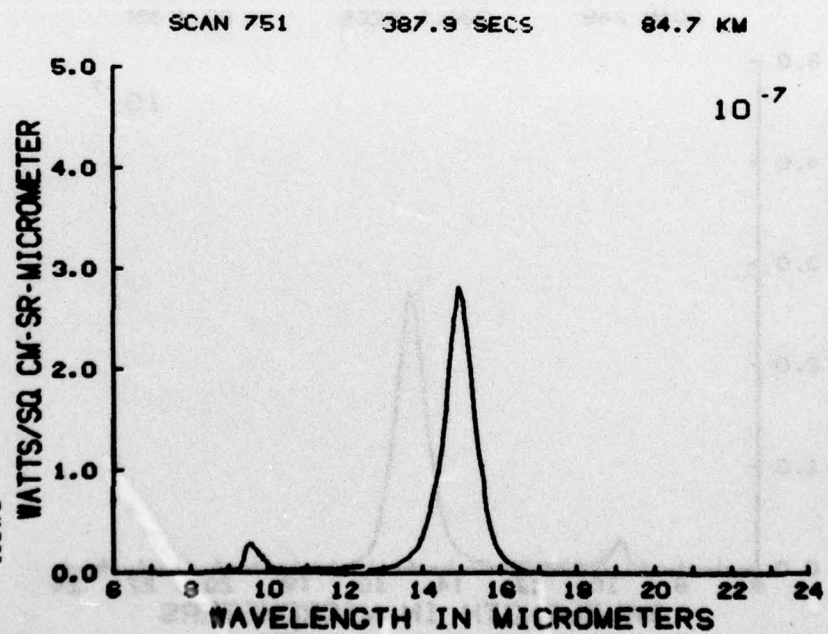


Figure C114

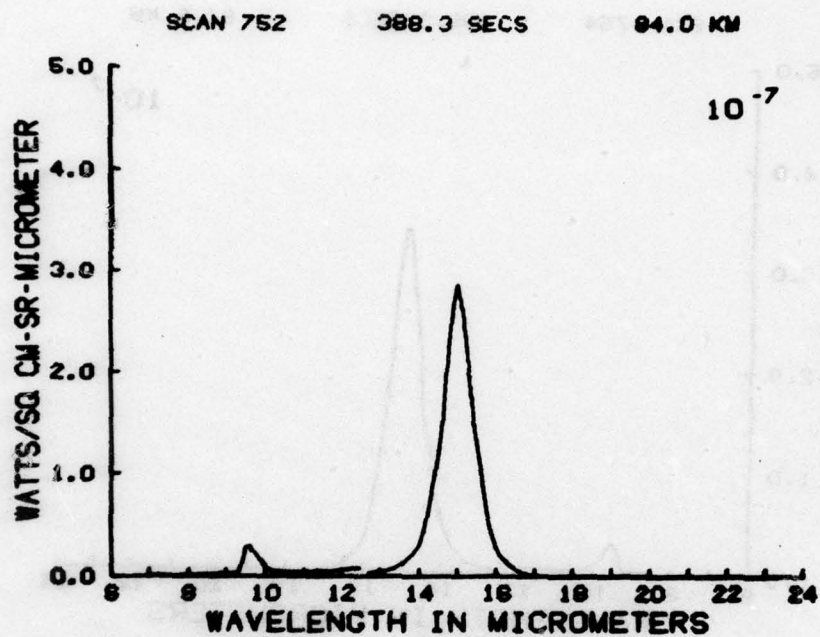


Figure C115

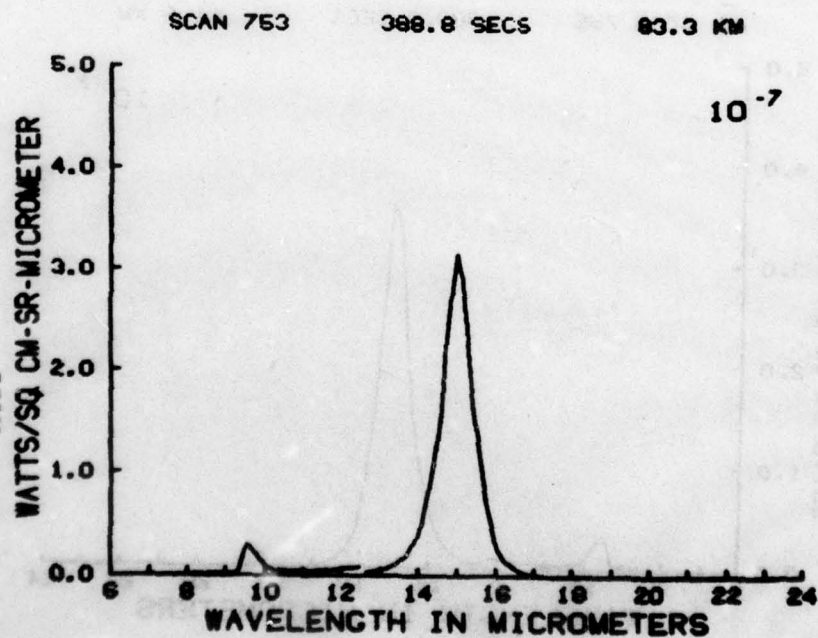


Figure C116

AD-A045 466

AIR FORCE GEOPHYSICS LAB HANSCOM AFB MASS  
LWIR (7-24-MICROMETER) MEASUREMENTS FROM THE LAUNCH OF A ROCKET--ETC(U)  
MAY 77 J W ROGERS, A T STAIR, N B WHEELER  
AFGL-TR-77-0113 DNA-HAES-64

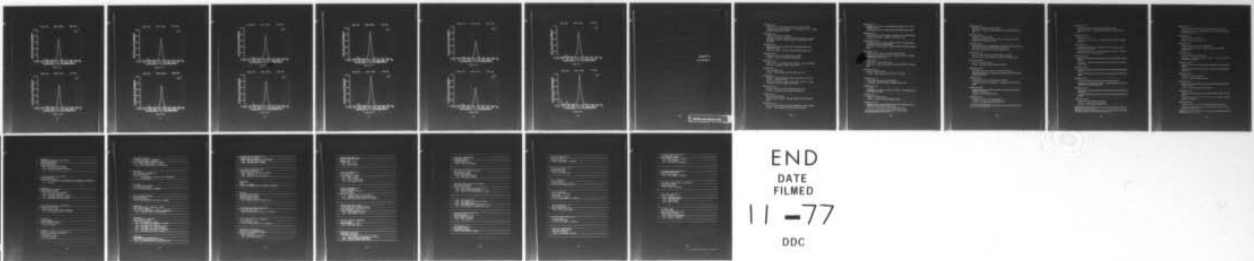
F/G 1/13

UNCLASSIFIED

NL

2 of 2

AD  
A045466



END  
DATE  
FILMED

11 -77

DDC



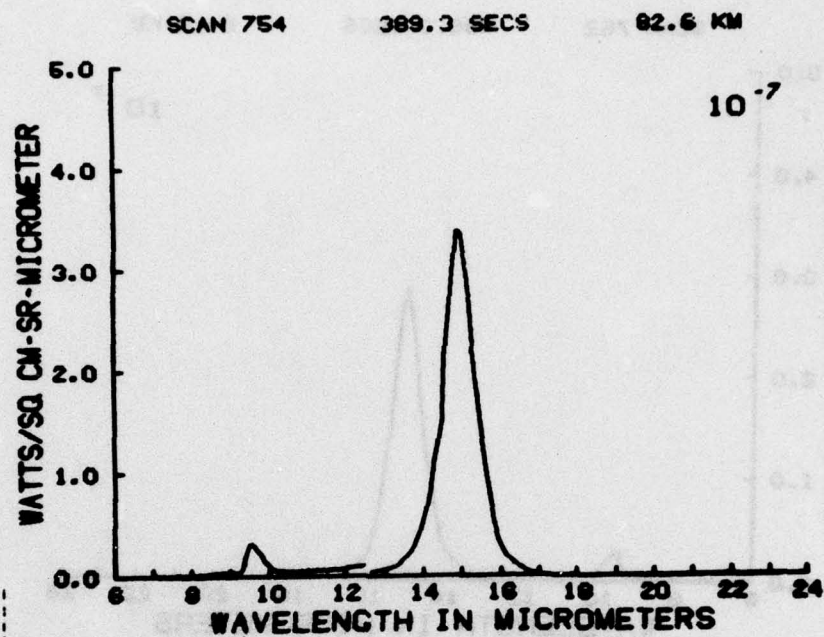


Figure C117

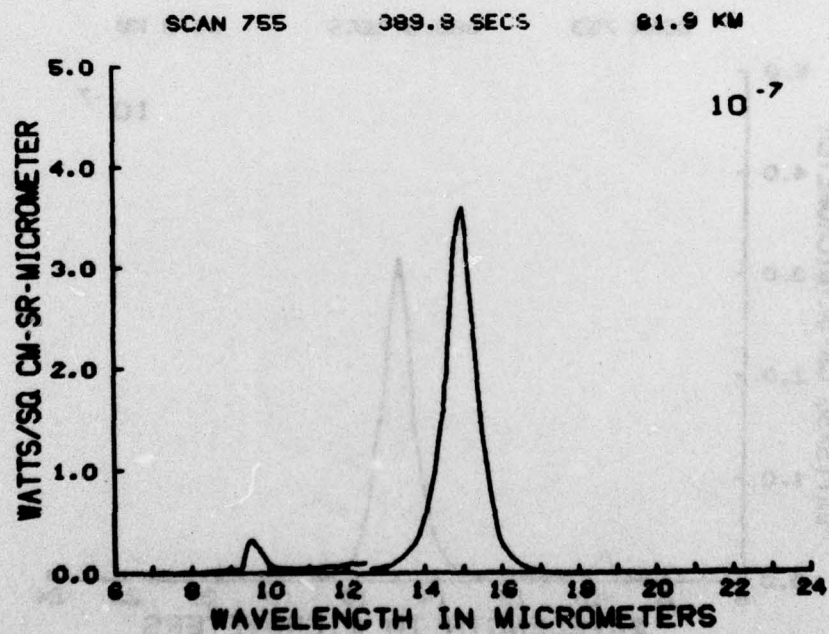


Figure C118

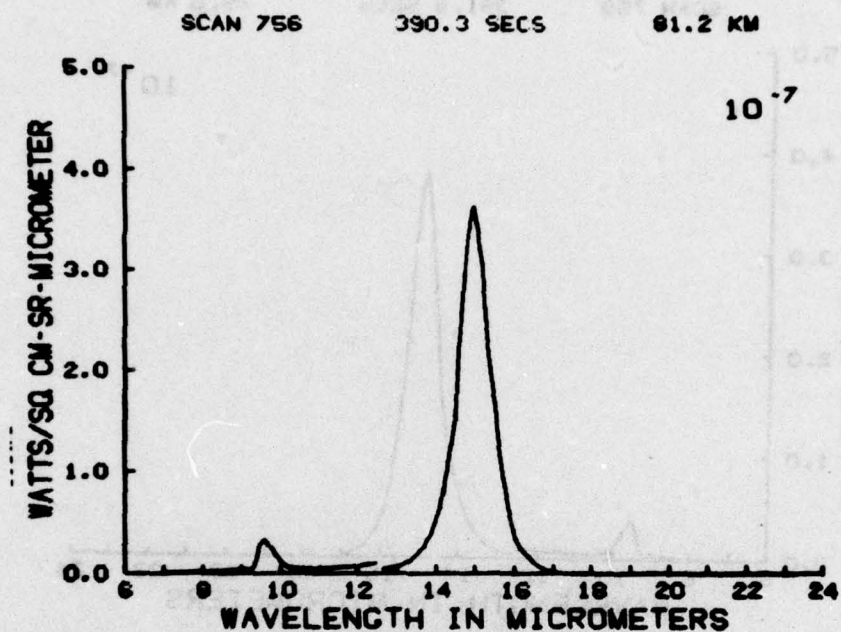


Figure C119

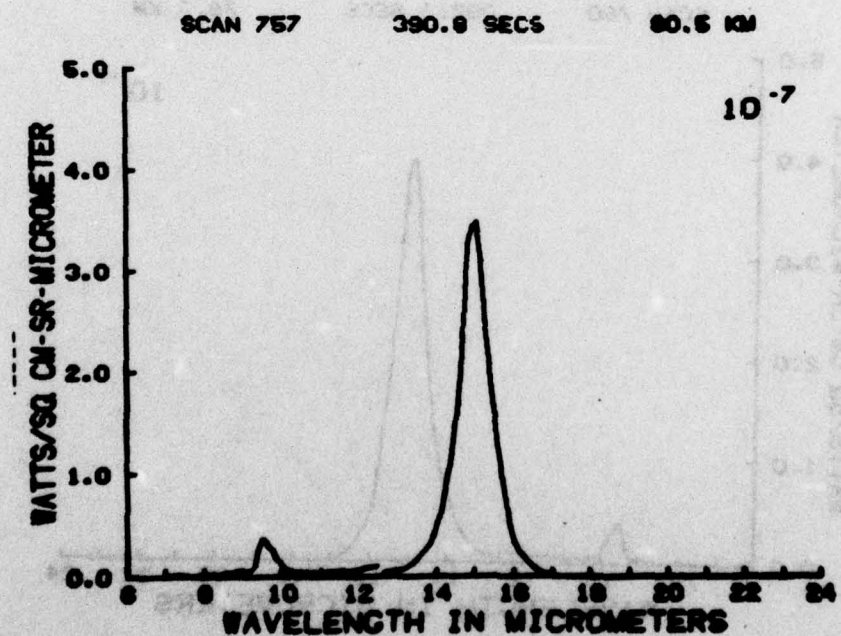


Figure C120



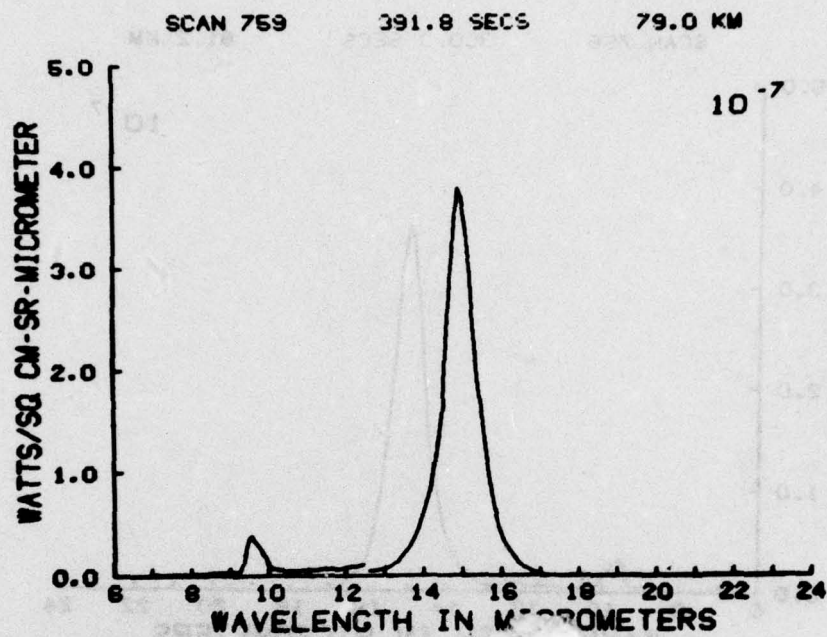


Figure C1

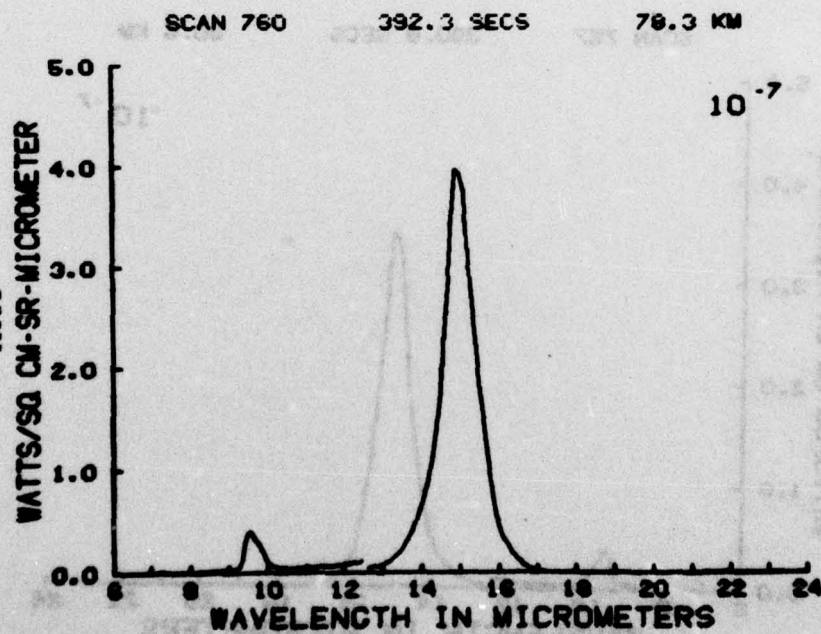


Figure C122



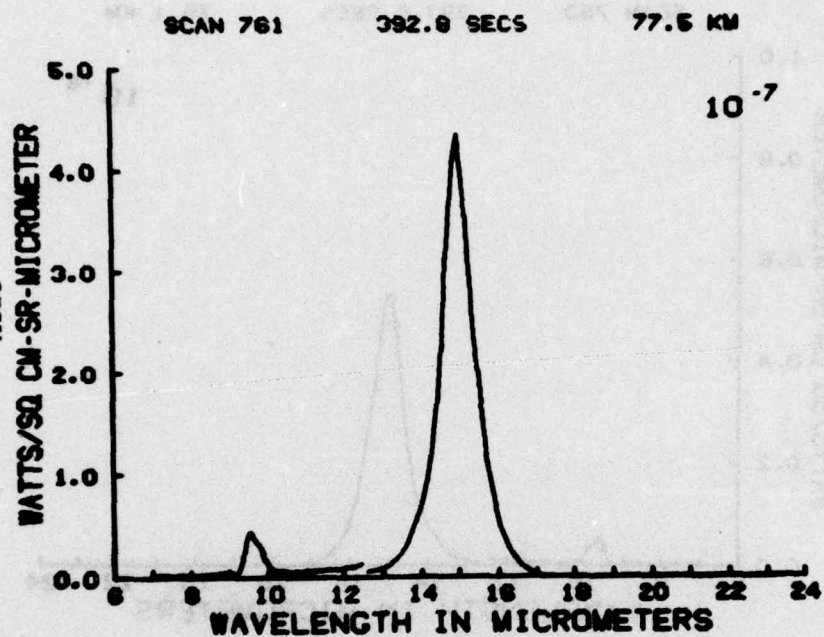


Figure C123

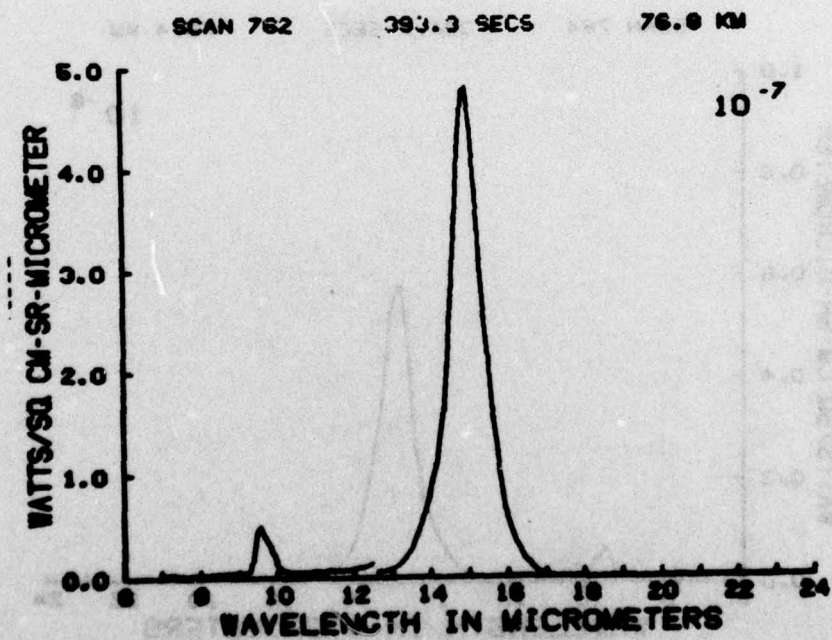


Figure C124

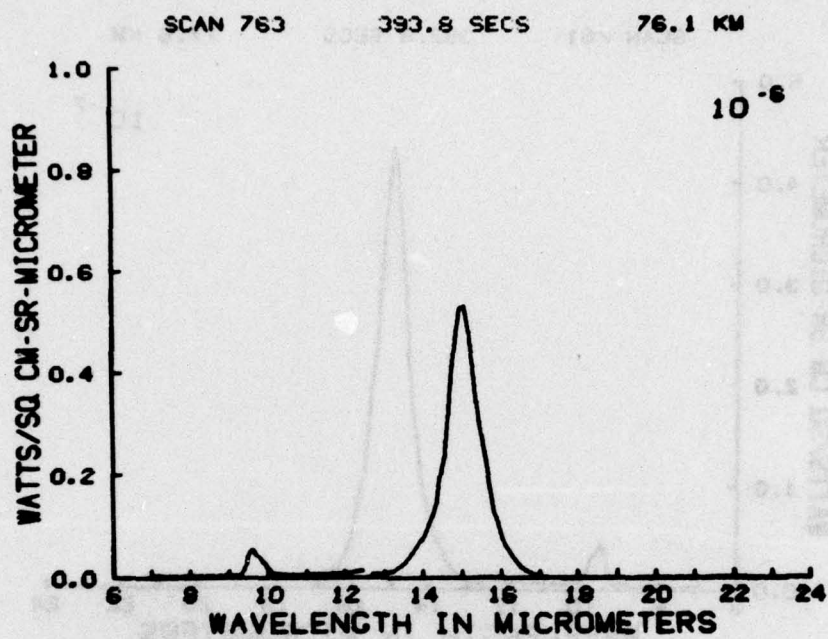


Figure C125

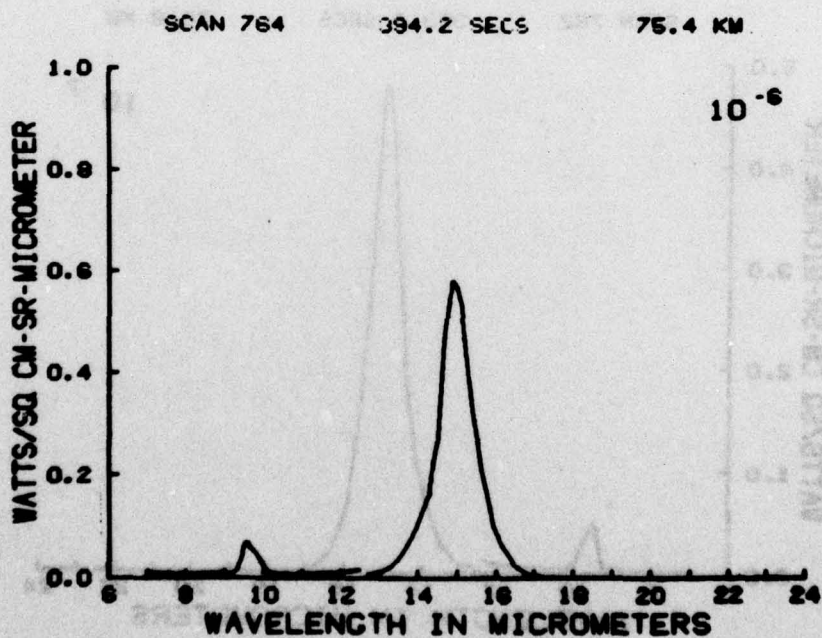


Figure C126



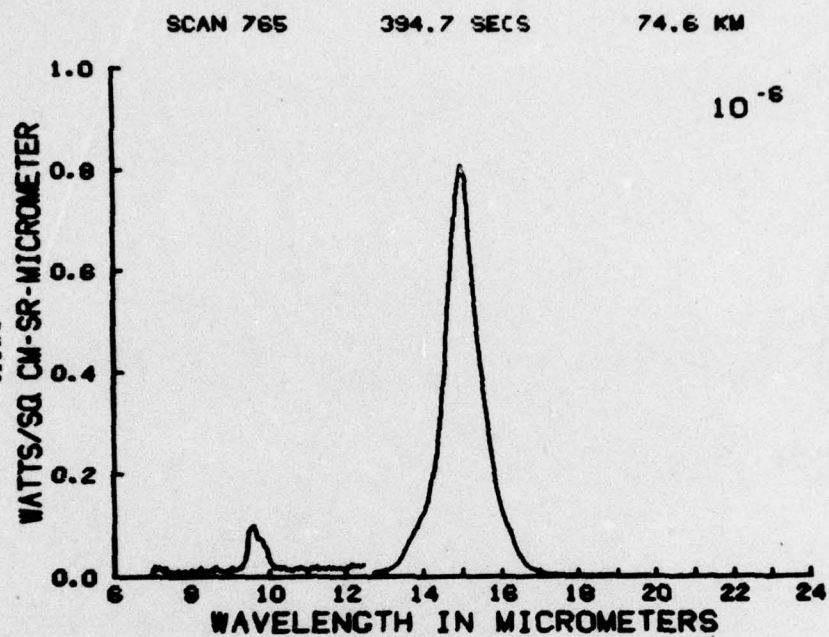


Figure C127

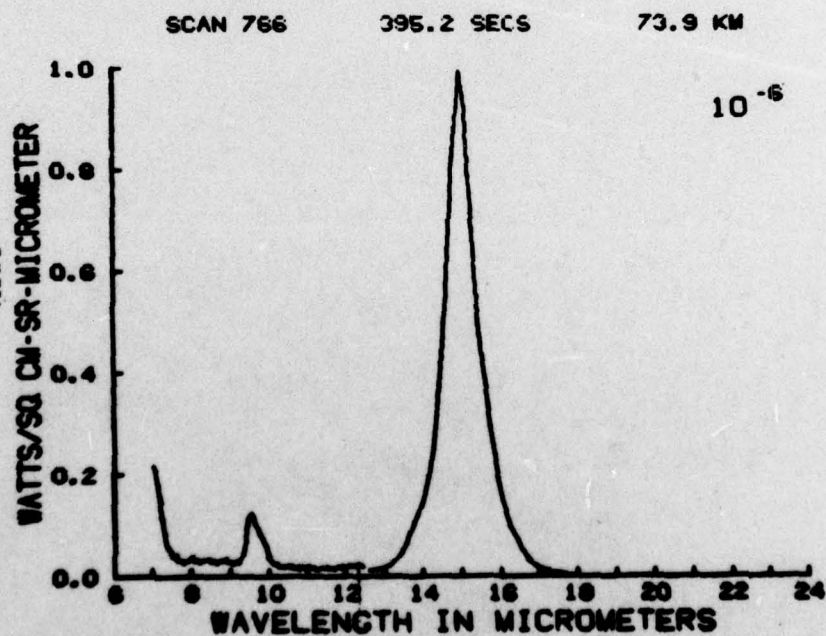


Figure C128



## Appendix D

### List of HAES Reports

HAES Report No. 1

*Rocket Launch of a SWIR Spectrometer into an Aurora (ICECAP 72)*

D.J. Baker, C.L. Wyatt, W.R. Pendelton, Jr. — Utah State, J.C. Ulwick — AFCRL;  
AFCRL-TR-74-0077, February 1974.

HAES Report No. 2

*Analysis of HAES Results: ICECAP 72*

W.P. Reidy, T.C. Degges, O.P. Manley, H.J. Smith, J.W. Carpenter — Visidyne,  
A.T. Stair, J.C. Ulwick — AFCRL, D.J. Baker — Utah State; DNA 3247F,  
April 1974.

HAES Report No. 3

*Rocket Instrumentation for ICECAP 73A, Auroral Measurements Program —  
Black Brant 18.205-1*

D.A. Burt, C.S. Davis — Utah State; AFCRL-TR-74-0195, February 1974.

HAES Report No. 4

*Data Reduction and Auroral Characterization for ICECAP*

I. Kofsky — Photometrics; DNA 3511F, January 1975.

HAES Report No. 5

*ICECAP Analysis: Energy Deposition and Transport in the Auroral Ionosphere*

R.D. Sears — Lockheed; DNA 3566F, November 1974

HAES Report No. 6

*Auroral Simulation Studies*

D. Archer — Mission Research Corp; DNA 3567T, April 1975.

HAES Report No. 7

*ICECAP 72 — Rocket Measurement Program for Investigation of Auroral IR  
Emissions — Black Brant 17.110-3.*

D.A. Burt, G.D. Allred, J.C. Kemp, L.C. Howlett, E.F. Pound, G.K. LeBaron  
— Utah State; AFCRL-TR-75-0001, September 1974.

HAES Report No. 8

*Design and Calibration of a Rocket-Borne Electron Spectrometer*

P.C. Neal — Utah State; AFCRL-TR-74-0629, December 1974.

HAES Report No. 9

*Near Infrared Auroral Spectra*

D. Baker, A. Steed, R. Huppi — Utah State; AFCRL-TR-75-0010, December  
1974.

HAES Report No. 10

*Arctic Code Electron Deposition Theory with Application to Project EXCEDE*

P.W. Tarr — Mission Research Corp; MRC-R-173, February 1975.



HAES Report No. 11

*Rocketborne Instrumentation for the Measurement of Electric Fields - Paiute  
Tomahawk 10.312-3*

L. Carl Howlett, R.J. Bell - Utah State; AFCRL-TR-75-0023, January 1975.

HAES Report No. 12

*Auroral Chemistry and Energy Deposition Calculations with the OPTAUR Code*

H.J.P. Smith, O.P. Manley - Visidyne; VI 266, February 1975.

HAES REPORT No. 13\*

*Theoretical Evaluation of Vertically Viewing and Earth-Limb Scanning Modes  
for Rocketborne Earth-Limb Measurements*

C.L. Wyatt, R.Y. Han, D.J. Baker -- Utah State; AFCRL-TR-75-0072, September  
1974.

HAES Report No. 14

*Ionospheric Effects Induced by Precipitating Auroral Electrons*

J.D. Cladis, G.T. Davidson, W.E. Francis, L.L. Newkirk, M. Walt - Lockheed;  
LMSC/D454890, February 1975.

HAES Report No. 15

*ICECAP 73A - Chatanika Radar Results*

M.J. Baron, N.J. Chang -- Stanford Research Institute; DNA 3531T, September  
1974.

HAES Report No. 16

*Numerical Modeling of Aurora*

T. Coffey - Naval Research Labs; NRL-MR-3120, October 1975.

HAES Report No. 17

*TMA Payload Field Services and Data Reduction*

J.F. Bedinger - GCA Corp; AFCRL-TR-75-0009, February 1975.

HAES Report No. 18

*Auroral NO*

E. Hyman, D.J. Strickland, P.S. Julianne, D.F. Strobel - Naval Research Labs;  
NRL-MR-3070, July 1975.

HAES Report No. 19

*Analysis of 4.3 $\mu$  ICECAP Data*

J. Kumer - Lockheed; AFCRL-TR-74-0334, July 1974.

HAES Report No. 20

*Cylindrical Langmuir Probe Measurements from Rocket Flights Covering the  
Period 31 January 1961 through 3 April 1974*

R.C. Wilson - Boston College; AFCRL-TR-75-0265, April 1975.

\*HAES number omitted from this report. If you are a recipient of this report, please add  
the appropriate HAES report number to the front cover.



**HAES Report No. 21**

***Data System Developed for Project ICECAP 74***

D.E. Delorey, P.N. Pruneau — Boston College; AFCRL-TR-75-0303, December 1974.

**HAES Report No. 22**

***Rocket-Borne Accelerator Module***

D. Shephard, J. Carpenter, W. Reidy, W. Sheean, T. Zehnpfennig — Visidyne; VI-289, AFCRL-TR-75-0379, July 1975.

**HAES Report No. 23**

***Instrumentation Analysis and Data Processing for Rocketborne LWIR Spectrometers (with Application to Rocket A18.006-2 of 22 March 1973)***

J.W. Rogers — AFCRL; AFCRL-TR-75-0535, December 1975.

**HAES Report No. 24**

***Auroral Simulation Studies in Support of ICECAP and EXCEDE***

D. Archer, P. Tarr — Mission Research Corp; MRC-R-211, September 1975.

**HAES Report No. 25\***

***Studies of Disturbed Ionospheres***

K. Baker — Utah State; AFCRL-TR-75-0342, June 1975.

**HAES Report No. 26\***

***Sky Radiance Calculations in the 0.5  $\mu$ m - 5.0  $\mu$ m Wavelength Range***

W.G.M. Blättner, M.B. Wells — Radiation Research Associates; AFCRL-TR-75-0317, RRA-T7501, May 1975.

**HAES Report No. 27**

***Data Reduction and Auroral Characterizations for ICECAP II***

I.L. Kofsky, R.B. Sluder, C.A. Trowbridge — Photometrics; PhM 05-76, October 1975.

**HAES Report No. 28\***

***Effective Recombination Coefficient of the Polar D Region Under Conditions of Intense Ionizing Radiation***

T.M. Watt — SRI; DNA 3663T, July 1975.

**HAES Report No. 29**

***Ionospheric Irregularities: HAES Program Support***

R.D. Sears — Lockheed; DNA 3782F, September 1975.

\*HAES number omitted from this report. If you are a recipient of this report, please add the appropriate HAES report number to the front cover.

HAES Report No. 30\*

*Development of a Liquid-Helium Cooled Rocketborne Spectrometer*

C.L. Wyatt, D.J. Baker — Utah State University; AFCRL-TR-75-0164, February 1975.

HAES Report No. 31\*

*SIMS Interferometer Study*

R.W. Esplin, D.J. Baker, R.J. Huppi — Utah State University; AFCRL-TR-75-0500, July 1975.

HAES Report No. 32

*Rocket Spectral Measurement of Atmospheric Infrared Emission During a Quiet Condition in the Auroral Zone*

N.B. Wheeler and A.T. Stair, Jr. — AFGL; G. Frodsham and D.J. Baker — Utah State University; AFGL-TR-76-0252, October 1976.

HAES Report No. 33\*

*Report on the Geophysical Description and the Available Data Associated with Rocket PF-BB-53*

G.J. Romick — Geophysical Institute, University of Alaska; AFCRL-TR-75-0040, January 1975.

HAES Report No. 34\*

*Report on the Geophysical Description and the Available Data Associated with Rocket PF-CI-97*

G.J. Romick, Geophysical Institute, University of Alaska; AFCRL-TR-75-0327, May 1975.

HAES Report No. 35

*A Correlation of Discrete and Diffuse Aurora With Particle Precipitation*

R.S. Caverly, G.J. Romick, and R.D. Sharp — Geophysical Institute, University of Alaska; AFCRL-TR-75-0508, August 1975.

HAES Report No. 36\*

*Report on the Geophysical Description and the Available Data Associated with Rocket PF-HJ-NJ-90*

G.J. Romick, Geophysical Institute, University of Alaska; AFCRL-TR-75-0362, December 1975.

HAES Report No. 37†

*ICECAP 73A Partial Reflection Sounder Results*

G. Falcon — ITS; DNA 3943F, November 1975.

\*HAES number omitted from this report. If you are a recipient of this report, please add the appropriate HAES report number to the front cover.

†DNA 3943F was erroneously issued as HAES Report No. 17 when in actuality it should have read "HAES Report No. 37." Holders of this report are urged to correct their copies.



HAES Report No. 38

*Rocket Measurement of OH Emission Profiles in the 1.56 and 1.99  $\mu$ m Bands*

W.F. Grieder, K.D. Baker — Utah State University and A.T. Stair, AFCRL; AFCRL-TR-76-0057, January 1976.

HAES Report No. 39

*ICECAP 74 Chatanika Radar Results*

M. Baron, SRI; DNA 3871T, October 1975.

HAES Report No. 40

*Analyses of High-Altitude Effects Simulation (HAES)*

W.P. Reidy, T.C. Degges, W. Neal — Visidyne; VI-311, AFGL-TR-76-0039, February 1976.

HAES Report No. 41

*Geometrical Aspects of Rocket Photometry*

W.F. Grieder — Utah State University, L.A. Whelan — Logicon Corp.; AFCRL-TR-76-0046, February 1976.

HAES Report No. 42\*

*Report on the Geophysical Description and Available Data Associated with Rocket PF-PT-81*

G.J. Romick, Geophysical Institute, University of Alaska; AFCRL-TR-74-0540, October 1974.

HAES Report No. 43

*ICECAP '75 Chatanika Radar Results*

T.M. Watt — SRI; DNA 4086F, August 1976.

HAES Report No. 44

*Results of Lower Ionospheric Measurements using the Partial Reflection Sounder During ICECAP '74*

G. Falcon — ITS; Report number not yet assigned.

HAES Report No. 45\*

*EXCEDE: SWIR EXPERIMENT — Quick Look Data Report of 28 February 1976 Launch*

R.R. O'Neil, A.T. Stair, Jr., J.C. Ulwick, R. Marcisi — AFGL; D. Burt — Utah State University; 3 March 1976.

HAES Report No. 46\*

*HIRIS EXPERIMENT — Quick Look Data Report of 1 April 1976 Launch*

A.T. Stair, Jr. and J.W. Rogers — AFGL; W.R. Williamson-Honeywell Radiation Center; AFGL-OP-TM 02, July 1976.

\*HAES number omitted from this report. If you are a recipient of this report, please add the appropriate HAES report number to the front cover.



HAES Report No. 47\*

*ICECAP '74 - Chatanika Radar Results*

P.D. Perreault, M.J. Baron - SRI; DNA 3871T, October 1975.

HAES Report No. 48\*

*Bias and Signal Processing Circuits for a Mass Spectrometer in the Project EXCEDE: SWIR Experiment*

R. Sukys, J.S. Rochefort, S. Goldberg - Northeastern University; AFGL-TR-76-0060, October 1975.

HAES Report No. 49

*Chatanika Radar Results during the EXCEDE Experiment*

T.M. Watt - SRI; DNA 4123T, September 1976.

HAES Report No. 50

*Rocketborne Measurements of Infrared Enhancements Associated with a Bright Auroral Breakup*

K.D. Baker, D.J. Baker - Utah State University, J.C. Ulwick, A.T. Stair - AFGL. Report number not yet assigned.

HAES Report No. 51

*LWIR (7-24  $\mu$ m) Measurements from the Launch of a Rocketborne Spectrometer into an Aurora (1973)*

J.W. Rogers, A.T. Stair, Jr., N.B. Wheeler - AFGL; C.L. Wyatt, D.J. Baker - Utah State University. AFGL-TR-76-0274.

HAES Report No. 52\*

*DNA Project 609 Radar: Auroral Backscatter Measurements*

R.T. Tsunoda, R.I. Presnell, T.N.C. Wang - SRI; DNA 3929F, February 1976.

HAES Report No. 53\*

*ICECAP Data Processing System*

D.E. Delorey and P.N. Pruneau - Boston College; AFGL-TR-76-0138, May 1976.

HAES Report No. 54

*Report on the Geophysical Description and Available Data Associated with Rocket PF-NH-89 (IC 507.11-2A)*

G.J. Romick, Geophysical Institute, University of Alaska; AFGL-TR-76-0010, January 1976

HAES Report No. 55

*Report on the Geophysical Description and Available Data Associated with Rocket PF-SH-92 (IC 519.07-1B)*

G.J. Romick, Geophysical Institute, University of Alaska; AFGL-TR-76-0007, January 1976

\*HAES number omitted from this report. If you are a recipient of this report, please add the appropriate HAES report number to the front cover.

## Appendix E

### Distribution List

PRECEDING PAGE BLANK-NOT FILMED



DIRECTOR  
DEFENSE ADVANCED RSCH PROJ AGENCY  
ARCHITECT BUILDING  
1400 WILSON BLVD.  
ARLINGTON, VA 22209  
OICY ATTN LTC W A WHITAKER  
OICY ATTN STD CAPT J JUSTICE  
OICY ATTN MAJOR GREGORY CANAVAN

DEFENSE DOCUMENTATION CENTER  
CAMERON STATION  
ALEXANDRIA, VA 22314  
(12 COPIES IF OPEN PUBLICATION, OTHERWISE 2 COPIES)  
12CY ATTN TC

DIRECTOR  
DEFENSE NUCLEAR AGENCY  
WASHINGTON, DC 20305  
OICY ATTN STTL TECH LIBRARY  
OICY ATTN STST ARCHIVES  
OICY ATTN RAAR CHARLES A BLANK  
OICY ATTN RAAR HAROLD C FITZ JR  
OICY ATTN RAAR MAJ JOHN CLARK

DIR OF DEFENSE RSCH & ENGINEERING  
DEPARTMENT OF DEFENSE  
WASHINGTON DC 20301  
OICY ATTN DD/SRSS DANIEL BROCKWAY  
OICY ATTN DD/SRSS RICHARD S RUFFINE

COMMANDER  
FIELD COMMAND  
DEFENSE NUCLEAR AGENCY  
KIRTLAND AFB, NM 87115  
OICY ATTN FCPR

CHIEF  
LIVERMORE DIVISION FLD COMMAND DNA  
LAWRENCE LIVERMORE LABORATORY  
P.O. BOX 808  
LIVERMORE, CA 94550  
OICY ATTN FCPL



COMMANDER/DIRECTOR  
ATMOSPHERIC SCIENCES LABORATORY  
U S ARMY ELECTRONICS COMMAND  
WHITE SANDS MISSILE RANGE, NM 88002  
OICY ATTN DRSEL-RL-SY-S F F NTLS  
OICY ATTN E BUTTERFIELD DRSEL-RL-SY-H

COMMANDER  
HARRY DIAMOND LABORATORIES  
2800 POWDER MILL ROAD  
ADELPHI MD 20783  
(COMMON-INNER ENVELOPE: ATTN: DRXDD-RRH)  
OICY ATTN DRXDD-VP

COMMANDER  
U S ARMY NUCLEAR AGENCY  
FORT BLISS, TX 79916  
OICY ATTN AYCA-NAW J RFRREFY

CHIEF OF NAVAL RESEARCH  
NAVY DEPARTMENT  
ARLINGTON, VA 22217  
OICY ATTN CODE 429 CDR RONALD J DREBLE

COMMANDER  
NAVAL ELECTRONICS LABORATORY CENTER  
SAN DIEGO, CA 92152  
OICY ATTN CODE 2200 1 VERNE E HILDEBRAND  
OICY ATTN CODE 2200 ILAN RYHMULLEN

DIRECTOR  
NAVAL RESEARCH LABORATORY  
WASHINGTON, DC 20375  
OICY ATTN DOUGLAS P MCNUTT  
OICY ATTN CODE 7127 CHARLES Y JOHNSON  
OICY ATTN CODE 2027 TECH LIA  
OICY ATTN CODE 7700 TIMOTHY P COFFEY  
OICY ATTN CODE 7701 JACK D BROWN  
OICY ATTN CODE 7750 DARNELL F STIMBEL  
OICY ATTN CODE 7750 PAUL JULUENNE

COMMANDER  
NAVAL SURFACE WEAPONS CENTER  
WHITE OAK, SILVER SPRING, MD 20910  
OICY ATTN CODE W4501 NAVY NUC PRNS OFF

AF GEOPHYSICS LABORATORY, AFSC

HANSCOM AFB, MA 01731

OICV ATTN LRB RENNETH S W CHAMPYHN

OICV ATTN OP JOHN S GARING

OICV ATTN OPR ALVA Y STAIR

AF WEAPONS LABORATORY, AFSC

KIRTLAND AFB, NM 87117

OICV ATTN DYT CAPT DAVID W GOFYZ

OICV ATTN SUL

OICV ATTN DYT LTC DON MITCHELL

COMMANDER

ASN

WPAFB, OH 45433

OICV ATTN ASD-YH-EX LTC ROBERTY LEVERETT

SANSO/SZ

POST OFFICE BOX 92960

WORLDWAY POSTAL CENTER

LOS ANGELES, CA 90009

(SPACE DEFENSE SYSTEMS)

OICV ATTN SZJ MAJOR LAWRENCE DUNN

DIVISION OF MILITARY APPLICATION

U S ENERGY RESEARCH & DEV ADMIN

WASHINGTON, DC 20545

OICV ATTN DDC CHN FOR MAJ D A HAYCOCK

LOS ALAMOS SCIENTIFIC LABORATORY

P.O. BOX 1663

LOS ALAMOS, NM 87545

OICV ATTN DDC CHN FOR R A JEFFRIES

DEPARTMENT OF COMMERCE

OFFICE OF TELECOMMUNICATIONS

INSTITUTE FOR TELECOM SCIENCE

BOULDER, CO 80302

OICV ATTN WILLIAM F DYLAUT

OICV ATTN GLENN FALCON



AERODYNE RESEARCH, INC.  
BEDFORD RESEARCH PARK  
CROSBY DRIVE  
BEDFORD, MA 01730  
OICY ATTN F BLEN  
OICY ATTN M CAMAC

AEROSPACE CORPORATION  
P.O. BOX 92957  
LOS ANGELES, CA 90009  
OICY ATTN T TAYLOR  
OICY ATTN R GROVE  
OICY ATTN R D HAWCLIFFE  
OICY ATTN HARRIS MAYER

DENVER: UNIVERSITY OF  
COLORADO SEMINARY  
DENVER RESEARCH INSTITUTE  
P.O. BOX 10127  
DENVER, CO 80270  
(ONLY 1 COPY OF CLASS RPTS)  
OICY ATTN SEC OFFICER FOR MR VAN ZYL  
OICY ATTN SEC OFFICER FOR DAVID MURCRAE

GENERAL ELECTRIC COMPANY  
TEMPO-CENTER FOR ADVANCED STUDIES  
816 STATE STREET (P.O. DRAWN 00)  
SANTA BARBARA, CA 93102  
OICY ATTN DASTAC ART PERVOK  
OICY ATTN WARREN S KNAPP

GENERAL RESEARCH CORPORATION  
P.O. BOX 3587  
SANTA BARBARA, CA 93105  
OICY ATTN JOHN ISF JR

GEOPHYSICAL INSTITUTE  
UNIVERSITY OF ALASKA  
FAIRBANKS, AK 99701  
(ALL CLASS ATTN: SECURITY OFFICER)  
OICY ATTN Y W DAVIS (UNCL ONLY)  
OICY ATTN NEAL BROWN (UNCL ONLY)



HONEYWELL INCORPORATED  
RADIATION CENTER  
2 FORBES ROAD  
LEXINGTON, MA 02173  
OICY ATTN W WILLIAMSON

INSTITUTE FOR DEFENSE ANALYSIS  
400 ARMY-NAVY DRIVE  
ARLINGTON, VA 22202  
OICY ATTN ERNEST RAUER  
OICY ATTN HANS WOLFHARD

LOCKHEED MISSILES AND SPACE COMPANY  
3251 HANOVER STREET  
PALM ALTO, CA 94304  
OICY ATTN JOHN R CLADIS DEPT 52-12  
OICY ATTN J R REAGAN D/52-12  
OICY ATTN RILLY M MCCORMAC DEPT 52-54

OICY ATTN TOM JAMES  
OICY ATTN ROBERT D SEARS DEPT 52-14  
OICY ATTN JOHN KUMER  
OICY ATTN MARTIN WALT DEPT 52-10  
OICY ATTN RICHARD G JOHNSON DEPT 52-12

MISSION RESEARCH CORPORATION  
735 STATE STREET  
SANTA BARBARA, CA 93101  
OICY ATTN P FISCHER  
OICY ATTN D ARCHER

PHOTOMETRICS, INC.  
442 WARRETT ROAD  
LEXINGTON, MA 02173  
OICY ATTN IRVING L KOFSKY

PHYSICAL DYNAMICS INC.

P.O. BOX 1089

BERKELEY, CA 94701

OICY ATTN JOSEPH R WORKMAN

PHYSICAL SCIENCES, INC.

30 COMMERCE WAY

WOBURN, MA 01801

OICY ATTN KURT WRAY

R & D ASSOCIATES

P.O. BOX 9895

MARINA DEL REY CA 90291

OICY ATTN FORREST GILMORE

R & D ASSOCIATES

1815 N. FT. MYER DRIVE

11TH FLOOR

ARLINGTON, VA 22209

OICY ATTN HERBERT J MITCHELL

RAND CORPORATION, THE

1700 MAIN STREET

SANTA MONICA, CA 90406

OICY ATTN JAMES OAKLEY

SCIENCE APPLICATIONS, INC.

P.O. BOX 2351

LA JOLLA, CA 92038

OICY ATTN DANIEL A HAMLIN

SPACE DATA CORPORATION

1331 SOUTH 26TH STREET

PHOENIX, AZ 85034

OICY ATTN EDWARD F ALLEN



STANFORD RESEARCH INSTITUTE  
333 RAVENSWOOD AVENUE  
MENLO PARK, CA 94025  
OICY ATTN WALTER G CHESTNUT  
OICY ATTN W HARRIS  
OICY ATTN RAY L LEADARRAND

STANFORD RESEARCH INSTITUTE  
1611 NORTH KENT STREET  
ARLINGTON, VA 22209  
OICY ATTN WARREN W BERNING

TECHNOLOGY INTERNATIONAL CORPORATION  
75 WIGGINS AVENUE  
BEDFORD, MA 01730  
OICY ATTN W P RHOIST

UTAH STATE UNIVERSITY  
LOGAN, UT 84321  
OICY ATTN DORAN BAKER  
OICY ATTN KAY BAKER  
OICY ATTN D BIRT  
OICY ATTN C WYATT

VISI-DYNE, INC.  
19 THIRD AVENUE  
NORTH WEST INDUSTRIAL PARK  
HURLINGTON, MA 01903  
OICY ATTN WILLIAM REIDY  
OICY ATTN J W CARPENTER  
OICY ATTN T C DEGGES